2011

Evaluation of the Selective Anti-Cancer Activity of Natural and Synthetic Alkaloids

Carly Griffin
University of Windsor

EVALUATION OF THE SELECTIVE ANTI-CANCER ACTIVITY OF NATURAL AND SYNTHETIC ALKALOIDS

by
Carly Griffin

A Dissertation
Submitted to the Faculty of Graduate Studies
through the Department of Chemistry and Biochemistry
in Partial Fulfillment of the Requirements for
the Degree of Doctor of Philosophy at the
University of Windsor

Windsor, Ontario, Canada
2011

Evaluation of the Selective Anti-Cancer Activity of Natural and Synthetic Alkaloids

by

Carly Griffin

APPROVED BY:

D.S. Riddick, External Examiner

University of Toronto

J. Hudson

Department of Biological Sciences

P. Vacratsis

Department of Chemistry & Biochemistry

L. Lee

Department of Chemistry & Biochemistry

S. Pandey, Advisor

Department of Chemistry & Biochemistry

O. Love, Chair of Defense

Department of Biological Sciences

6 January 2011

DECLARATION OF CO-AUTHORSHIP / PREVIOUS PUBLICATION

I. Declaration of Co-Authorship

I hereby declare that this thesis incorporates material that is the result of joint research, as follows:

This thesis incorporates the outcome of joint research efforts undertaken in collaboration with Dr. James McNulty, Dr. Caroline Hamm, Dr. Jerald Nair, Ms. Natasha Kekre, Ms. Natasha Sharda, Ms. Divya Sood and Mr. Aditya Karnik under the supervision of Dr. Siyaram Pandey. In all cases experimental design, execution, data analysis, interpretation, and manuscript preparation were performed by the author.*

- Collaboration with JM is covered in Chapters 2-6 of this thesis; this contribution was through provision of chemical compounds and write-up of synthesis details.
- Collaboration with CH is covered in Chapter 3 of this thesis; this contribution was through patient recruitment and clinical diagnosis.
- Collaboration with JN is covered in Chapter 4 of this thesis; this contribution was through provision of synthetic compounds and write-up of synthesis details.
- Collaboration with NK is covered in Chapter 2 of this thesis; this was a co-first authorship, where there was equal contribution to experimental design, data interpretation and manuscript preparation.
- Collaboration with NS and DS is covered in Chapter 3 of this thesis; this contribution was through performance of TUNEL and Caspase-activity experiments (viz. Figure 4 and 5).
- Collaboration with AK is covered in Chapter 5 of this thesis; this contribution was through standardization and performance of immunohistochemistry experiments (viz. Figure 5D).

*All authors read and approved the final manuscript prior to submission.

- Collaboration with others (non-authorship) is covered in Chapter 5 of this thesis; experimental setup by Ms. A. McLachlan and Ms. D. Gueorguieva (viz. Figure 3C), and materials (ws-CoQ10) provided by Dr. M. Sikorska (viz. Figure 3A, 3B, Supplementary Figure 2B).

I am aware of the University of Windsor Senate Policy on Authorship and I certify that I have properly acknowledged the contribution of other researchers to my thesis, and have obtained written permission from each of the co-authors to include the above materials in my thesis.

I certify that, with the above qualification, this thesis, and the research to which it refers, is the product of my own work.

II. Declaration of Previous Publication

This thesis includes **5** original papers that have been previously published, accepted or submitted for publication in peer-reviewed journals, as follows:

Thesis Chapter	Publication Title and Full Citation	Publication Status
Chapter 2	Kekre N, Griffin C, McNulty J, Pandey S. Pancratistatin causes early activation of caspase-3 and the flipping of phosphatidyl serine followed by rapid apoptosis specifically in human lymphoma cells. *Cancer Chemotherapy and Pharmacology.* 2005; 56(1): 29-38.	*Published*
Chapter 3	Griffin C, Hamm C, McNulty J, Pandey S. Pancratistatin induces apoptosis in clinical leukemia samples with minimal effect on non-cancerous peripheral blood mononuclear cells. *Cancer Cell International.* 2010; 10: 6	*Published*
Chapter 4	Griffin C, Sharda N, Sood D, Nair J, McNulty J, Pandey S. Selective cytotoxicity of pancratistatin-related natural *amaryllidaceae* alkaloids: evaluation of the activity of two new compounds. *Cancer Cell International.* 2007; 7: 10	*Published*
Chapter 5	Griffin C, Karnik A, McNulty J, Pandey S. Pancratistatin selectively targets cancer cell mitochondria and reduces growth of human colon tumor xenografts. *Molecular Cancer Therapeutics.* 2011; 10(1): 57-68.	*Accepted*
Chapter 6	Griffin C, McNulty J, Pandey S. Pancratistatin induces apoptosis and autophagy in metastatic prostate cancer cells. *International Journal of Oncology.* 2011 [Accepted].	*Accepted*

I certify that I have obtained a written permission from the copyright owners to include the above published materials in my thesis. I certify that the above material describes work completed during my registration as a graduate student at the University of Windsor.

I declare that, to the best of my knowledge, my thesis does not infringe upon anyone's copyright nor violate any proprietary rights and that any ideas, techniques, quotations, or any other material from the work of other people included in my thesis, published or otherwise, are fully acknowledged in accordance with the standard referencing practices. Furthermore, to the extent that I have included copyrighted material that surpasses the bounds of fair dealing within the meaning of the Canada Copyright Act, I certify that I have obtained a written permission from the copyright owners to include such materials in my thesis.

I declare that this is a true copy of my thesis, including any final revisions, as approved by my thesis committee and the Graduate Studies office, and that this thesis has not been submitted for a higher degree to any other University or Institution.

ABSTRACT

Cancer is a disease of uncontrolled cell growth and proliferation that is predicted to directly affect one-third of Canadians. Standard chemotherapy, which targets DNA or its replicative machinery, effectively eradicates cancer cells but also causes non-specific toxicity to non-cancerous cells. Pancratistatin is a natural alkaloid isolated from *Hymenocallis littoralis* found to selectively induce apoptosis (programmed cell death) in numerous human cancer cell lines with an insignificant effect on non-cancerous cells. The major objectives of this study were to: 1) assess the selectivity and efficacy of pancratistatin and synthetic derivatives on patient-obtained and commercially available leukemia models; 2) test the effect of pancratistatin on human colon and prostate cancer cells *in vitro* and *in vivo*; and 3) to determine the mechanism of action of pancratistatin. Results suggested that 1 μM pancratistatin induces apoptosis in leukemia *ex vivo* with an insignificant effect on non-cancerous peripheral blood mononuclear cells. Apoptosis was monitored by nuclear staining and phosphatidylserine exposure by microscopy and flow cytometry. Structure-activity relationship screening of synthetic derivatives of pancratistatin on leukemia (Jurkat) cells revealed that certain analogs retain activity of the native compound, albeit at higher concentrations. The effects of pancratistatin on colon (HCT116, HT-29) and prostate (LNCaP, DU145) cancer cell lines, expressing either the wild-type or functionally inactive p53 tumor suppressor protein, were studied using cell-based assays and animal models. Pancratistatin treatment caused increased production of reactive oxygen species, collapse of mitochondrial membrane potential, and release of the pro-apoptotic proteins cytochrome *c*, apoptosis-inducing factor and endonuclease G to the cytosol. Furthermore, pancratistatin induced cell death independent of p53, caspase activation or Bax expression. Importantly, components of the mitochondrial respiratory chain were deemed crucial for pancratistatin activity, as mtDNA-deficient 'Rho-0' cells were resistant to pancratistatin. A significant finding of this study was that pancratistatin reduced growth of human colon and prostate tumor xenografts in immune-compromised mice, was well-tolerated and determined to be non-toxic to vital organs compared to control. In conclusion, pancratistatin is a natural anti-cancer compound that selectively targets cancer cell mitochondria to induce apoptosis and significantly reduces growth of human tumor xenografts.

I dedicate this work in loving memory of my father, Glen Griffin, who lost his battle against colon cancer but will live forever in my heart.

ACKNOWLEDGEMENTS

First and foremost, I would like to acknowledge my supervisor, Siyaram Pandey, for his mentorship, guidance and support over the course of my studies. His enthusiasm and dedication to research is contagious and inspiring.

I would also like to acknowledge the efforts of my committee members, Dr. Vacratsis, Dr. Lee and Dr. Hudson, and thank all members of the Department of Chemistry and Biochemistry as well as the support staff at the University of Windsor, especially Marlene, whose advice has proven invaluable on multiple occasions.

To all lab mates past and present, thanks for the laughs and the memories. Thank you to all students on the "cancer project" over the years, Amanda, Meighan, Aditya, Peter, Sudipa, Pamela and Dennis. Thanks for bouncing ideas and theories back and forth with me and for all your contributions to the project. Special thanks to Mallika for sharing your expertise and advice, and for providing a voice of reason in times of adversity and doubt.

I would also like to thank all of the cancer patients who donated blood samples for this research, and the nurses and staff at the Windsor Regional Cancer Centre. Thank you Jafar Naderi for collecting non-cancerous blood samples from healthy volunteers.

Community support of this research has been overwhelming, and deserves acknowledgement; the Knights of Columbus, St. Clair Beach Council #9671 has raised awareness and contributed substantial financial support to the project since 2006.

Funding for this project was provided in part by the Lotte & John Hecht Memorial Foundation, Knights of Columbus Council #9671, Cancer Care Ontario, a Partnership Development Seed Grant from the Shastri Indo-Canadian Institute of Calgary, and by a CIHR Banting & Best Doctoral Fellowship.

Last but not least, I thank my husband and family for their continuous encouragement and support, which has helped me get through times of frustration and made my accomplishments worth celebrating.

TABLE OF CONTENTS

LIST OF TABLES

CHAPTER 3
Cancer Cell International (2010)

LIST OF FIGURES

CHAPTER 6
The Prostate (2011)

LIST OF APPENDICES

LIST OF ABBREVIATIONS

Abbreviation	Definition
5-FU	fluorouracil, pyrimidine analogue
ABCG2	ATP-binding cassette transporter
ADMET	absorption, distribution, metabolism, excretion, toxicity
AIF	apoptosis-inducing factor
ALL	acute lymphoid leukemia
AMD	*Amaryllidaceae*
AML	acute myeloid leukemia
AMPK	AMP-activated kinase
ANT	adenine nucleotide translocase
ATG	autophagy-related proteins
ATM	Ataxia telangiectasia mutated, a serine/threonine protein kinase
α-TOS	alpha-tocopheryl succinate
BA	betulinic acid
Bak	Bcl-2 homologous antagonist/killer protein
Bax	Bcl-2-associated X protein
Bcl-2	B-cell lymphoma-2
BH	Bcl-2 homology (domain)
CICD	caspase-independent (programmed) cell death
Chk1/2	Checkpoint kinase 1 / 2, serine/threonine protein kinases
CML	chronic myelogenous leukemia
CMML	chronic myelomonocytic leukemia
Complex I	NADH-ubiquinone oxidoreductase or NADH reductase
Complex II	succinate dehyrogenase
Complex III	ubiquinol cytochrome c reductase or cytochrome bc_1 complex
Complex IV	cytochrome *c* oxidase (alternate: COX)
Complex V	mitochondrial F_0-F_1 ATP synthase (alternate: F_0-F_1 ATPase)
CR	complete response
CRC	colorectal cancer
CYP3A4	human cytochrome P450 family member
CypD	cyclophilin D
Cyt c	cytochrome c
DAPI	4'-6-Diamidino-2-phenylindole, nuclear counterstain
DSB	double-strand breaks [DNA]
EC_{50}	effective concentration where 50% of maximal outcome is attained
EGCG	epigalocatechin gallate (constituent of green tea)
EndoG	endonuclease G
GLUT1	glucose transporter isoform 1
GSH	glutathione
H&E	Hematoxylin and Eosin
HK	hexokinase
IM	inner (mitochondrial) membrane
IMS	intermembrane space (of mitochondria)
IP	intra-peritoneal
IT	intra-tumor
JC-1	5,5′,6,6′-tetrachloro-1,1′,3,3′-tetraethyl-imidacarbocyanine iodide
LC3	microtubule-associated protein1 light-chain 3

MALDI–TOF	matrix-assisted laser desorption/ionization – time-of-flight
MDC	monodansylcadaverine
Mdm2	murine double-minute 2, an E3 ubiquitin ligase
MDS	myelodysplastic syndrome
MMP	mitochondrial membrane potential
MOMP	mitochondrial outer membrane permeabilization
MPTP	mitochondrial permeability transition pore
MRC	mitochondrial respiratory chain
mtDNA	mitochondrial DNA
mTOR	mammalian target of rapamycin
NAC	N-acetylcysteine
NCI	National Cancer Institute
Nox	NAD(P)H oxidase
Noxa	(latin for damage)
NR	no response
OM	outer (mitochondrial) membrane
PBMC	peripheral blood mono-nuclear cells
PBS	phosphate buffered saline
PEITC	beta-phenylethyl isothiocyanate
PM-MTOX1	phenotype microarray - mitochondrial toxicity plate type 1
PR	partial response
PST	pancratistatin
Puma	p53-upregulated modulator of apoptosis
ROS	reactive oxygen species
SAR	structure-activity relationship
s.c.	sub-cutaneous
sdAbs	single-domain antibodies or intrabodies
SDH	succinate dehydrogenase
Smac/DIABLO	Second-mitochondria derived activator of caspases / Direct IAP Binding Protein with low pI
TAM	Tamoxifen
Taxol	paclitaxel
TMRM	tetramethylrhodamine methyl ester perchlorate
TUNEL	terminal transferase dUTP nick-end labelling
VDAC	voltage-dependent anion channel
Vp-16	etoposide
ws-CoQ_{10}	water-soluble coenzyme Q_{10} (alternate abbreviation: Q10)

CHAPTER 1

General Introduction

CANCER

Background

Cancer is a major health issue in Canada that is predicted to develop in nearly one third of the population (Canadian Cancer Society, 2010). Cancer arises from normal tissues of the body and can stem from many different cell types. The majority of tumors are carcinomas, which develop from epithelial tissues such as the lungs, skin, intestines and mammary glands. Sarcomas, which arise from non-epithelial cells like fibroblasts and osteoblasts, and cancers of hematopoietic tissue, occur with less frequency (Weinberg, 2007). Development of cancer is attributed to various factors including exposure to environmental carcinogens, unhealthy lifestyle, and genetic predisposition. These factors contribute to tumorigenesis by damaging genetic material, which is normally repaired or triggers senescence or elimination of the cell depending on extent of damage. Accumulation of multiple mutations is required for the progression of cancer from *in situ* dysplasia to malignant tumor (Weinberg, 2007). According to Hanahan and Weinberg (2000), the various genetic alterations acquired by cancer cells ultimately manifest as six essential properties considered the "hallmarks of cancer": growth signal autonomy and resistance to anti-growth signals; ability to invade and metastasize; unlimited replication potential; sustained angiogenesis; and escape of apoptosis (Hanahan and Weinberg, 2000). This thesis will focus on carcinomas originating from secretory cells (prostate and colorectal adenocarcinoma) and leukemia.

Leukemia

Leukemia, specifically acute myeloid leukemia (AML), is the most common childhood cancer and a leading cause of cancer-related death in people under forty (Jemal *et al,* 2010). Leukemia is a cancer that arises from hematopoietic tissues and is typically categorized as acute or chronic, according to progression rate and blast phenotype, and either myelogenous or lymphocytic depending on the cell lineage involved (Weinberg, 2007). Acute leukemia progresses quickly and contains high numbers of blast (immature undifferentiated) cells; chronic leukemia progresses relatively more slowly and generally has a lower blast count (Harris *et al,* 1999). Myeloid progenitors normally differentiate into granulocytes and monocytes, and lymphocytic progenitors become T-cells and B-cells of the immune system (Lehninger *et al,* 2000).

Leukemia leads to accumulation of immature white blood cells that do not function properly or hinder the ability of red blood cells to function. The causes of leukemia are unknown for the majority of patients; however, exposure to high doses of radiation or carcinogens, such as benzene, as well as genetic abnormalities and family history have been attributed to higher risk of developing leukemia (Chokkalingam and Buffler, 2008). A genetic abnormality responsible for the onset of chronic myelogenous leukemia (CML) is the translocation of chromosomes 9 and 22, which forms the Philadelphia chromosome (Ph) resulting in the Bcr-Abl fusion gene that translates a constitutively active tyrosine kinase (Druker, 2008). This unique feature enabled development of imatinib, a targeted tyrosine kinase inhibitor that is very effective against Ph+ cases of CML, but exerts selective pressure that generates resistance (Chabner and Roberts, 2005). At present, the only curative therapy for leukemia is allogeneic stem cell transplantation, but is associated with a high risk of fatal complications (Druker, 2008).

Colorectal Adenocarcinoma

Colorectal cancer (CRC) is the second-leading cause of cancer-related death in Canada, behind lung cancer (Canadian Cancer Society, 2010). This is a dire statistic considering that recommended routine colonoscopy screenings can detect and remove polyps, and surgical resection of stage I CRC is associated with >90% long-term survival (Worthley and Leggett, 2010). Sporadic CRC develops from multiple and sequential genetic mutations, a process known as the multi-hit theory of carcinogenesis (Fearon and Vogelstein, 1990). Particularly for CRC, the sequential multiple mutations are well-documented. The first 'hit' induces loss-of-function of the *APC* (Adenomatous polyposis coli) tumor suppressor gene, typically followed by an activating mutation of the *RAS* oncogene, which precedes inactivating mutations of the *TP53* tumor suppressor gene (Fearon and Vogelstein, 1990; Knudson, 2001). Further mutations are a result of the chromosomal instability that ensues after the loss of *TP53*, leading to the development of malignant carcinoma (Knudson, 2001). Chromosomal instability generates highly heterogeneous cancers that are fatal if diagnosed in advanced stages due to the rapid rate of proliferation and extent of invasion and metastasis (Worthley and Leggett, 2010). The standard line of adjuvant (post-operative) chemotherapy for earlier stage CRC is combination of fluorouracil (5-FU), leucovorin (LV) and oxaliplatin, referred to collectively as FOLFOX, and is generally successful albeit with serious toxic side-effects (Goodwin

and Asmis, 2009). Patients with metastatic CRC (mCRC) may initially respond to therapy, but commonly relapse and succumb to the disease within two years (Goodwin and Asmis, 2009).

Prostate Cancer

Prostate carcinoma is the leading cancer in men over 50, and the second-leading cause of cancer-related death of North American men (Jemal *et al,* 2010). Prostate cancer generally presents as hormone-dependent (androgen-receptor positive) and in most cases, remission is achieved by endocrine therapy. Fatality associated with this disease is a result of relapse with advanced hormone refractory (androgen-receptor independent) metastatic cancer (Radhakrishnan *et al,* 2010). Androgen hormones are important players in the differentiation, development and normal functioning of the prostate gland, and are believed to contribute to abnormal growth in prostate carcinogenesis (Nieto *et al,* 2007).

The initiating event(s) in the development of prostate cancer remain unknown and are up for debate. Similar to many other types of cancer, the risk factors include exposure to environmental carcinogens and poor diet; and prostate cancer is considered an age-related disease, as the median age of onset is over 55 years (Nieto *et al,* 2007). Recently, it was reported that increased reactive oxygen species (ROS) produced as a by-product of normal cell metabolism not only contributes to the process of aging, but may have an essential role in the development of cancer, including prostate cancer (Khandrika *et al,* 2009). New insights into the molecular changes involved in metastatic prostate cancer have enabled use of targeted therapies as adjuncts to the standard care of chemotherapy (Fizazi *et al,* 2010). Today, advanced metastatic prostate cancer is treated with docetaxel-based chemotherapy, and clinical trials to test the effectiveness of combinations with monoclonal antibodies or tyrosine-kinase inhibitors are ongoing (Fizazi *et al,* 2010).

CANCER METABOLISM

An alternate method to specifically target cancer cells is to exploit the extensive metabolic reprogramming commonly observed in many types of cancer. In addition to the aforementioned six essential changes in cancer cell physiology, cancer cell mitochondria are known to be structurally and functionally different than their normal cell counterparts (Figure 1) (Fulda *et al,* 2010a). Cancer cell mitochondria have extensive metabolic reprogramming allowing them to rely on glycolysis for production of adenosine 5'-triphosphate (ATP), despite high oxygen tension (DeBerardinis, 2008). This phenomenon is known as aerobic glycolysis or the Warburg effect, as it was first described by Otto Warburg in the 1920's (Warburg, 1956; Nijsten and van Dam, 2009). Cancer cells essentially bypass oxidative phosphorylation, the main energy production process in normal cells, and manage to thrive on upregulation of glucose import and metabolism (Kaelin and Thompson, 2010). Moreover, cancer cells have increased levels of gluconeogenesis, reduced pyruvate oxidation and increased lactic acid production (Modica-Napolitano and Singh, 2002). These metabolic differences between normal and cancer cells may be the primary cause of cancer, as proposed by Warburg, but the more likely explanation is that altered metabolism is an adaptation to support malignancy (Nijsten and van Dam, 2009; Fulda *et al,* 2010a). Aerobic glycolysis allows a cancer cell to generate ATP in varying oxygen conditions, which is advantageous for survival and proliferation (DeBerardinis, 2008).

To this end, there are three key changes to mitochondrial metabolic processes that result from elevated oncogenic signalling or loss-of-function mutations of tumor suppressors (Fulda *et al,* 2010a). One of these changes is the binding of hexokinase (HK) to the voltage-dependent anionic channel (VDAC) on the outer mitochondrial membrane in cancer cells (Mathupala *et al,* 2010). Hexokinase converts glucose to glucose-6-phosphate, a rate-limiting step of glycolysis that requires ATP. By binding to VDAC, HK is in close proximity to the export of residual ATP produced in the mitochondria (Mathupala *et al,* 2010; Fulda *et al,* 2010a). VDAC is a component of the mitochondrial permeability transition pore (MPTP), a dynamic structure comprised of VDAC on the outer mitochondrial membrane, adenine nucleotide translocase (ANT) and cyclophilin D (cypD) on the inner mitochondrial membrane that is reversibly permeable to solutes < 1.5 kDa (Halestrap *et al,* 2002).

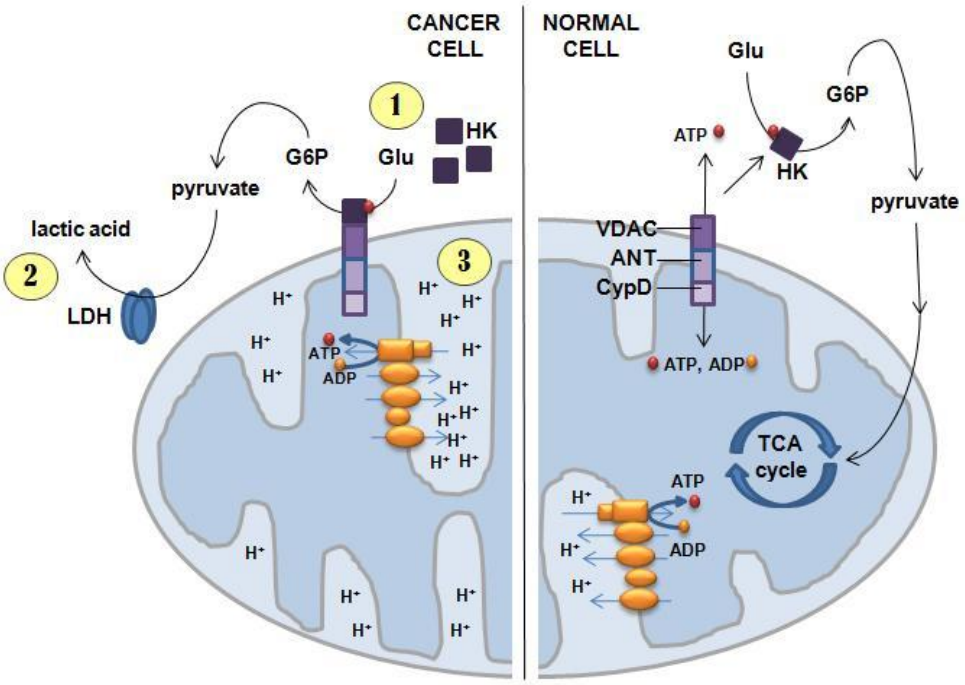

Figure 1. The key metabolic alterations in cancer cell mitochondria that may contribute to the vulnerability of cancer cells, compared to normal cell counterparts. Cancer cell mitochondria are structurally and functionally different in three ways: **1**) hexokinase is bound to VDAC on the outer mitochondrial membrane to facilitate glycolysis; **2**) the end product of glycolysis, pyruvate, is preferentially converted to lactic acid leading to acidification of the tumor microenvironment; and **3**) the decreased rate of mitochondrial ATP production leads to hyperpolarization of the mitochondria, compared to normal mitochondria.

A second key change in cancer cell metabolism is increased lactic acid production and efflux (Hockenbery, 2010). In normal conditions the end product of glycolysis (pyruvate) is converted to acetyl coenzyme A (acetyl CoA), which enters the citric acid cycle to generate substrates (NADH, $FADH_2$) required for oxidative phosphorylation. In cancer cells, pyruvate is preferentially converted to lactic acid by lactate dehydrogenase, which diverts energy production away from the mitochondria and contributes to acidification of the tumor microenvironment (Nijsten and van Dam, 2009). An acidic microenvironment is proposed to enhance invasive and metastatic potential of tumor cells by degrading components of the extracellular matrix (Robey *et al,* 2009).

The third key change is the observed hyperpolarization of cancer cell mitochondria compared to normal counterparts, due to reduced dissipation of the mitochondrial membrane potential as a result of increased glycolytic ATP production (Modica-Napolitano and Singh, 2002; Fulda *et al,* 2010a; Hockenbery, 2010). In normal cells an electrochemical gradient is established across the inner mitochondrial membrane as protons (H^+) are pumped into the intermembrane space (IMS) by complexes I, III and IV during cellular respiration. The potential energy of built up protons is used to drive synthesis of ATP from ADP and inorganic phosphate (P_i) by ATP synthase (Lehninger *et al,* 2000). In contrast, malignant tumor cells produce up to 75% of their ATP requirements by glycolysis, and thus the electrochemical gradient generated by mitochondrial respiratory chain (MRC) complexes is largely unused for ATP generation, even in aerobic conditions, leading to hyperpolarization (Mathupala *et al,* 2010).

These key metabolic changes, as well as improper lipid remodelling of mitochondrial (and other organelle) membranes due to the rapid proliferation rate of cancer cells, indicate that cancer cell mitochondria may be more susceptible to disruption (Alirol and Martinou, 2006). These generally conserved features of cancer cell mitochondria present an attractive target for cancer therapy, specifically those designed to stimulate mitochondrial-mediated apoptosis.

APOPTOSIS

Apoptosis is a physiological process of programmed cell death important for normal tissue development and homeostasis, and elimination of virally infected or degenerate cells (Kerr *et al,* 1972). Apoptosis is a tightly regulated energy-requiring process that is stimulated by various cellular stresses, such as chemotherapy and oxidative stress (Fulda *et al,* 2010b). Characteristic features of apoptosis include nuclear fragmentation, chromatin condensation, plasma membrane blebbing, cell shrinkage and formation of apoptotic bodies (Reed, 2000). Apoptotic bodies are small-membrane-surrounded fragments that are easily engulfed by phagocytes so as not to elicit an immune response (Reed, 2000).

Dysregulated apoptosis has been implicated in numerous diseases including the two leading causes of death in Canada: cardiovascular disease (CVD) and cancer (Fulda *et al,* 2010b). Interestingly, CVD is associated with excessive apoptosis and cancer development is associated with evasion of apoptosis (Fulda, 2009). The two main signalling pathways of apoptosis are the extrinsic and intrinsic pathways (Figure 2). The extrinsic pathway is dependent on death-receptor stimulation, and the intrinsic pathway is activated in response to DNA damage through the mitochondria (Kroemer *et al,* 2007). Activation of either pathway leads to activation of caspases; cysteine-dependent aspartic-directed proteases that act as the final executioners of apoptosis by cleaving nuclear and cytoplasmic substrates.

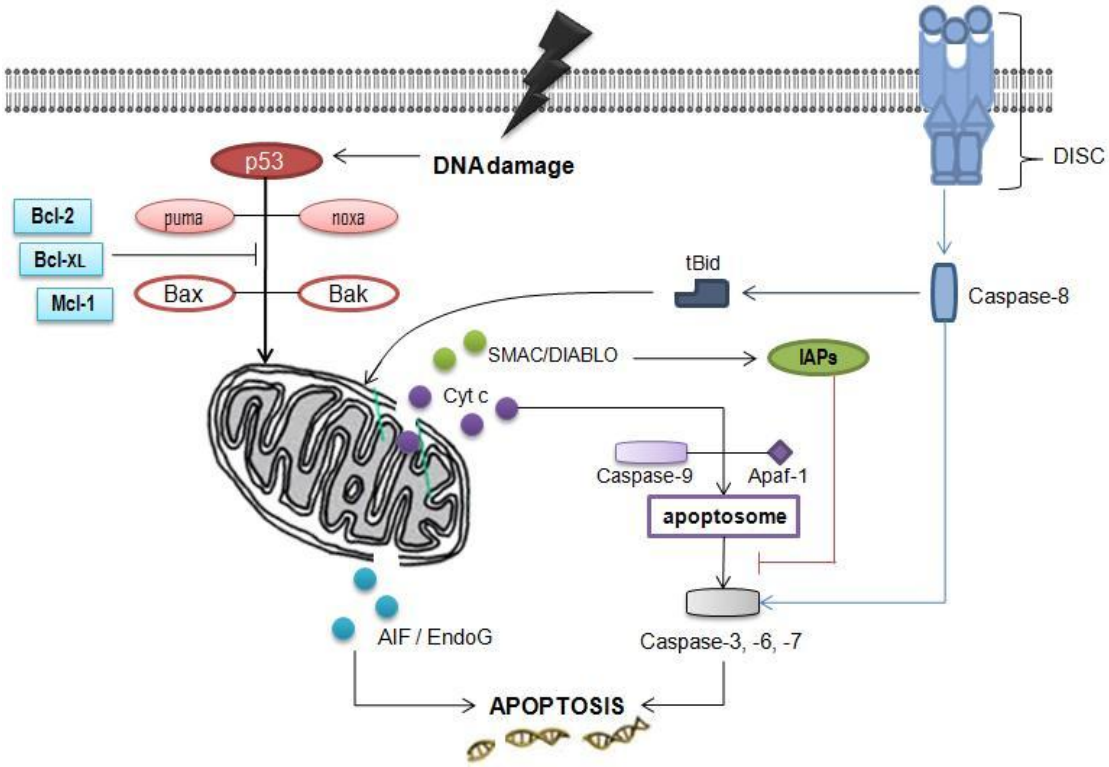

Figure 2. Extrinsic and intrinsic pathways of apoptosis. The extrinsic pathway is dependent on death receptor stimulation by the appropriate ligand, causing death receptor trimerization and recruitment of death effector domains and pro-caspase-8 that together make up the death-inducing signalling complex (DISC). Activation of caspase-8 leads to activation of caspase-3, and/or tBid (BH3-only protein). The intrinsic pathway is orchestrated by p53-activation of pro-apoptotic Bcl-2 family proteins in response to DNA damage. This leads to mitochondrial outer membrane permeabilization (MOMP) (*not shown*). Permeabilization of the mitochondria is irreversible and causes release of pro-apoptotic factors leading to caspase-dependent (Cyt *c*, SMAC/DIABLO, Omi/HtrA2) or caspase-independent (AIF, Endo G) apoptosis.

Extrinsic Pathway of Apoptosis

The extrinsic pathway of apoptosis is triggered by stimulation of death receptors on the plasma membrane by their respective ligands. The TNF (tumor-necrosis factor) superfamily of death receptors, such as Fas and TRAIL receptors, oligomerize upon binding with their ligands, FasL and TRAIL (TNF-related apoptosis-inducing ligand). Receptors then bind to adapter proteins, such as Fas-associated death domain (FADD) through an exposed death domain (DD). In complex with the receptor, the death effector domain (DED) on FADD binds with the DED on pro-caspase-8 (Reed, 2000). Assimilation of these proteins constitutes the death inducing signalling compex (DISC), which cleaves and activates caspase-8 (Green and Evan, 2002). Caspase-8 and -10 are initiator caspases that become activated upstream of effector caspase-3, -6, and -7 (Kroemer *et al,* 2007). Caspase-8 provides a link between the extrinsic and intrinsic pathways of apoptosis, through an alternate mechanism whereby caspase-8 cleaves and activates the pro-apoptotic Bcl-2 family protein Bid (to truncated Bid, or tBid). Pro-apoptotic tBid then interacts with anti-apoptotic Bcl-2 family proteins on the mitochondrial outer membrane to promote mitochondrial-mediated apoptosis (Billen *et al,* 2008).

Intrinsic Pathway of Apoptosis

The intrinsic pathway of apoptosis can be induced by multiple signals such as DNA damage, hypoxia and growth factor deprivation, which activate tumor suppressor p53, a transcription factor that increases expression of pro-apoptotic members of the Bcl-2 family of proteins (Chipuk and Green, 2006; Giménez-Bonafé *et al,* 2009). The Bcl-2 protein family is comprised of both anti- and pro-apoptotic members; and pro-apoptotic proteins are further classified as multi-domain or BH3-only proteins (Gogvadze *et al,* 2009). Anti-apoptotic members include the archetypal Bcl-2, as well as Bcl-XL, Bcl-w and Mcl-1, all of which contain all four Bcl-2 homology domains (BH1-4) and reside mainly in the mitochondrial outer membrane (OM) (Kroemer *et al,* 2007; Letai, 2008). Pro-apoptotic multi-domain Bcl-2 family proteins Bax and Bak contain three BH domains (BH1-3) and are the key proteins responsible for mitochondrial outer membrane permeabilization (MOMP) (Letai, 2008; Brenner and Mak, 2009). In normal physiological conditions, Bax is cytosolic and Bak resides in the OM; upon activation by pro-apoptotic stimuli Bax translocates to the OM and Bak changes conformation (Fulda *et al,* 2010a). Lastly, the BH3-only pro-apoptotic proteins are subdivided depending on their role as

either direct activators of Bax and Bak (Bim and tBid), or as derepressors of anti-apoptotic proteins (Bad, Bik, Puma, Noxa) (Bouchier-Hayes *et al,* 2005; Brenner and Mak, 2009; Letai, 2008). Recently, cytoplasmic p53 has been suggested to act as a BH3-only protein in the activation of Bax, though it is not clear whether as a direct activator or derepressor (Green and Kroemer, 2009). Once activated, Bax and Bak form hetero- and/or homo-oligomers that create channels permitting the rapid and complete release of toxic proteins, such as cytochrome *c* and AIF (apoptosis inducing factor) previously contained in the IMS (Armstrong, 2006; Kroemer *et al,* 2007). MOMP is widely considered to be 'the point of no return' after which cells cannot be rescued (Armstrong, 2006; Gogvadze *et al,* 2009). In addition to the release of pro-apoptotic factors following MOMP, there is subsequent loss of mitochondrial membrane potential (MMP) due to uncoupling of the MRC (Fulda *et al,* 2010a).

An alternate method that causes dissipation of MMP is opening of the mitochondrial permeability transition pore (MPTP) to a high-conductance state (Gogvadze *et al,* 2009). MPTP opening can be stimulated by accumulation of reactive oxygen species (ROS) and/or calcium overload (Gogvadze *et al,* 2009). An unregulated influx of solutes flows through opened MPTP, which causes swelling of the matrix and rupture of the OM (MOMP) leading to cell death (Kinnally and Antonsson, 2007).

Cell Death Effectors Released from Mitochondria

The toxic proteins released from the mitochondria following its permeabilization fall into three main categories: direct caspase activators; indirect caspase activators; and caspase-independent pro-apoptotic factors. Cytochrome *c* forms a complex with apoptosis-protease activating factor (apaf-1) and pro-caspase-9 called the apoptosome, whose primary function is to cleave and activate caspase-9. Caspase-9, like caspase-8, is an initiator caspase that cleaves and activates downstream effector caspases 3, 6 and 7 (Pradelli *et al,* 2010). The indirect caspase activators, Smac/DIABLO and Omi/HtrA2, bind and inhibit the inhibitor of apoptosis proteins (IAPs), which are endogenous caspase inhibitory proteins (Brenner and Mak, 2009; Kroemer *et al,* 2007). Activation of effector caspases is often portrayed as the last step in the signalling pathway of apoptosis; however, it should be noted that the substrates of effector caspases include poly (ADP-ribose) polymerase (PARP), cytoskeletal and nuclear matrix proteins (Reed, 2000).

Along with the caspase-dependent cytotoxic factors, pro-apoptotic caspase-independent proteins, AIF and Endonuclease G (EndoG) are also released from the mitochondria following MOMP (Pradelli *et al,* 2010). These proteins bypass caspase activation to induce a distinct form of programmed cell death, called caspase-independent programmed cell death (CICD) (Constantinou *et al,* 2009). EndoG is a mitochondrial endonuclease that translocates to the nucleus following release from the mitochondria and induces DNA fragmentation and CICD (Pradelli *et al,* 2010). The flavoprotein AIF is anchored to the IM in the IMS and is required for maintenance of the MRC in physiological conditions (Millan and Huerta, 2009; Pradelli *et al,* 2010). In response to MOMP, AIF gets cleaved and activated by calpain or cathepsin proteases and is released to the cytosol where it induces large-scale DNA fragmentation and CICD (Millan and Huerta, 2009). Recent studies indicate that AIF is down-regulated in metastatic colon cancer, which may contribute to chemotherapy resistance (Millan and Huerta, 2009).

Evasion of apoptosis is considered a hallmark of cancer cells, and is also attributed to acquired resistance of metastatic tumor cells to chemotherapeutic agents (Fulda, 2009). All tumor cells, however heterogeneous or advanced, are imbalanced towards proliferation and reduced cell death through overexpression of anti-apoptotic proteins and/or down-regulation or loss-of-function of pro-apoptotic proteins (Green and Evan, 2002). There have been major advances in the treatment of metastatic tumors with the development and application of small molecules that target Bcl-2 family proteins to induce MOMP and inevitably cell death (as reviewed in Fulda *et al,* 2010a; Giménez-Bonafé *et al,* 2009; Hockenbery, 2010). The pro-survival process of autophagy has also been implicated as a possible mechanism of resistance to cell death in tumor cells (Dalby *et al,* 2010).

AUTOPHAGY

Autophagy is a physiological process that enables digestion of proteins, macromolecules and organelles (Kroemer *et al,* 2007). It is a catabolic process tightly regulated by autophagy-related proteins (ATG) that become activated downstream of inactivation of mammalian target of rapamycin (mTOR) kinase (Dalby *et al,* 2010; Essick and Sam, 2010). Activation of autophagy results in formation of phagophores that elongate and fuse together to engulf proteins within a mature autophagosome. The autophagosome then fuses with intracellular lysosomes (now an autophagolysosome), which leads to digestion of the engulfed macromolecules by lysosomal hydrolases (Essick and Sam, 2010).

Autophagy is a temporary survival mechanism triggered by nutrient deprivation, hypoxia and/or metabolic stress; it effectively clears away damaged or long-lived proteins and recycles the intermediate metabolites to meet essential energy requirements (Fulda *et al,* 2010b). Alternatively, sustained autophagy in response to conditions of continuous stress causes autophagic cell death, either via self-cannibalism or induction of apoptosis (Dalby *et al,* 2010). This supposed duality of autophagy has recently generated tremendous controversy in regards to the role of autophagy in tumorigenesis and chemo-resistance, and the complex interplay between autophagy and apoptosis (Dalby *et al,* 2010). It is suggested that Beclin-1, an essential autophagy gene, acts as a tumor suppressor because its mutation leads to defective (reduced) autophagy associated with malignant transformation (Fimia and Piacentini, 2010; Dalby *et al,* 2010). Conversely, tumor cells have been reported to use autophagy as a means of survival in the harsh conditions of the tumor microenvironment and in the face of chemotherapy-induced insults (Dalby *et al,* 2010). Recent research supports these contradictory roles of autophagy in cancer. Some studies suggest induction of autophagy as a novel therapeutic strategy for the treatment of prostate and pancreatic cancers (DiPaola *et al,* 2008; Ullén *et al,* 2010; Dalby *et al,* 2010). Others report the effectiveness of autophagy inhibition against chemo-resistant breast and colon cancers (Qadir *et al,* 2008; Sasaki *et al,* 2010).

Crosstalk *between Autophagy and Apoptosis*

There is significant crosstalk between autophagy and apoptosis signalling pathways, and the mechanisms by which one modulates and/or activates the other are not fully understood (Figure 3) (Dalby *et al,* 2010). Autophagy and apoptosis have common regulators, can exert similar effects and have shared activation stimuli (e.g., Bcl-2 family members, cell death, hypoxic/metabolic stress) (Fimia and Piacentini, 2010). The anti-apoptotic protein Bcl-2, as well as related proteins Bcl-XL, Bcl-w and Mcl-1, reportedly interact with the novel BH3-only protein Beclin-1, which is critical for autophagosome formation (Fulda *et al,* 2010b). This interaction inhibits autophagy and autophagic cell death. Moreover, inhibition of Beclin-1 and the cysteine protease Atg4, involved in the elongation step of autophagy, reportedly occurs by caspases and contributes to inhibition of autophagy; and calpain-cleavage of Atg5, also involved in elongation, induces apoptosis (Fimia and Piacentini, 2010; Levine, 2007). Tumor suppressor p53 induces autophagy and/or apoptosis through its cytosolic and nuclear effects in response to DNA damage and other stressors (Olovnikov *et al,* 2009; Fimia and Piacentini, 2010). Oxidative stress, i.e., increased production of reactive oxygen species (ROS), can also induce apoptosis and autophagy (Essick and Sam, 2010). Although the interplay between these two pathways is undeniable, the question remains as to whether autophagy works to promote or prevent cancer.

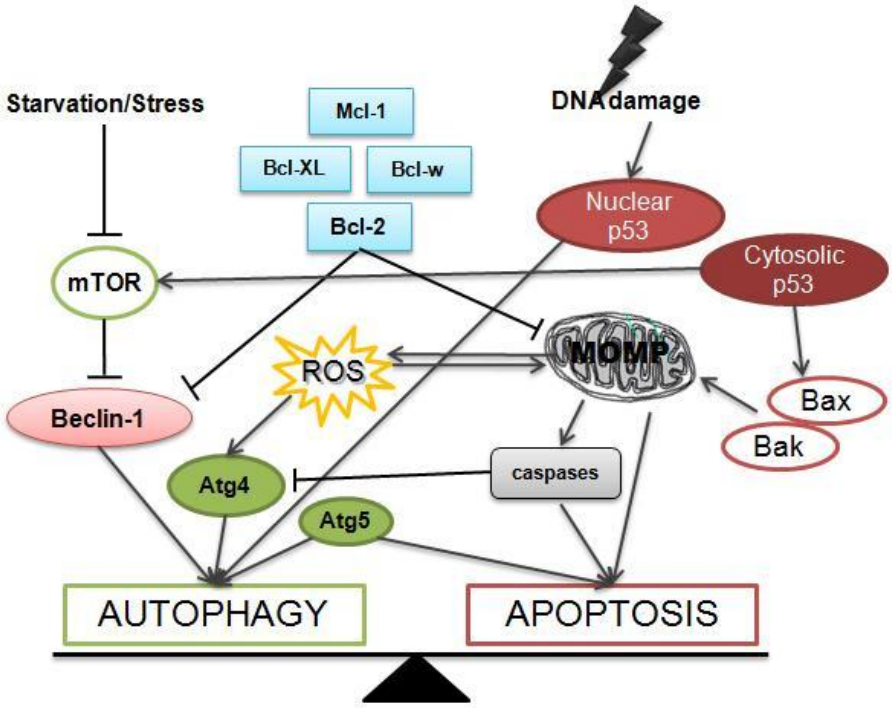

Figure 3. Mechanisms of crosstalk between autophagy and apoptosis. Bcl-2 is over-expressed in many cancers and mediates inhibition of both autophagy and apoptosis, indicating that inhibition of autophagy promotes tumorigenesis. Tumor suppressor p53 activates both pathways in response to cellular stress, suggesting that autophagy induction prevents tumorigenesis. The supposed roles of autophagy in cancer development and resistance to treatment are currently under intense scrutiny.

REACTIVE OXYGEN SPECIES

Reactive oxygen species (ROS) are generated during normal oxidative phosphorylation as a result of improper or incomplete electron transfer by complexes I, and III of the MRC (Gogvadze *et al,* 2009). ROS is a collective term that refers to highly reactive molecules such as superoxide anion (O_2•−), hydrogen peroxide (H_2O_2) and hydroxyl radical (OH•) (Fulda *et al,* 2010b). The deleterious effects of these pro-oxidants are managed by an anti-oxidant defence system comprised of catalase and super-oxide dismutase enzymes and glutathione that quench and neutralize ROS (Fulda *et al,* 2010b). While low to moderate amounts of ROS may have beneficial effects on regulation of cell proliferation and gene expression, increased ROS production results in oxidative stress-induced damage to proteins, lipids and DNA, which has implications in diseases including diabetes, Parkinson's disease and cancer (Valko *et al,* 2007; Fulda *et al,* 2010b).

ROS and Apoptosis

Mitochondria are the central players in the intrinsic pathway of apoptosis and are also the major producers of ROS. Mitochondrial permeabilization and cell death can be stimulated by increased ROS production (Ralph *et al,* 2010). ROS reportedly modifies two thiol groups on the ANT, an IM component of the MPTP, which stimulates pore opening and solute influx (Gogvadze *et al,* 2009). Furthermore, mitochondrial release of cytochrome *c* (Cyt *c*) is facilitated by ROS. Cyt *c* is bound to the IM in the IMS by electrostatic and hydrophobic interactions with the mitochondrial phospholipid, cardiolipin. Oxidation of cardiolipin causes release of Cyt *c* to the IMS, allowing it to dissociate through channels formed by Bax/Bak in the OM (MOMP) (Gogvadze *et al,* 2009). Another target of ROS is mitochondrial DNA (mtDNA), which encodes for 13 essential subunits of MRC complexes I, III, IV and V critical for proper oxidative phosphorylation (Chen *et al,* 2009). mtDNA is especially vulnerable to ROS-induced damage due to its close proximity to the source of ROS (MRC complexes) and its lack of protective histones (Valko *et al,* 2007). Moreover, oxidative damage to mtDNA may cause genetic instability and disruption of proper MRC function, leading to elevated ROS production, stimulating a vicious cycle with detrimental effects on the cell (Gogvadze *et al,* 2009).

ROS and Autophagy

Oxidative stress-induced damage to proteins and organelles can induce pro-survival autophagy or autophagic cell death, depending on the extent of the damage (Kroemer *et al,* 2007). Sub-apoptotic stress that causes MMP in only a small fraction of mitochondria induces 'mitophagy', a process of pro-survival autophagy that specifically removes dysfunctional mitochondria (Kroemer *et al,* 2007). However, extensive oxidative stress, causing damage to MRC components and production of even more ROS, is associated with autophagic cell death and apoptosis (Essick and Sam, 2010). ROS induces autophagy by modulating key signalling proteins, such as Beclin-1. Under normal conditions Beclin-1 is negatively regulated by anti-apoptotic Bcl-2 family proteins, but pathological levels of ROS can activate the ubiquitin-proteosome system, leading to activation of Beclin-1 by degradation of Bcl-2 resulting in autophagic cell death (Essick and Sam, 2010).

ROS and Cancer

Oxidative stress is involved in the aging process, and generally one's risk of developing cancer increases with age. Oxidative damage to either nuclear or mitochondrial DNA is implicated in the early steps of carcinogenesis (Valko *et al,* 2007). Depending on the site, oxidative damage to DNA can result in induction or repression of transcription, altered signal transduction and/or replication errors, all of which contribute to genetic instability (Valko *et al,* 2007). Recent studies suggest that tumor cells are under constant stress from their microenvironment, and have increased levels of intracellular ROS (Khandrika *et al,* 2009; Fulda *et al,* 2010b). Prostate cancer in particular is reported to have elevated levels of intracellular ROS and overexpression of NAD(P)H oxidase (Nox), which facilitates NAD(P)H-dependent generation of superoxide anion (O_2•−) and is thought to contribute to tumor growth (Khandrika *et al,* 2009; Graham *et al,* 2010). Further, the p53 tumor suppressor, which is mutated in approximately 50% of human cancers, is a major activator of anti-oxidant defence mechanisms (DeBerardinis, 2008; Olovnikov *et al,* 2009). With respect to its apoptosis-inducing capacity, molecules that promote ROS production may be novel therapeutics, proposed to selectively target cancer cells by elevating ROS levels beyond a tolerable threshold to induce MOMP and cell death (Fulda *et al,* 2010a; Chen *et al,* 2010).

p53 TUMOR SUPPRESSOR

The quintessential tumor suppressor p53 is a transcription factor that regulates mechanisms of DNA damage response, cell cycle arrest, apoptosis, autophagy and metabolism through its nuclear and cytoplasmic functions (Lane, 1992; Green and Kroemer, 2009). Approximately half of all human cancers have inactivating mutations of p53, while the rest have adapted ways to override the tumor suppressor function of p53 (Weinberg, 2007). Under normal conditions, p53 is regulated by the ubiquitin-proteasome system, triggered by p53-mediated transcription of Mdm2. In response to damaging effects of radiation, chemotherapy and/or hypoxia, p53 is phosphorylated by kinases such as ATM, Chk1 and Chk2, which work to stabilize the protein (Weinberg, 2007; Fulda *et al,* 2010b).

The mechanisms of p53-mediated apoptosis are well studied. Activated p53 accumulates in the nucleus to facilitate expression of pro-apoptotic proteins like Bax, puma and noxa (Chipuk and Green, 2006). Interestingly, cytosolic p53 also acts to induce apoptosis in a manner similar to BH3-only proteins; p53 has been shown to bind Bcl-2 and Bcl-XL, as well as Bax and Bak, to induce MOMP (Mihara *et al,* 2003; Gogvadze *et al,* 2008). Puma (Figure 4) is suggested to modulate the cytoplasmic pool of p53 by binding with anti-apoptotic Bcl-2 proteins, thus releasing p53 to activate Bax/Bak (Green and Kroemer, 2009).

The mechanisms of autophagy regulation by p53 are contradictory. The most direct role discovered thus far is the expression of DRAM (damage-regulated autophagy modulator) (Figure 4) by p53 (Crighton *et al,* 2006). DRAM is a lysosomal protein that induces autophagy, is required for p53-induced cell death and is reportedly down-regulated in cancer (Crighton *et al,* 2006). Indirect regulation of autophagy by p53 may involve AMPK (AMP-activated kinase) activation and mTOR inhibition (Olovnikov *et al,* 2009). In response to DNA damage p53 activates AMPK, which serves to maintain the balance of energy (AMP:ATP), leading to inhibition of mTOR and thus induction of autophagy (Buzzai *et al,* 2007; Olovnikov *et al,* 2009). In contrast, reports indicate that cytoplasmic p53 is a strong inhibitor of autophagy, and cells with loss-of-function mutations of p53 show hyperactive autophagy (Tasdemir *et al,* 2008).

Novel functions of p53 in the regulation of glucose metabolism have been discovered that account for the Warburg effect in cancer cells. The recently discovered p53 target gene *TIGAR* (*TP53*-induced glycolysis and apoptosis regulator) (Figure 4)

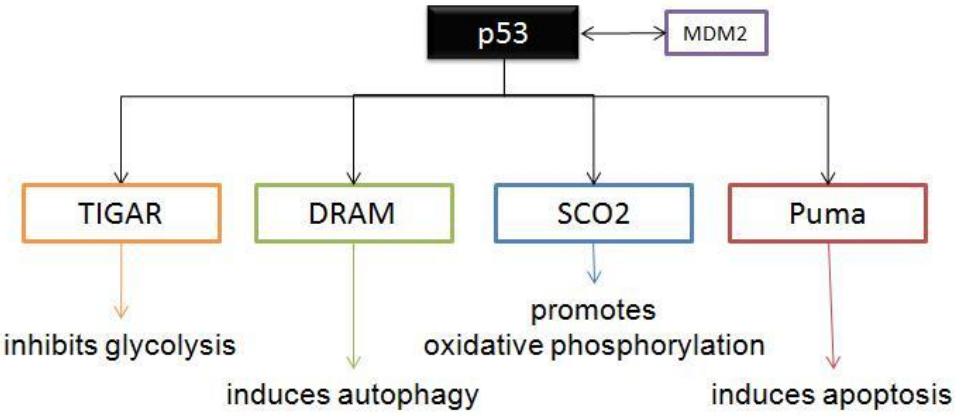

Figure 4. The master regulator p53. In normal physiological conditions, p53 is regulated by Mdm2. In response to stress/damage, p53 coordinates multiple pathways with the overall goal of tumor suppression. The p53 target TIGAR (TP53-induced glycolysis and apoptosis regulator) can block glycolysis at the fructose-6-phosphate step and diverts catabolism of glucose towards the pentose phosphate pathway. The p53 target DRAM (damage-regulated autophagy modulator) can induce pro-survival autophagy or autophagic cell death. SCO2 (synthesis of *cytochrome c* oxidase-2) is activated by basal levels of p53 to promote oxidative phosphorylation. The p53 target puma (p53-upregulated modulator of apoptosis), a BH3-only protein, induces apoptosis by triggering Bax- and Bak-mediated mitochondrial outer membrane permeabilization (MOMP; *not shown*).

encodes a protein that is homologous to the bisphosphatase domain of 6-phosphofructo-2-kinase (Bensaad *et al,* 2006). TIGAR lowers fructose-2,6-bisphosphate levels in cells, effectively inhibiting glycolysis and redirecting glucose catabolism to the pentose phosphate pathway to generate nucleotides needed for DNA repair (Bensaad *et al,* 2006; Green and Chipuk, 2006). Another novel target of p53 is SCO2 (synthesis of *cytochrome c* oxidase-2) (Figure 4), a protein required for proper assembly of MRC complex IV, which is reportedly upregulated by basal levels of p53 (Matoba *et al,* 2006).

Taken together, mutations in p53 contribute to genetic instability, accumulation of damaged proteins and organelles, decreased apoptosis, down-regulation of mitochondrial respiration and increased glycolysis. The recently discovered metabolism-related regulatory roles of p53 provide a clear explanation of factors that support aerobic respiration in cancer cells, originally observed by Otto Warburg in the 1920s.

CURRENT CANCER THERAPY

The current standard of care for cancer is adjuvant chemotherapy that elicits a cell death response, typically by causing damage to the DNA or interfering with its replicative machinery (Chabner and Roberts, 2005). Cancer therapeutic agents are generally categorized as (standard) chemotherapy, targeted therapy or natural products.

Chemotherapy

Standard chemotherapy is used for treatment of advanced stage cancer and is generally administered following surgical resection of the primary tumor mass (adjuvant chemotherapy). Aside from improvements to stability and toxicity, chemotherapy has not dramatically changed since the mid-1970s (Chabner and Roberts, 2005). For instance, the front-line of therapy for advanced colorectal carcinoma, one of the most fatal cancers, is 5-fluorouracil (5-FU), a pyrimidine analogue that inhibits DNA synthesis and has been used to treat cancer for over half a century (Goodwin and Asmis, 2009). Other drugs that have been used for decades against cancer include anti-metabolites like methotrexate, DNA alkylating agents such as cyclophosphamide or cisplatin, anti-mitotics like paclitaxel, and topoisomerase inhibitors like etoposide and camptothecins (Chabner and Roberts, 2005). While their long-track record implies superior utility in the fight against cancer, it belies the serious toxic effects associated with drugs that have such universally-vital targets and is always combined with agents that offer protection of normal cells (Blagosklonny, 2005; Chabner and Roberts, 2005).

Targeted Therapy

Development of targeted therapy resulted from increased understanding of the complex molecular and genetic changes associated with cancer. The first breakthrough targeted therapy was imatinib for the treatment of (Ph+) CML nearly a decade ago, which paved the way for new targeted molecules against other types of cancer (Chabner and Roberts, 2005). Soon after, monoclonal antibodies developed against oncogenic receptor tyrosine kinases (HER-2, Herceptin; EGF-R, Cetuximab) and growth factors (VEGF, Gefitinib) were approved for clinical use (Blagosklonny, 2005; Goodwin and Asmis, 2009). Hormone-dependent cancers can be effectively prevented and treated with endocrine therapy, such as tamoxifen for breast cancer. Tamoxifen is an estrogen-receptor antagonist that has been used in the fight against breast cancer for nearly 30

years (Wang *et al,* 2009). Recent studies indicate that tamoxifen also inhibits components of the MRC, leading to increased ROS production and apoptotic cell death (Parvez *et al,* 2008; Chatterjee *et al,* 2011). These targeted therapies are often used in combination with standard chemotherapy to enhance the cancer cell-killing effect (Goodman and Asmis, 2009; Fizazi *et al,* 2009). Unfortunately, tumors adapt to the selective pressures of targeted therapy, and gain resistance to treatment and metastatic capabilities (Don and Hogg, 2004; Letai, 2008; Fulda *et al,* 2010a).

Natural Products

There has been a recent revival in the development of natural products as anti-cancer agents, based on their historical use in folk, Ayurvedic and traditional Chinese medicine (Deorukhkar *et al,* 2007; Fulda and Kroemer, 2009). Plants and microorganisms are incredible sources of diverse phytochemicals, classified into various families such as alkaloids, flavinoids and isothiocyanates, with potential medicinal properties (Deorukhkar *et al,* 2007). In addition to the well known natural products used as standard chemotherapy, such as paclitaxel (obtained from the bark of the Pacific Yew tree) or etoposide (derived from roots of the mayapple plant), new products that directly target the mitochondria to induce cell death are of current interest (Chen *et al,* 2010; Fulda and Kroemer, 2009; Fulda *et al,* 2010a). Exemplary models of a new class of mitochondrial-targeting anti-cancer agents, called *mitocans*, include the natural products betulinic acid, phenylethyl isothiocyanate, resveratrol and α-tocopheryl succinate, among others (Ralph and Neuzil, 2009; Biasutto *et al,* 2010). Due to the direct-targeted action of these agents on the mitochondria, they may bypass mechanisms of resistance to standard chemotherapy by tipping cancer cells over the 'point-of-no-return' that is mitochondrial outer membrane permeabilization (MOMP).

Natural Mitocans

Betulinic acid (BA) is a natural phytochemical found in various plants worldwide, including white-barked birch trees used by Native Americans as a folk remedy (Fulda and Kroemer, 2009). BA is proposed to induce mitochondrial outer membrane permeabilization (MOMP) and loss of mitochondrial membrane potential (MMP) in a manner that can be inhibited by bongkrekic acid, an inhibitor of the mitochondrial permeability transition pore (MPTP) (Fulda and Kroemer, 2009). It has been speculated

that BA increases ROS production to stimulate loss of MMP; however the mitochondrial target of BA remains unknown (Ralph and Neuzil, 2009). BA is currently under evaluation as a topical agent in phase I/II cancer prevention clinical trials (Fulda and Kroemer, 2009).

Phenylethyl isothiocyanate (PEITC) is found in cruciferous vegetables such as watercress, broccoli and cabbage, and is considered a chemo-preventative agent (Chen *et al,* 2010; Xiao *et al,* 2010). Recent studies show that PEITC inhibits the glutathione (GSH) anti-oxidant system, leading to increased ROS production, MOMP and apoptosis selectively in cancer cells (Xiao *et al,* 2010; Wu *et al* 2010). PEITC is currently being tested in a Phase II cancer prevention clinical trial (Chen *et al,* 2010).

Resveratrol is a flavinoid polyphenol found in the skin of red grapes, wine and blueberries (Deorukhkar *et al,* 2007; Chen *et al,* 2010). Polyphenols are often touted for their anti-oxidant properties, but can also act as pro-oxidants in cancer cells with already elevated levels of intracellular ROS (Biasutto *et al,* 2010). Although multiple possible effects of resveratrol have been reported (Chen *et al,* 2010; Deorukhkar *et al,* 2007), recent studies indicate that resveratrol inhibits synthetic and hydrolytic function of the F_1-ATPase, thereby inhibiting mitochondrial ATP synthesis leading to cell death due to ROS over-production (Fulda *et al,* 2010a; Ralph and Neuzil, 2009). Resveratrol is currently undergoing phase II clinical trials against colorectal cancer (Chen *et al,* 2010).

Alpha-tocopheryl succinate (α-TOS) is a vitamin E analogue that has been shown to target the ubiquinone-binding site on MRC complex II, preferentially in cancer cell mitochondria, triggering increased ROS production (Dong *et al,* 2009). Interestingly, mtDNA-deficient cells resisted the effect of α -TOS, defining the mitochondria as a crucial component for its anti-cancer activity (Fulda *et al,* 2010a). Furthermore, studies indicate that α-TOS is deprotonated at neutral pH, but becomes significantly more protonated in the acidic tumor microenvironment, resulting in enhanced uptake and activity in cancer cells (Biasutto *et al,* 2010). Alpha-TOS is currently in pre-clinical development (Chen *et al,* 2010). Together, these studies showcase the potential of natural products as anti-cancer agents that induce apoptosis specifically in cancer cells by directly acting on the mitochondria.

PANCRATISTATIN

Pancratistatin is an *Amaryllidaceae* alkaloid isolated from the bulbs of the Hawaiian spider lily (*Hymenocallis littoralis*) (Pettit *et al,* 1993). Extracts from the *Amaryllidaceae* family of plants have been used in folk medicine for the management of cancer and other ailments dating back centuries (Pettit *et al,* 1993; Kornienko and Evidente, 2008). Recent research efforts have focused on pancratistatin, narciclasine and related constituents (Figure 5), which are considered the most important metabolites responsible for the therapeutic benefits of these plants (Kornienko and Evidente, 2008). Studies from our laboratory indicate that pancratistatin induces loss of MMP and increased ROS production, leading to apoptosis in several different types of cancer including colon, prostate and breast carcinomas, leukemia, melanoma and glioblastoma, with minimal toxicity to non-cancerous counterpart cells (Griffin *et al,* 2010; Griffin *et al,* 2011a; Griffin *et al,* 2011b; Siedlakowski *et al,* 2008; Chatterjee *et al,* 2011). It has been shown that pancratistatin does not target the DNA or have anti-mitotic properties (like other natural products, e.g., anthracyclines, taxanes, vinca alkaloids); however, the target of pancratistatin remains elusive (Kekre *et al,* 2005; Griffin *et al,* 2011a). The high medicinal potential of this alkaloid, and the time-consuming and expensive multi-step process of extraction from the natural source, have fuelled major efforts to produce pancratistatin using a biosynthetic approach (McNulty *et al,* 2008; Pettit *et al,* 1993; Rinner *et al,* 2004a).

Other Amaryllidaceae Alkaloids

Lycorine was the first alkaloid isolated from bulbs of the *Amaryllidaceae* family of plants; its anti-tumor properties were being studied nearly 40 years before the more oxygenated constituents (Figure 5) were identified (Hudlicky *et al,* 2002). Lycorine reportedly has anti-tumor, anti-viral, anti-malarial and anti-inflammatory effects, and may also inhibit ascorbic acid biosynthesis (Liu *et al,* 2009). Recent studies indicate that lycorine activates caspase-3, 8 and 9, and also modulates the expression of anti-apoptotic Bcl-2 family member, Mcl-1, leading to apoptosis in leukemia cells (Liu *et al,* 2004; Liu *et al,* 2009).

Narciclasine, lycoricidine (also referred to as 7-deoxynarciclasine in literature) and 7-deoxypancratistatin are all natural *Amaryllidaceae* alkaloids of the same type as

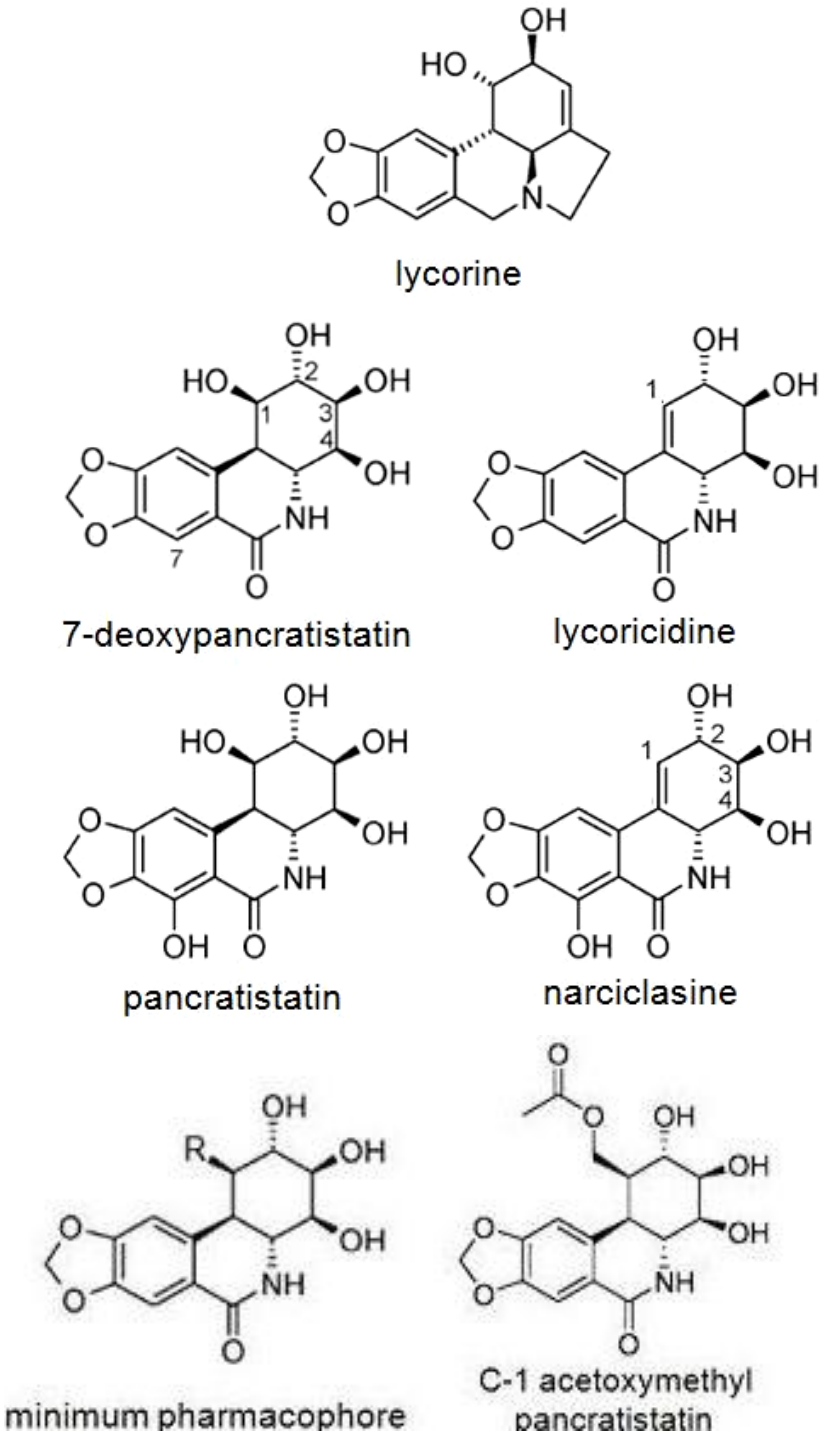

Figure 5. Representative members of the *Amaryllidaceae* family of alkaloids, the minimum pharmacophore and a recently synthesized derivative with comparable activity.

pancratistatin (McNulty *et al,* 2008). To date, the majority of reports on lycoricidine and 7-deoxypancratistatin detail various approaches for their synthesis, with little focus on biological activity. These compounds lack the free phenolic hydroxyl group (at C-7) that the more oxygenated forms (pancratistatin and narciclasine) possess, which accounts for their higher (10-fold or more) biological activity, i.e., anti-tumor and anti-viral (Rinner *et al,* 2004b). Narciclasine, isolated from the bulbs of different varieties of daffodil (*Narcissus*), is known to modulate plant growth; florists know that arranging fresh-cut daffodils in a vase with other flowers will have a negative effect on their appearance and will significantly shorten their vase-life (Kornienko and Evidente, 2008). Recent studies suggest that, at nanomolar concentrations, narciclasine suppresses growth and proliferation of glioblastoma multiforme cancer cells by inhibiting protein synthesis pathways (LeFranc *et al,* 2009; Van Goietsenoven *et al,* 2010). Earlier studies reported that, at pharmacologic doses (micromolar range), narciclasine induces apoptosis in breast and prostate cancer cells, characterized by cytochrome *c* release from the mitochondria and caspase activation (Dumont *et al,* 2007).

Synthetic Derivatives

Targeted design and synthesis of *Amaryllidaceae* constituents has been driven by their historical medicinal properties, the complex extraction process and limited yield of these compounds from their natural sources (McNulty *et al,* 2008; Pettit *et al,* 1993; Rinner *et al,* 2004a). Numerous synthetic derivatives of native pancratistatin have been subject to SAR (structure-activity relationship)-based screening efforts, which helped to identify the minimally active anti-cancer pharmacophore of pancratistatin (Griffin *et al,* 2007; McNulty *et al,* 2008). Recently, SAR-based screening of 7-deoxypancratistatin derivatives has revealed, for the first time, a C-1 acetoxymethyl derivative with promising anti-cancer activity comparable to that of native pancratistatin (Collins *et al,* 2010).

Despite the historical medical usage of *Amaryllidaceae* alkaloids and the extensive research efforts on pancratistatin and its congeners, these compounds have not yet advanced to clinical trials for the treatment of human cancers (Hudlicky *et al,* 2002; Kornienko and Evidente, 2008; Collins *et al,* 2010). Identification of the site and mechanism of action of pancratistatin will provide crucial information required for advancement to clinical application.

HYPOTHESIS and OBJECTIVES

This research aims to determine the efficacy and selectivity of pancratistatin and to elucidate its mechanism of action using *in vitro*, *ex vivo* and *in vivo* models of leukemia, colon and/or prostate cancer. Our working hypothesis is that pancratistatin targets the mitochondria of cancer cells to induce apoptosis with minimal effect on non-cancerous cells or tissues, and thus would improve cancer patient outcomes if used in the clinical treatment of human cancer.

This hypothesis will be tested through the following objectives:

- Evaluate the efficacy and selectivity of pancratistatin on cultured and patient-obtained leukemia models
- Determine the mechanism of action and anti-tumor efficacy of pancratistatin in colon and prostate cancer using *in vitro* and *in vivo* models
- Assess the biological activity of synthetic derivatives of pancratistatin compared to the native natural structure

Results obtained through this study will identify the molecular effects of treatment with pancratistatin and synthetic derivatives on cancer cells, and provide rationale for pharmaceutical development of pancratistatin, or active synthetic analogues, and progression to clinical trials.

REFERENCES

Alirol E, Martinou JC. Mitochondria and cancer: is there a morphological connection? Oncogene 2006; 25: 4706-4716.

Armstrong JS. Mitochondria: a target for cancer therapy. Br J Pharmacol 2006; 147: 239-248.

Bensaad K, Tsuruta A, Selak MA, *et al*. TIGAR, a p53-inducible regulator of glycolysis and apoptosis. Cell 2006; 126: 107-120.

Biasutto L, Dong LF, Zoratti M, Neuzil J. Mitochondrially targeted anti-cancer agents. Mitochondrion 2010; 10: 670–681.

Billen LP, Shamas-Din A, Andrews DW. Bid: a Bax-like BH3 protein. Oncogene 2008; 27(S1): S93-S104.

Blagosklonny MV. How cancer could be cured by 2015. Cell Cycle 2005; 4(2): 269-278.

Bouchier-Hayes L, Lartigue L, Newmeyer DD. Mitochondria: pharmacological manipulation of cell death. J Clin Invest 2005; 115(10): 2640-2647.

Brenner D, Mak TW. Mitochondrial cell death effectors. Curr Opin Cell Biol 2009; 21(6): 871-877.

Buzzai M, Jones RG, Amaravadi RK, *et al*. Systemic treatment with the antidiabetic drug metformin selectively impairs p53-deficient tumor cell growth. Cancer Res 2007; 67 (14): 6745-6752.

Canadian Cancer Society's Steering Committee: Canadian Cancer Statistics 2010. Toronto: Canadian Cancer Society, 2010. April 2010, ISSN 0835-2976.

Chabner BA, Roberts TG. Timeline: Chemotherapy and the war on cancer. Nat Rev Cancer 2005; 5(1): 65-72.

Chatterjee SJ, McNulty J, Pandey S. Sensitization of human melanoma cells by tamoxifen to apoptosis induction by pancratistatin, a nongenotoxic natural compound. Melanoma Res 2011. 2010 Mar 17 [Epub ahead of print].

Chen G, Wang F, Trachootham D, Huang P. Preferential killing of cancer cells with mitochondrial dysfunction by natural compounds. Mitochondrion 2010; 10(6): 614-625.

Chen JQ, Cammarata PR, Baines CP, Yager JD. Regulation of mitochondrial respiratory chain biogenesis by estrogens/estrogen receptors and physiological, pathological and pharmacological implications. Biochim Biophys Acta 2009; 1793(10): 1540-1570.

Chipuk JE, Green DR. Dissecting p53-dependent apoptosis. Cell Death Diff 2006; 13: 994–1002.

Chokkalingam AP, Buffler PA. Genetic susceptibility to childhood leukaemia. Radiat Prot Dosimetry 2008; 132(2): 119-129.

Collins J, Rinner U, Moser M, *et al*. Chemoenzymatic synthesis of Amaryllidaceae constituents and biological evaluation of their C-1 analogues. The next generation synthesis of 7-deoxypancratistatin and trans-dihydrolycoricidine. J Org Chem 2010; 75(9): 3069-3084.

Constantinou C, Papas KA, Constantinou AI. Caspase-indpendent pathways of programmed cell death: the unravelling of new targets of cancer therapy? Curr Cancer Drug Targets 2009; 9: 717-728.

Crighton D, Wilkinson S, O'Prey J, *et al*. DRAM, a p53-induced modulator of autophagy, is critical for apoptosis. Cell 2006; 126(1): 121-134.

Dalby KN, Tekedereli I, Lopez-Berenstein G, Ozpolat B. Targeting the prodeath and prosurvival functions of autophagy as novel therapeutic strategies in cancer. Autophagy 2010; 6(3): 322-329.

DeBerardinis RJ. Is cancer a disease of abnormal cellular metabolism? New angles on an old idea. Genet Med 2008; 10(11): 767-777.

Deorukhkar A, Krishnan S, Sethi G, Aggarwal BB. Back to basics: how natural products can provide the basis for new therapeutics. Expert Opin Investig Drugs 2007; 16(11): 1753-1773.

DiPaola RS, Dvorzhinski D, Thalasila A, Garikapaty V, Doram D, May M, *et al*. Therapeutic starvation and autophagy in prostate cancer: a new paradigm for targeting metabolism in cancer therapy. Prostate 2008; 68(16): 1743-1752.

Don AS, Hogg PJ. Mitochondria as cancer drug targets. Trends Mol Med 2004; 10(8): 372-378.

Dong LF, Freeman R, Liu J, *et al*. Suppression of tumor growth in vivo by the mitocan alpha-tocopheryl succinate requires respiratory complex II. Clin Cancer Res 2009; 15(5): 1593-1600.

Druker BJ. Translation of the Philadelphia chromosome into therapy for CML. Blood 2008; 112(13): 4808-4817.

Dumont P, Ingrassia L, Rouzeau S, *et al*. The Amaryllidaceae isocarbostyril narciclasine induces apoptosis by activation of the death receptor and/or mitochondrial pathways in cancer cells but not in normal fibroblasts. Neoplasia 2007; 9(9): 766-776.

Essick EE, Sam F. Oxidative stress and autophagy in cardiac disease, neurological disorders, aging and cancer. Oxid Med Cell Longev 2010; 3(3): 168-177.

Fearon ER, Vogelstein B. A genetic model for colorectal tumorigenesis. Cell 1990; 61(5): 759-767.

Fimia GM, Piacentini M. Regulation of autophagy in mammals and its interplay with apoptosis. Cell Mol Life Sci 2010; 67: 1581–1588.

Fizazi K, Sternberg CN, Fitzpatrick JM, Watson RW, Tabesh M. Role of targeted therapy in the treatment of advanced prostate cancer. BJU Int 2010; 105(6): 748-767.

Fulda S, Galluzzi L, Kroemer G. Targeting mitochondria for cancer therapy. Nat Rev Drug Discov 2010(**a**); 9(6): 447-464.

Fulda S, Gorman AM, Hori O, Samali A. Cellular stress responses: Cell survival and cell death. Int J Cell Biol 2010(**b**); 2010(214074): 1-23.

Fulda S, Kroemer G. Targeting mitochondrial apoptosis by betulinic acid in human cancers. Drug Discov Today 2009; 14(17-18): 885-890.

Fulda S. Tumor resistance to apoptosis. Int J Cancer 2009; 124: 511-515.

Giménez-Bonafé P, Tortosa A, Pérez-Tomás R. Overcoming drug resistance by enhancing apoptosis of tumor cells. *Curr Cancer Drug Targets* 2009; 9(3): 320-340.

Gogvadze V, Orrenius S, Zhivotovsky B. Mitochondria as targets for chemotherapy. Apoptosis 2009; 14: 624-640.

Gogvadze V, Orrenius S, Zhivotovsky B. Mitochondria in cancer cells: what is so special about them? Trends Cell Biol 2008; 18(4): 165-173.

Goodwin RA, Asmis TR. Overview of Systemic Therapy for Colorectal Cancer. Clin Colon Rectal Surg 2009; 22(4): 251–256.

Graham KA, Kulawiec M, Owens KM, Li X, Desouki MM, Chandra D, Singh KK. NADPH oxidase 4 is an oncoprotein localized to mitochondria. Cancer Biol Ther 2010; 10(3): 223-231.

Green DR, Chipuk JE. P53 and metabolism: inside the TIGAR. Cell 2006; 126: 30-32.

Green DR, Evan GI. A matter of life and death. Cancer Cell 2002; 1: 19-30.

Green DR, Kroemer G. Cytoplasmic functions of the tumor suppressor p53. Nature 2009; 458(7242): 1127-1130.

Griffin C, Hamm C, McNulty J, Pandey S. Pancratistatin induces apoptosis in clinical leukemia samples with minimal effect on non-cancerous peripheral blood mononuclear cells. Cancer Cell Int 2010; 10: 6.

Griffin C, Karnik A, McNulty J, Pandey S. Pancratistatin selectively targets cancer cell mitochondria and reduces growth of human colon tumor xenografts. Mol Can Ther 2011a; 10(1): 57-68

Griffin C, McNulty J, Pandey S. Pancratistatin induces apoptosis and autophagy in metastatic prostate cancer cells. 2011b [Accepted in Int J Oncol].

Griffin C, Sharda N, Sood D, Nair J, McNulty J, Pandey S. Selective cytotoxicity of pancratistatin-related natural Amaryllidaceae alkaloids: evaluation of the activity of two new compounds. Cancer Cell Int 2007; 7: 10.

Halestrap AP, McStay GP, Clarke SJ. The permeability transition pore complex: another view. Biochimie 2002; 84: 153-166.

Hanahan D, Weinberg RA. The hallmarks of cancer. Cell 2000; 100: 57-70.

Harris N, Jaffe E, Diebold J, *et al*. The World Health Organization classification of neoplastic diseases of the hematopoietic and lymphoid tissues. Ann Oncol 1999; 10 (12): 1419–1432.

Hockenbery DM. Targeting mitochondria for cancer therapy. Environ Mol Mutagen 2010; 51(5): 476-489.

Hudlicky T, Rinner U, Gonzalez D, *et al*. Total synthesis and biological evaluation of Amaryllidaceae alkaloids: narciclasine, ent-7-deoxypancratistatin, regioisomer of 7-deoxypancratistatin, 10b-epi-deoxypancratistatin, and truncated derivatives. J Org Chem 2002; 67(25): 8726-8743.

Jemal A, Siegel R, Xu J, Ward E. Cancer statistics, 2010. CA Cancer J Clin 2010; 60(5): 277-300.

Kaelin WG, Thompson CB. Cancer: Clues from cell metabolism. Nature Q&A 2010; 465: 562-564.

Kekre N, Griffin C, McNulty J, Pandey S. Pancratistatin causes early activation of caspase-3 and the flipping of phosphatidyl serine followed by rapid apoptosis

specifically in human lymphoma cells. Cancer Chemother Pharmacol 2005; 56(1): 29-38.

Kerr JF, Wyllie AH, Currie AR. Apoptosis: a basic biological phenomenon with wide-ranging implications in tissue kinetics. Br J Cancer 1972; 26: 239-257.

Khandrika L, Kumar B, Koul S, Maroni P, Koul HK. Oxidative stress in prostate cancer. Cancer Lett 2009; 282(2): 125-136.

Kinnally KW and Antonsson B. A tale of two mitochondrial channels, MAC and PTP, in apoptosis. Apoptosis 2007; 12: 857-868.

Knudson AG. Two genetic hits (more or less) to cancer. Nature Rev Cancer 2001; 1: 157-162.

Kornienko A, Evidente A. Chemistry, biology, and medicinal potential of narciclasine and its congeners. Chem Rev 2008; 108: 1982–2014.

Kroemer G, Galluzzi L, Brenner C. Mitochondrial membrane permeabilization in cell death. Physiol Rev 2007; 87: 99-163.

Lane DP. Cancer. p53, guardian of the genome. Nature 1992; 358(6381): 15-16.

Lefranc F, Sauvage S, Van Goietsenoven G, *et al*. Narciclasine, a plant growth modulator, activates Rho and stress fibers in glioblastoma cells. Mol Cancer Ther 2009; 8(7): 1739-1750.

Lehninger AL, Nelson DL, Cox MM. Principles of Biochemistry. WH Freeman & Company, 3rd Edition, 2000. Pgs. 225-227.

Letai AG. Diagnosing and exploiting cancer's addiction to blocks in apoptosis. Nat Rev Cancer 2008; 8(2): 121-132.

Levine B. Cell biology: Autophagy and cancer. Nature Q&A 2007; 446: 745-747.

Liu J, Hu WX, He LF, Ye M, Li Y. Effects of lycorine on HL-60 cells via arresting cell cycle and inducing apoptosis. FEBS Lett 2004; 578(3): 245-250.

Liu XS, Jiang J, Jiao XY, Wu YE, Lin JH, Cai YM. Lycorine induces apoptosis and down-regulation of Mcl-1 in human leukemia cells. Cancer Lett 2009; 274(1): 16-24.

Mathupala SP, Ko YH, Pedersen PL. The pivotal roles of mitochondria in cancer: Warburg and beyond and encouraging prospects for effective therapies. Biochim Biophys Acta 2010; 1797(6-7): 1225-1230.

Matoba S, Kang JG, Patino WD, *et al*. p 53 regulates mitochondrial respiration. Science 2006; 312: 1650-1653.

McNulty J, Nair JJ, Griffin C, Pandey S. Synthesis and biological evaluation of fully functionalized seco-pancratistatin analogues. J Nat Prod 2008; 71(3): 357-363.

Mihara M, Erster S, Zaika A, *et al*. p53 has a direct apoptogenic role at the mitochondria. Mol Cell 2003; 11(3): 577-590.

Millan A, Huerta S. Apoptosis-inducing factor and colon cancer. J Surg Res 2009; 151: 163-170.

Modica-Napolitano JS, Singh KK. Mitochondria as targets for detection and treatment of cancer. Expert Rev Mol Med 2002; 4(9): 1-19.

Nieto M, Finn S, Loda M, Hahn WC. Prostate cancer: Re-focusing on androgen receptor signaling. Int J Biochem Cell Biol 2007; 39(9): 1562-1568.

Nijsten MWN, van Dam GM. Hypothesis: Using the Warburg effect against cancer by

reducing glucose and providing lactate. Med Hypotheses 2009; 73: 48-51.

Olovnikov IA, Kravchenkoa JE, Chumakov PM. Homeostatic functions of the p53 tumor suppressor: Regulation of energy metabolism and antioxidant defence. Sem Can Biol 2009; 19: 32-41.

Parvez S, Tabassum H, Banerjee BD, Raisuddin S. Taurine prevents tamoxifen-induced mitochondrial oxidative damage in mice. Basic Clin Pharmacol Toxicol 2008; 102(4): 382-387.

Pettit GR, Pettit GR III, Backhaus RA, Boyd MR, Meerow, AW. Antineoplastic Agents 256. Cell Growth Inhibitory Isocarbostyrils from *Hymenocallis*. J Nat Prod 1993; 56: 1682.

Pradelli LA, Beneteau M, Ricci JE. Mitochondrial control of caspase-dependent and -independent cell death. Cell Mol Life Sci 2010; 67: 1589-1597.

Qadir MA, Kwok B, Dragowska WH, To KH, Le D, Bally MB, Gorski SM. Macroautophagy inhibition sensitizes tamoxifen-resistant breast cancer cells and enhances mitochondrial depolarization. Breast Cancer Res Treat 2008; 112: 389–403.

Radhakrishnan S, Miranda E, Ekblad M, Holford A, Pizarro MT, Lemoine NR, Hallde G. Efficacy of oncolytic mutants targeting prb and p53 pathways is synergistically enhanced when combined with cytotoxic drugs in prostate cancer cells and tumor xenografts. Hum Gene Ther 2010; 21: 1311–1325.

Ralph SJ, Neuzil J. Mitochondria as targets for cancer therapy. Mol Nutr Food Res 2009; 53: 9-28.

Ralph SJ, Rodríguez-Enríquez S, Neuzil J, Moreno-Sánchez R. Bioenergetic pathways in tumor mitochondria as targets for cancer therapy and the importance of the ROS-induced apoptotic trigger. Mol Aspects Med 2010; 31(1): 29-59.

Reed JC. Mechanisms of apoptosis. Am J Pathol 2000; 157(5); 1415-1430.

Rinner U, Hillebrenner HL, Adams DR, Hudlicky T, Pettit GR. Synthesis and biological activity of some structural modifications of pancratistatin. Bioorg Med Chem Lett 2004(**a**); 14(11): 2911-2915.

Rinner U, Hudlicky T, Gordon H, Pettit GR. A beta-carboline-1-one mimic of the anticancer Amaryllidaceae constituent pancratistatin: synthesis and biological evaluation. Angew Chem Int Ed Engl 2004(**b**); 43(40): 5342-5346.

Robey IF, Baggett BK, Kirkpatrick ND, Roe DJ, Dosescu J, Sloane BF, *et al*. Bicarbonate increases tumor pH and inhibits spontaneous metastases. Cancer Res 2009; 69: 2260–2268.

Sasaki K, Tsuno NH, Sunami E, Tsurita G, Kawai K, Okaji Y, *et al*. Chloroquine potentiates the anti-cancer effect of 5-fluorouracil on colon cancer cells. BMC Cancer 2010; 10: 370.

Siedlakowski P, McLachlan-Burgess A, Griffin C, Tirumalai SS, McNulty J, Pandey S. Synergy of pancratistatin and Tamoxifen on breast cancer cells in inducing apoptosis by targeting mitochondria. Cancer Biol Ther 2008; 7(3): 376-384.

Tasdemir E, Maiuri MC, Galluzzi L, *et al*. Regulation of autophagy by cytoplasmic p53. Nat Cell Biol 2008; 10: 676-687.

Ullén A, Farnebo M, Thyrell L, Mahmoudi S, Kharaziha P, Lennartsson L, *et al*. Sorafenib induces apoptosis and autophagy in prostate cancer cells in vitro. Int J Oncol 2010; 37(1): 15-20.

Valko M, Leibfritz D, Moncol J, Cronin MT, Mazur M, Telser J. Free radicals and antioxidants in normal physiological functions and human disease. Int J Biochem Cell Biol 2007; 39(1): 44-84.

Van Goietsenoven G, Hutton J, Becker JP, *et al*. Targeting of eEF1A with Amaryllidaceae isocarbostyrils as a strategy to combat melanomas. FASEB J 2010; 24(11): 4575-4584.

Wang T, You Q, Huang FS, Xiang H. Recent advances in selective estrogen receptor modulators for breast cancer. Mini Rev Med Chem. 2009; 9(10): 1191-1201.

Warburg O. On respiratory impairment in cancer cells. Science 1956; 124: 269-270.

Weinberg RA. The biology of cancer. Garland Science Taylor & Francis Group, LLC, 2007. Pgs. 26-39; 310-323.

Worthley DL, Leggett BA. Colorectal cancer: molecular features and clinical opportunities. Clin Biochem Rev 2010; 31(2): 31-38.

Wu X, Zhu Y, Yan H, *et al*. Isothiocyanates induce oxidative stress and suppress the metastasis potential of human non-small cell lung cancer cells. BMC Cancer 2010; 10: 269.

Xiao D, Powolny AA, Moura MB, *et al*. Phenethyl isothiocyanate inhibits oxidative phosphorylation to trigger reactive oxygen species-mediated death of human prostate cancer cells. J Biol Chem 2010; 285(34): 26558-26569.

CHAPTER 2

Pancratistatin causes early activation of caspase-3 and the flipping of phosphatidyl serine followed by rapid apoptosis specifically in human lymphoma cells

BACKGROUND

Despite an extensive research effort to conquer cancer, this disease remains largely irremediable. The research effort towards cancer has become centralized around the mechanism of apoptosis since its discovery (Kerr *et al,* 1972). Apoptosis is a physiological process involving a cell suicide program that is essential in normal development and tissue homeostasis (Corcoran *et al,* 1994; Green *et al,* 1998). This process is characterized by cell shrinkage and nuclear condensation (Jaattela, 2002). The biochemical pathways involved in apoptosis offer a variety of targets for inducing the cell suicide program that eliminates cancer cells. Several research groups have been successful in inducing apoptosis by targeting specific components of the cell (Hu and Kavanagh, 2003). Most of the currently used anti-cancer treatments, including chemotherapeutics and radiotherapies, are capable of triggering apoptotic cell death in cancer cells by causing DNA damage. Unfortunately, these treatments come with the consequence of causing toxicity to normal cells due to the fact that cancer cells tend to differ from normal cells in their DNA replication mechanism and rate of proliferation. For example, etoposide (Vp-16), a topoisomerase II inhibitor, is known to be a genotoxic anti-cancer drug (Boose and Stopper, 2000) that may exhibit this toxicity against normal cells. This damage to normal cells is most relevant in the recurrence of cancer in patients because mutations caused by these therapies may predispose normal cells to become cancerous. There are very few anti-cancer drugs that are capable of targeting receptors or other components of the cell without producing any genotoxic effects.

Current therapies thought to be non-genotoxic include paclitaxel and tamoxifen (Abal *et al,* 2003; Bursch *et al,* 1996). Since the discovery of the potent anti-cancer activity of the natural product paclitaxel, scientific efforts have been made to find other natural products capable of specifically targeting cancerous cells. Although it was believed that paclitaxel induces non-genotoxic apoptosis by stabilizing tubulin, it has only recently been shown to be genotoxic (Cunha *et al,* 2001). Recently, natural products such as N-thiolated β-lactam and a labdane diterpene have been found to specifically target cancer cells in inducing apoptosis. However, the concentrations of these compounds required to induce apoptosis are high and their toxicity against normal blood cells is not known (Kazi *et al,* 2004; Souza-Fagundes *et al,* 2003). Pancratistatin is a natural compound first isolated in 1992 from the spider lily (Pettit *et al,* 1993). It has been shown to have anti-neoplastic and cytostatic activity (Luduena *et al,* 1992; Pettit *et al,*

1993), but its biochemical mechanism of action is still unknown. The critical evaluation of the specificity and efficacy of pancratistatin in targeting cancer cells and its toxicity against normal noncancerous cells are yet to be established.

In the present work, we evaluated the efficacy of pancratistatin in inducing apoptosis in Human lymphoma (Jurkat) cells and its effect on normal non-cancerous mononculeated blood cells. Since blood is one of the body's first lines of defense and all blood cells get exposed to any drug administered, it was important for us to determine the toxicity of pancratistatin against normal nucleated blood cells (lymphocytes).We report an interesting and exciting finding that pancratistatin is capable of effectively inducing apoptosis specifically in cancerous cells within a short period of time at a very low concentration. Interestingly, in all experiments, no toxic effect of pancratistatin treatment was found in normal blood cells. More importantly, no DNA damage was detected following pancratistatin treatment of these cells. On the other hand, Vp-16 was clearly genotoxic to cancerous as well as normal blood cells. We further studied the mechanism of action of pancratistatin by investigating the effects of pancratistatin on caspase-3 activation, ROS production and DNA damage by sensitive procedures. The results of these experiments were further compared with those of experiments with the currently used chemotherapeutic agent, Vp-16. An interesting observation made with regard to the mechanism of action of pancratistatin in cancer cells was the rapid activation of caspase-3 and flipping of phosphatidylserine to the outer leaflet of the plasma membrane in the pathway of apoptosis. These results collectively suggest that pancratistatin could be a very effective and nontoxic alternative for anti-cancer therapy.

METHODS

Cell cultures

A human lymphoma cell line (Jurkat cells) was purchased from ATCC (Manassas VA). These cells were grown and maintained in an incubator set at 37°C with an atmosphere containing 5% CO_2 and of 95% humidity. These cells were cultured in RPMI-1640 medium supplemented with 10% fetal bovine serum (FBS) and 40 µg/ml gentamicin (Life Technologies, Mississauga ON). Human nucleated blood cells were purified from whole blood obtained from healthy male and female volunteers as approved by the University of Windsor ethical committee, REB# 04-060. Whole blood (7 ml) was collected into a BD Vacutainer CPT Tube (Cell Preparation Tube) obtained from Becton Dickinson (Franklin Lakes NJ). The whole blood was centrifuged in a table-top low-speed centrifuge at 500 x *g* for 30 min at 25°C. The red blood cells went through the polyester gel and the top layer containing mononuclear cells, platelets and plasma was collected. These cells were kept in the same incubator as the Jurkat cells (37°C, 5% CO_2 and 95% humidity).

Cell treatment

For the induction of apoptosis by treatment with pancratistatin, Jurkat cells were grown to 70% confluence and then treated for varying periods of time. Pancratistatin was isolated from Hymenocallis following the literature scheme (99% pure) (Pettit *et al,* 1993). Jurkat cells were directly treated with pancratistatin at a concentration of 1 µM or as indicated. Normal nucleated blood cells were treated in a similar manner after being purified from whole blood. In a parallel set of separate experiments involving Vp-16 treatments, Vp-16 (Sigma Chemical Company, Mississauga, Ontario) was also directly added to the culture medium, but to a final concentration of 10 µM (which is the concentration currently used clinically).

Cellular staining and viability assay

To examine the viability of Jurkat cells after treatment, a cell suspension was added to 20 µl of 0.4% Trypan Blue dye (Life Technologies). Using a hemocytometer (Fisher Scientific), both dead (Trypan blue-positive) and live cells were counted four times. The results were then calculated and tabulated as percentage of dead cells using Microsoft Excel 6.0 software. To examine apoptotic morphology changes, the Jurkat

cells and lymphocytes were grown and treated, and then stained with cell-permeable Hoechst 33342 (Molecular Probes, Eugene OR) at a final concentration of 10 µM and incubated for 5 min at 37°C. The cells were then examined under a fluorescent microscope (Leica DM IRB, Germany) and both phase-contrast and fluorescent pictures were taken. Five fields with at least 100 cells/field were used to count apoptotic versus live cells (where brightly stained cells with condensed nuclei were considered apoptotic). These results were then calculated and tabulated as percentage of apoptotic cells using Microsoft Excel 6.0 software. The pictures at higher magnification were compiled using Adobe Photoshop 7.0 software.

Comet assay

The comet assay was performed using a slight modification of a previously published method (Naderi *et al,* 2003). Briefly, the slides were pre-coated with 0.10% agarose and left to dry for at least 30 min. The desired cell suspension was added to 50 µl of 0.75% warm low-melting point agarose and immediately spread over the pre-coated slide. The slides were placed at 4°C for 5 min to solidify, and then immersed in cold lysis buffer (2.5 mM NaCl, 100 mM Na2EDTA, 10 mM Tris at pH 10, 1% Triton X-100, 10% DMSO) for 1 h at 4°C. Following incubation, slides were washed in alkaline electrophoresis buffer (0.3 M NaOH and 1 mM Na_2EDTA at pH >13). The DNA was electrophoresed at 300 mA for 30 min, washed in neutralizing buffer (0.4 M Tris, pH 7.5) and stained with 10 µM Hoechst 33342. The cells were examined under a fluorescent microscope (Leica DM IRB) and fluorescence pictures were taken. All pictures were processed using Adobe Photoshop 7.0 software.

Annexin-V binding assay

After treating Jurkat cells and lymphocytes, the Annexin-V binding assay was conducted using a purchased kit and the manufacturer's protocol (Cat. No. A13201, Molecular Probes). After treatment, cells were washed in phosphate-buffered saline (PBS) and resuspended in Annexin-V binding buffer (10 mM HEPES/NaOH pH 7.5, 140 mM NaCl, 2.5 mM $CaCl_2$), containing 1:50 Annexin-V AlexaFluor 488 conjugate for 15 min at 25°C. Cells were then examined under a fluorescent microscope (Leica DM IRB), and fluorescence pictures were taken. All pictures were processed using Adobe Photoshop 7.0 software.

Caspase-3 activity

The caspase-3 assay was performed using a previously published method (Naderi *et al,* 2003). To determine the caspase-3 activity, the total protein from Jurkat or lymphocyte cell lysates was incubated with a fluorogenic substrate (DEVD-AFC), a tetrapeptide sequence corresponding to the substrate cleavage site. The caspase assay was carried out according to the manufacturer's protocol (Enzyme System Products, USA). The fluorescence was measured at an excitation wavelength of 400 nm and emission wavelength of 505 nm using a Spectra Max Gemini XS (Molecular Devices, Sunnyvale CA). Caspase-3 activity was calculated per microgram of protein, and protein concentration was determined with BioRad protein assay reagent (BioRad, Mississauga ON) using bovine serum albumin as a standard. Microsoft Excel 6.0 software was used for data representation and statistical analysis.

Mitochondrial membrane potential

Control and treated Jurkat cells were stained with 0.5 µM Mitotracker CM-XH2-Ros dye (Molecular Probes) to determine mitochondrial membrane potential. After 30 min at 37°C, Jurkat cells were centrifuged and resuspended in PBS. The cells were examined under a fluorescent microscope (Leica DM IRB). Fluorescence pictures were taken; all pictures were processed using Adobe Photoshop 7.0 software.

Measurement of total ROS generation

After cells were treated, production of total reactive oxygen species (ROS) in Jurkat cells and lymphocytes was measured using the membrane permeable dye 2',7'-dichlorofluorescein diacetate (H_2DCFDA) (Molecular Probes) and a slight modification of a previously published procedure (Siraki *et al,* 2002). The cells were incubated with H_2DCFDA at 37°C for 30 min, and fluorescence was measured at an excitation wavelength of 500 nm and emission wavelength of 524 nm using a Spectra Max Gemini XS multiwell plate fluorescence reader (Molecular Devices). Fluorescence readings were expressed in terms of the total cell count per well, determined using Trypan blue staining. Microsoft Excel 6.0 software was used for data representation and statistical analysis.

H2AX staining

Jurkat cells and lymphocytes were grown and treated, and the pellet was resuspended in 4% paraformaldehyde and incubated. The cell suspension was added to slides pre-coated with 0.01% poly-L-lysine (Sigma) and allowed to dry. The slides were washed with PBS three times for 5 min each time and incubated in 70% ethanol for 5 min. The slides were washed again and then incubated in 10% FBS in PBS for 1 h followed by an additional washing with PBS. After incubation for 1 h with the primary antibody, 1:300 anti-phosphohistone H2AX (Upstate Biotechnology, Lake Placid NY), the slides were washed again with PBS. The cells were then incubated in secondary antibody, 1:200 anti-mouse IgG-conjugated to FITC (Sigma) for 1 h and washed with PBS. The slides were stained with Hoechst 33342 and washed again with PBS. A glass coverslip was mounted over the dried slides using Cytoseal mounting medium (VWR, Mississauga ON). The slides were examined under a confocal microscope (BioRad MRC600) using oil immersion and pictures were taken. All pictures were processed using Adobe Photoshop 7.0 software.

RESULTS

Induction of apoptosis by pancratistatin in Jurkat cells

In order to evaluate the efficacy of pancratistatin in inducing cell death in cancer cells, we carried out experiments to determine the concentration- and time-dependent effects of pancratistatin on Jurkat cells. Jurkat cells were treated with different concentrations of pancratistatin for 6 h and stained with Hoechst dye, and apoptotic cells were counted as described in ‘‘Materials and methods’’. At a concentration as low as 500 nM, pancratistatin was efficient in causing approximately a third of the cells to undergo apoptosis (Figure 1A). At 1 µM, however, more than 70% of the Jurkat cells were apoptotic, meaning that apoptosis was effectively being induced. Hence, in all following experiments, this effective concentration of 1 µM was used.

Further examination of the time kinetics of cell death triggered by 1 µM pancratistatin indicated that apoptosis was detected as early as within 1 h of treatment (Figure 1B). More than 90% of the Jurkat cells displayed apoptotic morphology after 24 h of treatment whereas normal blood cells remained unaffected (Figure 1B). Results of Trypan blue staining to determine the number of permeable (dead) cells (Figure 1C) indicated that apoptotic cells were eventually becoming necrotic. This is evident by a higher percentage of apoptotic cells than dead cells within a short time of treatment, as seen by comparing data from figure 1B and 1C.

Apoptotic characteristics including cellular and nuclear morphology and biochemical features were studied in Jurkat cells with various times of pancratistatin treatment. Hoechst staining clearly indicated typical nuclear morphological changes induced by apoptosis, such as increased brightness of the nuclei and nuclear condensation (Figure 1D). DNA fragmentation is another key feature of apoptosis that was examined by using the comet assay as previously described (Naderi *et al,* 2003). The presence of a comet after 24 h indicated that massive apoptotic DNA fragmentation had occurred in most of the Jurkat cells (Figure 1E).

A specific biochemical characteristic of apoptosis is the flipping of phosphatidyl serine from the inner leaflet of the plasma membrane to the outer leaflet. This change can be observed as an increase in fluorescence due to the binding of the Annexin-V AlexaFluor conjugate to phosphatidyl serine. As shown in figure 1F, Annexin-V binding was obvious after 1 h of pancratistatin treatment in Jurkat cells, indicating early activation of the pathway of apoptosis.

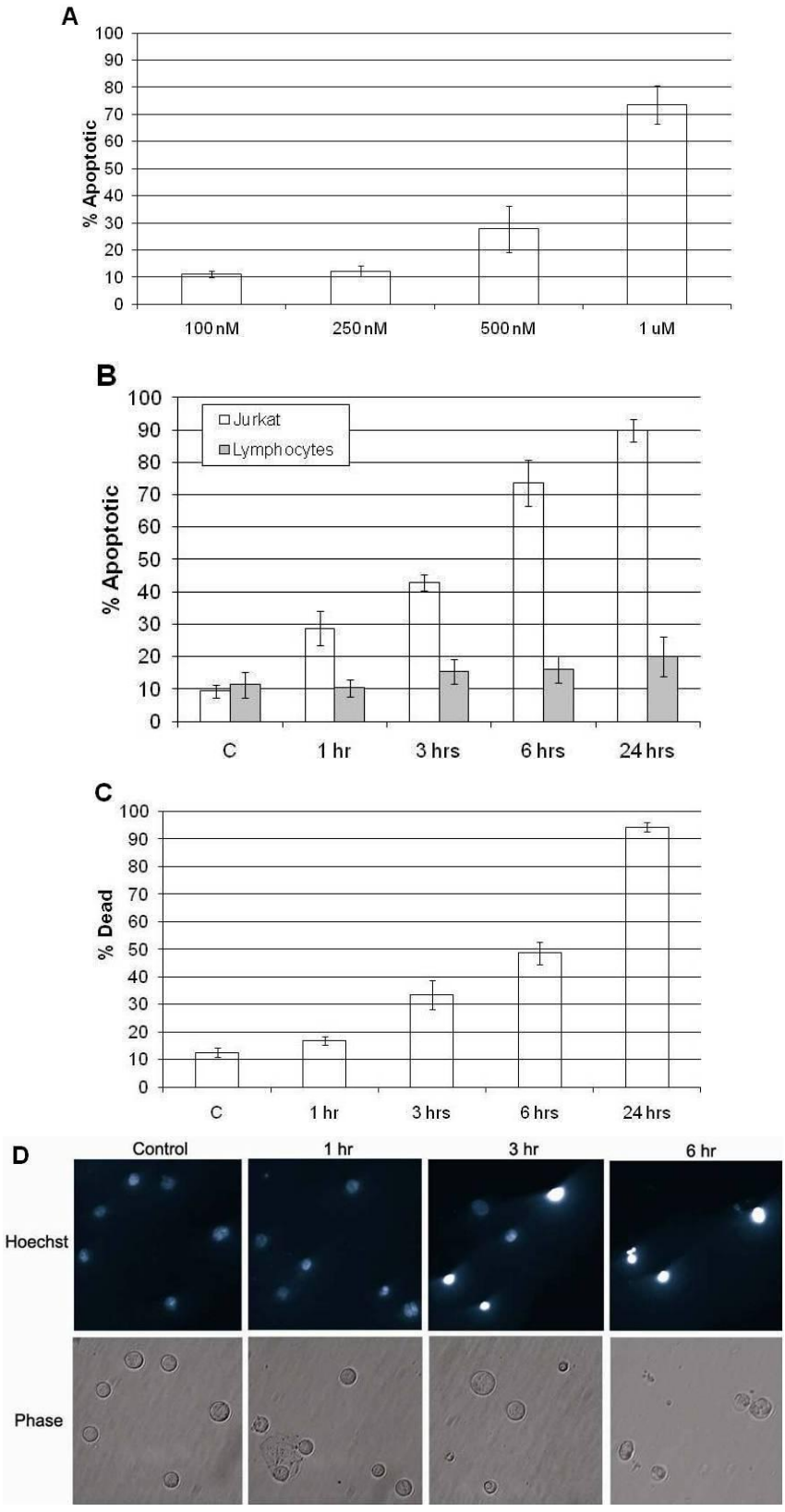
A
% Apoptotic
100
90
80
70
60
50
40
30
20
10
0
100 nM
250 nM
500 nM
1 uM
B
% Apoptotic
Jurkat
Lymphocytes
C
1 hr
3 hrs
6 hrs
24 hrs
C
% Dead
D
Control
1 hr
3 hr
6 hr
Hoechst
Phase

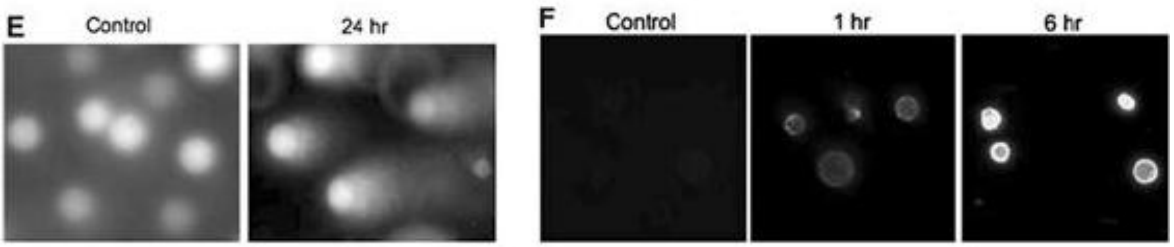

Figure 1. Induction of apoptosis in Jurkat cells treated with different concentrations of pancratistatin. (**A**) Jurkat cells were treated with various concentrations of pancratistatin as indicated. After 6 h of treatment, cells were stained with Hoechst dye and the percentage of apoptotic cells (the apoptotic index) determined. A minimum of five different fields at 100x magnification were counted and an average was taken for each experiment. The standard error was calculated using the data from three separate sets of experiments. (**B**) Induction of apoptosis over time in Jurkat (open columns) and normal blood cells (shaded columns) treated with pancratistatin. Jurkat or normal blood cells were treated with 1 µM pancratistatin for the indicated times. The apoptotic index was calculated as described above using a minimum of five different fields per experiment at 100x magnification. The standard error was calculated using the data from three separate sets of experiments. (**C**) Trypan blue staining for dead and live Jurkat cells treated with pancratistatin. Jurkat cells were treated with pancratistatin for the indicated times. The cells were then stained with Trypan blue dye so that the number of dead cells could be determined. The results are presented as the percentage of permeable (dead) cells. A minimum of eight different fields at 100x magnification were counted and an average was taken for each experiment. The standard error was calculated using the data from three separate sets of experiments. (**D**) Nuclear and cellular morphology of Jurkat cells treated with pancratistatin. The cells were treated with pancratistatin at 1 µM for the indicated times. Cells were then stained with Hoechst to examine nuclear morphology. Apoptosis is evident in cells with bright, condensed and rounded nuclei. (**E**) DNA degradation in Jurkat cells treated with pancratistatin as indicated by the comet assay. Jurkat cells were treated with either solvent (control, 0.001% DMSO) or 1 µM pancratistatin for 24 h. DNA degradation is indicated by the comet-like images due to migration of damaged DNA during electrophoresis. (**F**) Induction of the flipping of phosphatidyl serine in the plasma membrane of Jurkat cells by 1 µM pancratistatin treatment. Fluorescence indicates the flipping of phosphatidyl serine to the outer leaflet of the plasma membrane. Pictures were taken at 400x magnification.

These results collectively illustrate that pancratistatin is a very potent inducer of apoptosis in Jurkat cells. Normal nucleated blood cells including lymphocytes are not affected by pancratistatin.

Normal lymphocytes purified from a healthy person are the best candidates to determine the effect of pancratistatin on non-cancerous cells in comparison to the effect on cancerous Jurkat cells. These cells respond differently than Jurkat cells when subjected to pancratistatin treatment under similar conditions. We investigated the sensitivity of nucleated blood cells including lymphocytes to pancratistatin by quantifying the degree of apoptosis as with Jurkat cells. Unlike the Jurkat cells, the apoptotic index of the pancratistatin-treated lymphocytes did not increase over a significant amount of time (up to 24 h, Figure 1B). Furthermore, the nuclear shrinkage and brightness detected in Jurkat cells were not visible in the normal lymphocytes (Figure 2A). This suggests that apoptosis was not being induced in normal non-cancerous blood cells. Moreover, there was no increase in fluorescence following the Annexin-V binding assay (Figure 2B), implying that this apoptotic event was not present following treatment of lymphocytes with pancratistatin. The pathway of apoptosis is therefore not activated by pancratistatin in normal lymphocytes as it is in Jurkat cells.

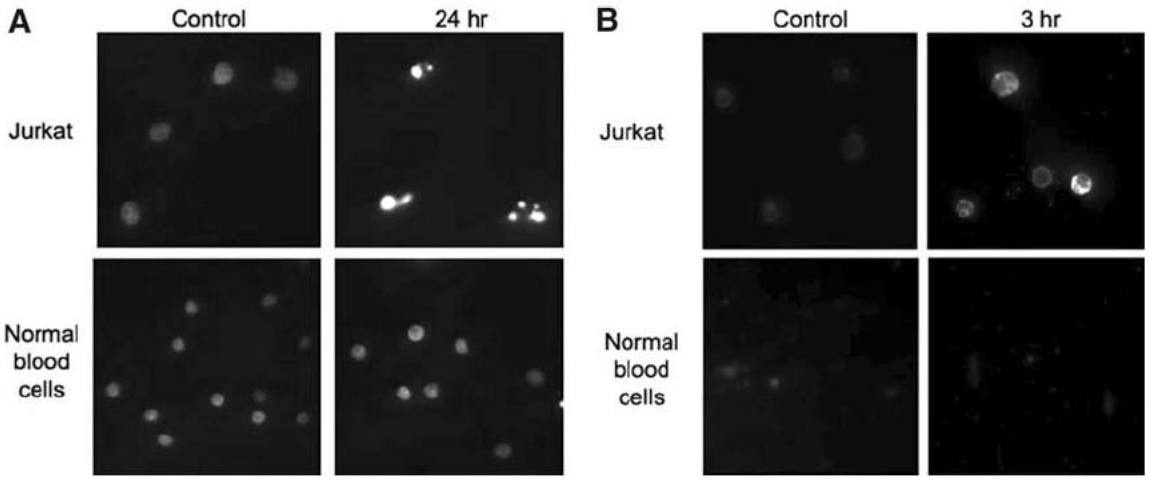

Figure 2. Pancratistatin selectively induces apoptosis in cancer cells. (**A**) Nuclear morphology of Jurkat (cancerous) and normal blood cells (non-cancerous peripheral blood mononuclear cells) treated with pancratistatin. Cells were treated with solvent (control, 0.001% DMSO) or 1 µM pancratistatin for 24 h. Apoptosis is evident in cells with bright, condensed and rounded nuclei. (**B**) Specific induction of the flipping of phosphatidyl serine in the plasma membrane of Jurkat cells by pancratistatin treatment. After 3 h of treatment with 1 µM pancratistatin, the Annexin-V binding assay was performed. Fluorescence indicates the flipping of phosphatidyl serine to the outer leaflet of the plasma membrane only in Jurkat cells, not in normal blood cells. Pictures were taken at 400x magnification.

Pancratistatin provokes early activation of caspase-3 in Jurkat cells, but not in normal lymphocytes

Caspase-3 is a required component of the apoptotic machinery which is activated specifically in the pathway of apoptosis. To determine whether pancratistatin treatment caused caspase-3 activation, the activity of caspase-3 was assayed in cell extracts prepared at different times after pancratistatin treatment. There was an early increase in caspase-3 activity upon treatment of Jurkat cells (Figure 3) indicating that caspase-3 might be involved in the early phase of apoptosis induced by pancratistatin in Jurkat cells. This increase in activity was not evident in lymphocytes; again illustrating that pancratistatin does not induce apoptosis in lymphocytes *(data not shown)*.

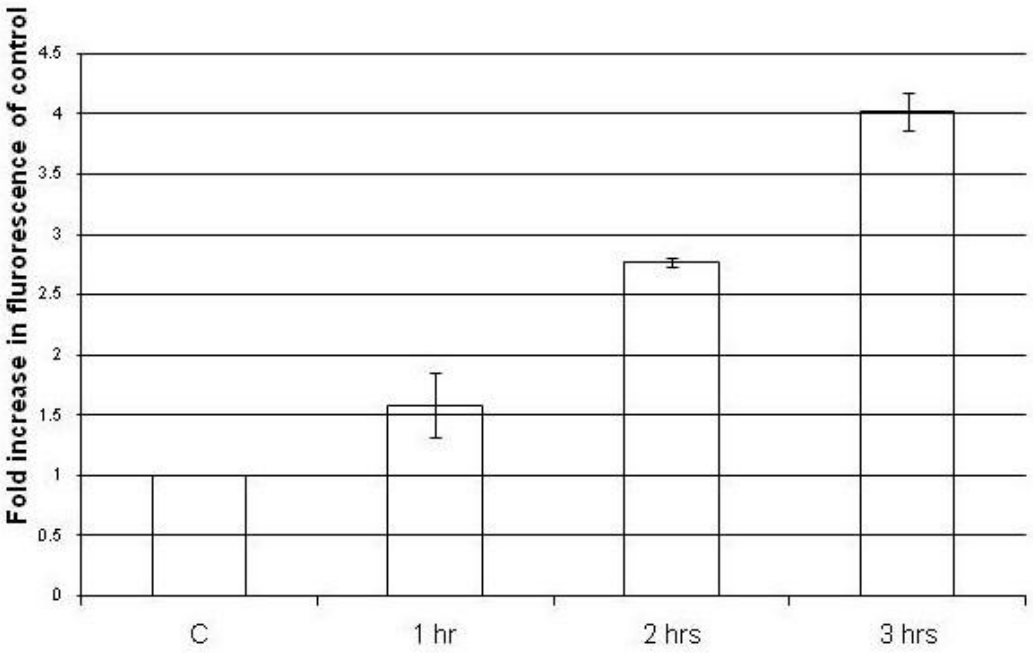

Figure 3. Early activation of caspase-3 in Jurkat cells treated with pancratistatin. The caspase-3 assay was performed as described in Materials and methods. The average of nine readings was used to determine the reading for each well. A minimum of three wells were run per experiment and the average was taken for each experiment. The results were calculated per microgram of protein and the standard error was calculated using the data from three separate sets of experiments.

Role of mitochondria in pancratistatin-induced apoptosis in Jurkat cells

The collapse of the mitochondrial membrane potential is a common event in the apoptotic pathway that leads to mitochondrial dysfunction and production of ROS. Mitotracker Red staining was carried out as described in Materials and methods to assess the mitochondrial membrane potential. Figure 4A clearly illustrates that the mitochondrial membrane potential in Jurkat cells was not lost prior to activation of caspase-3 by pancratistatin treatment. Furthermore, total cellular ROS was measured using the redox-sensitive fluorescent dye DCFDA, and the readings further confirmed that the production of ROS occurred after activation of caspase-3 (Figure 4B). There was minimal ROS production relative to Jurkat cells in normal blood cells *(data not shown)*.

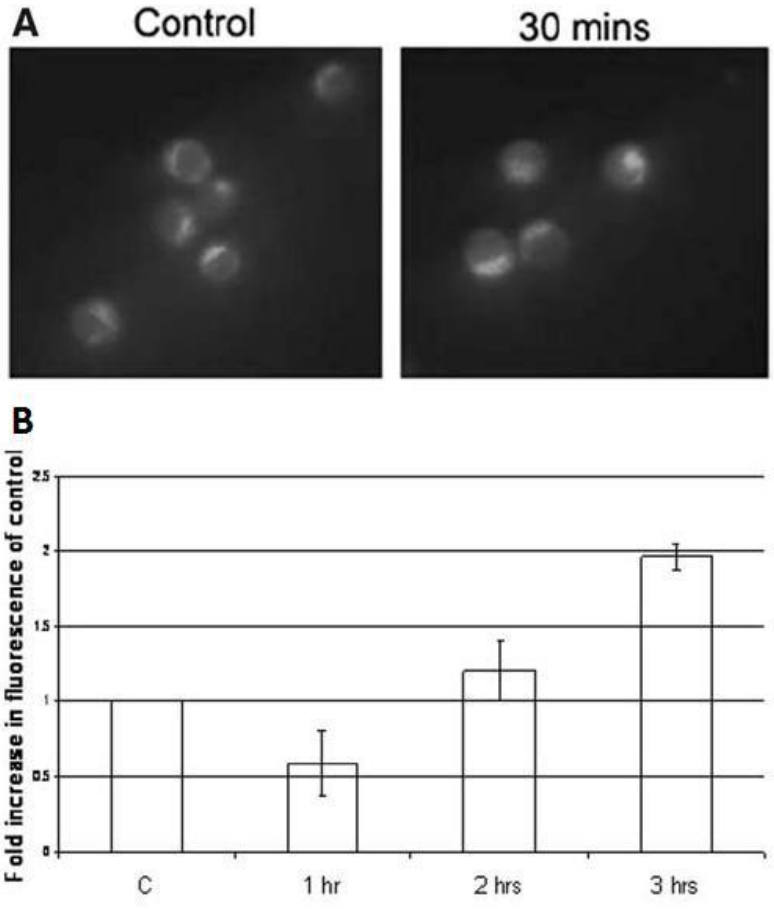

Figure 4. The effect of pancratistatin treatment on the mitochondrial membrane potential of Jurkat cells. (**A**) Jurkat cells were treated with solvent (control, 0.001% DMSO) or 1 µM pancratistatin for 30 min and stained with Mitotracker Red; fluorescence indicates that the mitochondrial membrane potential is intact. Pictures were taken at 400x magnification. (**B**) Generation of ROS in Jurkat cells treated with pancratistatin determined using DCFDA. The average of nine readings was used to determine the reading for each well. A minimum of three wells were run per experiment and the average was taken for each experiment. The results were calculated per 10 000 cells and standard error was calculated using the data from three separate sets of experiments.

Pancratistatin is a non-genotoxic inducer of apoptosis as compared to Vp-16

Pancratistatin treatment of Jurkat cells caused caspase-3 activation and ROS production within 3 h, but no comet had been produced at this time. This indicates that DNA degradation is not an early event in the pathway of apoptosis induced by pancratistatin in Jurkat cells. On the other hand, Vp-16 had clearly produced comets at this time (Figure 5A). This absence of DNA degradation by pancratistatin at an early phase, and its presence in a later phase indicates that DNA degradation is a result of the apoptotic mechanism. With Vp-16, the DNA damage was detected very early, which indicates that apoptosis was caused by DNA damage. These results signify that pancratistatin is a non-genotoxic inducer of apoptosis in Jurkat cells in contrast to Vp-16 which is a known genotoxic anti-cancer drug. In order to rule out the possibility of DNA double-strand breaks (DSB) caused by pancratistatin, we performed antiphosphohistone H2AX immunostaining. This assay is one of the most sensitive methods of detecting DNA fragmentation in mammalian cells (Rothkamm and Löbrich, 2003). Phosphorylation of the histone H2AX, symbolized as γ-H2AX, is one of the earliest events of DNA repair in response to DSB. Hence a positive staining indicates the presence of DSB (Martin, 2001; Bassing *et al,* 2002; Huang *et al,* 2004). As shown in figure 5B, pancratistatin did not stain for H2AX at the early time point of 3 h. This illustrates that indeed pancratistatin does not induce DSB in Jurkat cells; however we cannot rule out the possibility of single-strand breaks. A positive staining in Vp-16-treated cells confirms that this drug truly is a genotoxic anti-cancer drug.

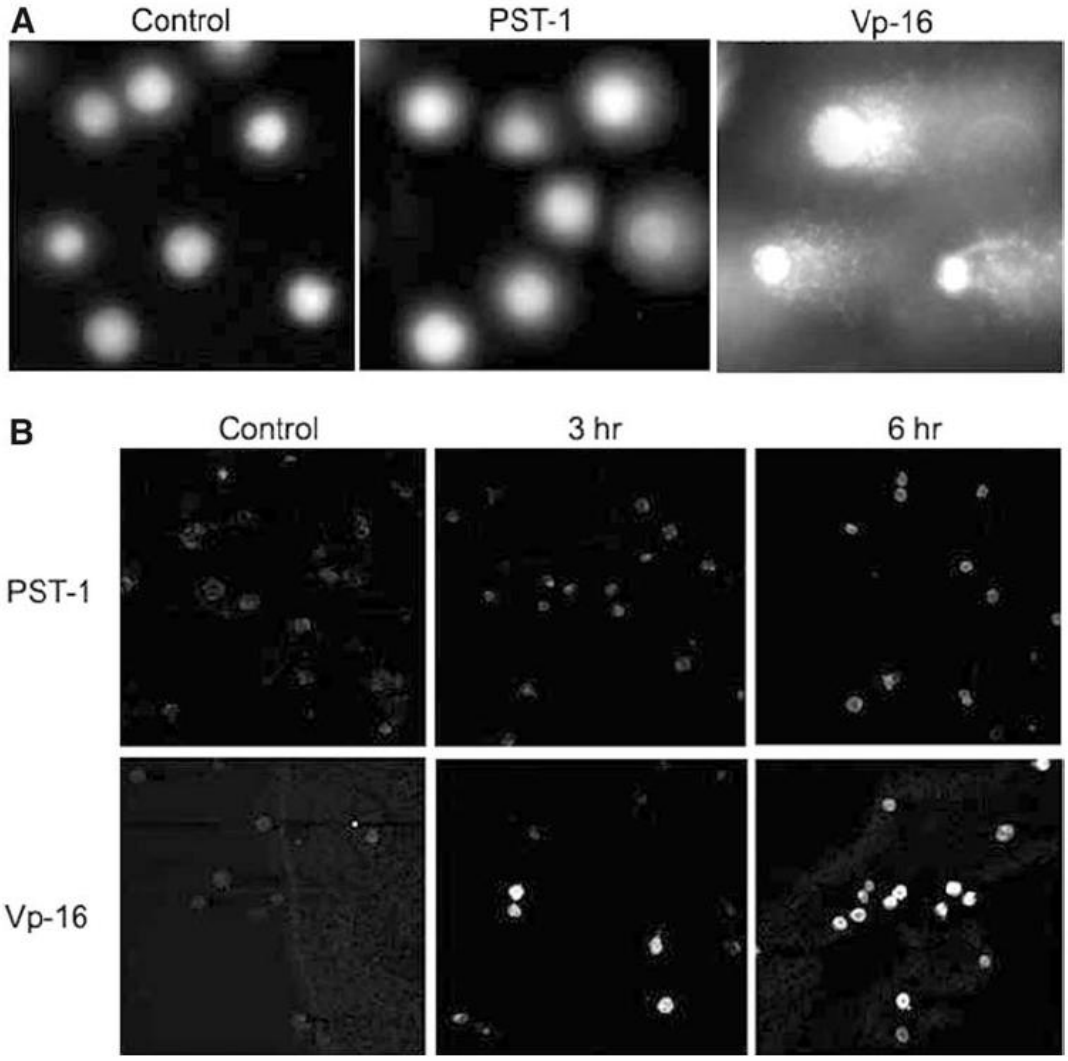

Figure 5. Detection of DNA degradation at an early phase of treatment in Jurkat cells. (**A**) Jurkat cells were treated with solvent (control, 0.001% DMSO), 1 µM pancratistatin (PST-1) or 10 µM Vp-16 for 3 h. The comet assay was then performed as described. DNA degradation is indicated by the comet-like images due to migration of damaged DNA during electrophoresis. Pictures were taken at 400x magnification. (**B**) Detection of DNA DSB by H2AX staining. Cells were treated with solvent (control, 0.001% DMSO), 1 µM pancratistatin (PST-1) or 10 µM Vp-16 for various times as indicated. Bright fluorescence indicates the presence of DNA DSB. Pictures were taken at 600x magnification, using oil immersion.

Vp-16 induces genotoxicity in normal cells

Although it has clearly been proven that Vp-16 (a topoisomerase-II inhibitor) is genotoxic to cancerous cells (Boose and Stopper, 2000), we decided to test its effect on the DNA of normal blood cells. Vp-16 treatment caused DNA damage as seen by comet formation, demonstrating its genotoxic effect on lymphocytes (Figure 6A). The absence of comets in normal blood cells (lymphocytes) treated with pancratistatin indicated that it may not cause DNA damage (Figure 6A). These results indicate that Vp-16 is genotoxic to Jurkat cells as well as normal lymphocytes whereas pancratistatin did not show any sign of genotoxicity to normal nucleated blood cells even after 24 h. This was further confirmed by the fact that no H2AX staining was observed following pancratistatin treatment, but was clearly evident following Vp-16 treatment (Figure 6B). Therefore, unlike Vp-16, pancratistatin specifically induces apoptosis in Jurkat cells, but does not seem to affect lymphocytes.

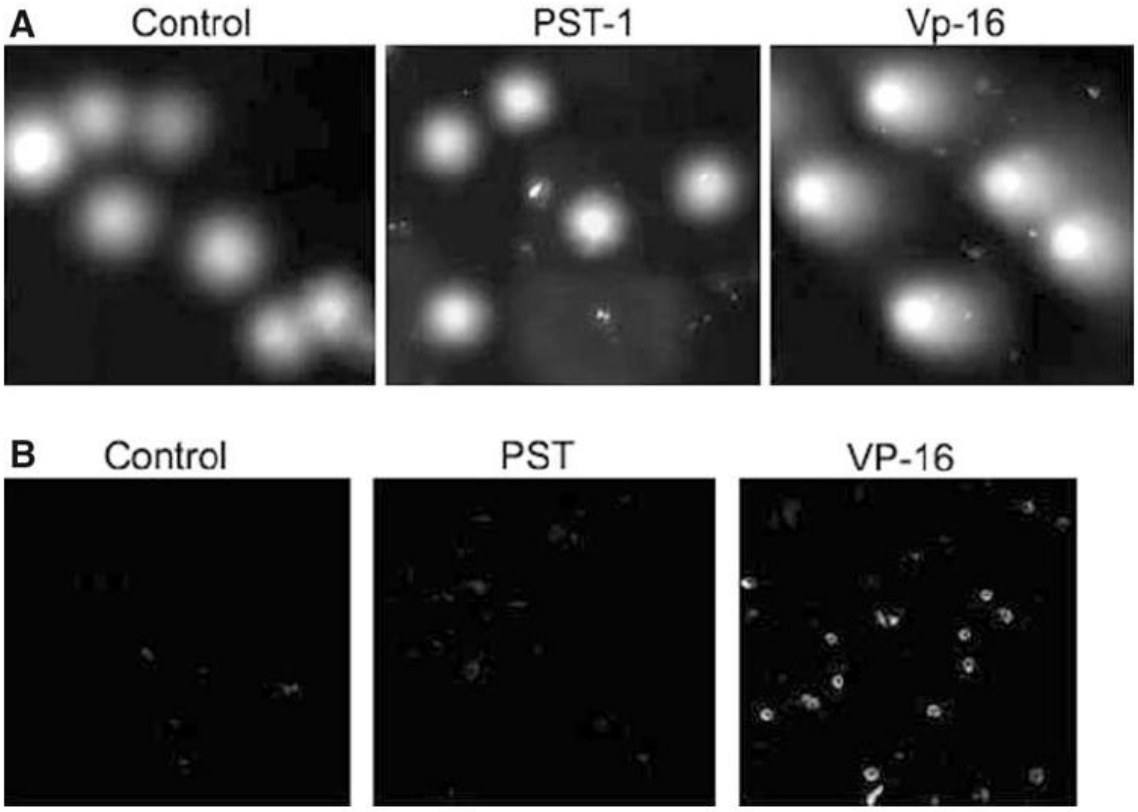

Figure 6. Effect of pancratistatin and Vp-16 treatment on the DNA integrity of normal blood cells. (**A**) Normal blood cells were treated with solvent (control, 0.001% DMSO), 1 µM pancratistatin (PST) or 10 µM Vp-16 for 24 h. The comet assay was then performed as described. DNA degradation is indicated by the comet-like images due to migration of damaged DNA during electrophoresis. Pictures were taken at 400x magnification. (**B**) Detection of DNA double-strand breaks (DSB) in normal blood cells treated with Vp-16. Cells were treated with solvent (control, 0.001% DMSO), 1 µM pancratistatin (PST) or 10 µM Vp-16 for 3 h. Fluorescence indicates the presence of DNA DSB. Pictures were taken at 600X magnification using oil immersion.

DISCUSSION

We report here for the first time that pancratistatin is selective in inducing apoptosis strictly in cancerous cells (specifically Jurkat cells). Second, since the chemical structure of pancratistatin does not resemble any existing genotoxic chemicals, DNA is unlikely to be a direct target of this drug. Due to the desperation for a treatment, genotoxic drugs are currently being used to target this disease. Unfortunately, we have found that some of these drugs, such as Vp-16 and paclitaxel are toxic to normal blood cells.

Although pancratistatin has been studied for many years, most of the research done on this drug has been in the field of organic chemistry (Khan *et al,* 1999; McNulty *et al,* 2001; Kim *et al,* 2002). For this reason, little information is available regarding its biochemical activity. However, it has been found that the pharmacophore of this drug is capable of specifically killing cancerous cells by inducing apoptosis.

The rapid and efficient induction of classical apoptosis by a very low concentration of pancratistatin in human lymphoma cells illustrates that this chemical is very specifically targeting a biochemical component of the apoptotic pathway. More importantly, however, is the fact that pancratistatin left the normal blood cells unaffected both biochemically and morphologically after 24 h. We have also tested the effect of pancratistatin on other normal non-cancerous cells, including dividing human fibroblasts, and human embryonic endothelial cells, and have found that it is not affecting the population doubling or viability of these cells (McLachlan *et al*., unpublished results). On the other hand, Vp-16, a commonly used chemotherapeutic agent, causes DNA damage in normal nucleated cells. This suggests that pancratistatin is a more specific inducer of apoptosis in cancer cells than currently used drugs such as Vp-16. We have also observed that paclitaxel causes apoptosis in normal nucleated cells *(data not shown)*. Although the efficacy of pancratistatin was highest in Jurkat cells, we have shown that it is also effective in inducing apoptosis in various cancer cell lines, including human breast cancer (MCF-7), rat hepatoma (5123) and neuroblastoma (SH-SY5Y) cells.

What is therefore the biochemical target of pancratistatin? DNA is a less likely target of pancratistatin action since is not structurally similar to any known genotoxic drugs. Our results from the comet assay further confirmed that indeed there is no early DNA degradation, but that DNA fragmentation is a late event in the apoptotic cascade resulting from pancratistatin treatment. In contrast, Vp-16 caused massive DNA damage

at an early phase (3 h). Furthermore, we applied H2AX staining, a sensitive technique to monitor DNA DSB. This indicated that pancratistatin did not induce DSB, whereas Vp-16 caused DSB soon after treatment. These experiments imply that pancratistatin could be a non-genotoxic compound that induces apoptosis by targeting non-genomic targets.

It is commonly accepted that a mitochondrial target can trigger apoptosis. This would suggest that pancratistatin might be targeting the mitochondrial membrane. However, this possibility was ruled out because our preliminary results indicated that within a short time of treatment, there was neither depolarization of the mitochondrial membrane nor production of ROS.

Interestingly, during the first hour, the apoptotic events triggered by pancratistatin were found to be the flipping of phosphatidyl serine on the plasma membrane and the activation of caspase-3. Surprisingly, this activation of caspase-3 came before that of caspase-8 which was found to be activated only after 3 h of treatment (refer to Appendix B, Figure 1). This evidence leads to two possibilities: pancratistatin directly activates caspase-3 or pancratistatin is targeting an enzyme on the plasma membrane. Incubation of a cell extract from untreated Jurkat cells with pancratistatin did not result in the activation of caspase-3 thus indicating that pancratistatin was not directly interacting with caspase-3 *(data not shown)*.

The other possible mechanism includes interaction with the plasma membrane and cytosolic proteins as a target for pancratistatin. Receptor-mediated Fas induced-apoptosis in Jurkat cells is one of the best-studied biochemical pathways (Ashkenazi and Dixit, 1998). It is generally believed that caspase-8 is recruited to the death-inducing signalling complex (DISC) following oligomerization of the Fas receptor. It is this initiator caspase of DISC that cleaves and activates caspase-3 as well as the Bid protein (Chinnaiyan *et al,* 1995). Intriguingly, it has been recently shown that caspase-3 is recruited to the DISC and processed to its active form before activation of caspase-8 or mitochondrial depolarization (Aouad *et al,* 2004). Recently evidence has also been found suggesting that caspase-3 may be present in the plasma membrane of the cell (Aouad *et al,* 2004). It is possible that pancratistatin may be directly targeting the Fas receptors on the plasma membrane of blood lymphoma cells which further activates caspase-3 followed by the activation of caspase-8. This is our hypothesis currently under investigation. Our preliminary results have indicated that indeed there is a significant

increase in caspase-3 activity following pancratistatin treatment in the plasma membrane fraction of Jurkat cells *(data not shown)*.

With this mechanism of action, why are normal cells not being affected by pancratistatin? This could be due to the expression of the Fas receptors which is found to be greater in blood lymphoma cells than normal blood cells. Furthermore, in fast-dividing cancer cells, the plasma membrane tends to run short of lipids, perhaps changing the fluidity of the membrane.

CONCLUSIONS

We are aggressively pursuing this hypothesized mechanism of action of pancratistatin in cancerous cells. Current investigation is underway to determine exactly what the biochemical targets of pancratistatin are on blood lymphoma cells. Given the significance of our *in vitro* results, pancratistatin could be a much better chemotherapeutic agent than those presently available.

REFERENCES

Abal M, Andreu JM, Barasoain I. Taxanes: microtubule and centrosome targets, and cell cycle dependent mechanisms of action. Curr Cancer Drug Targets 2003; 3: 193-203.

Aouad SM, Cohen LY, Sharif-Askari F, Haddad EK, Alam A, Sekaly RP. Caspase-3 is a component of Fas death-inducing signaling complex in lipid rafts and its activity is required for complete caspase-8 activation during Fas-mediated cell death. J Immunol 2004; 172(4): 2316-2323.

Ashkenazi A, Dixit VM. Death receptors: signaling and modulation. Science 1998; 281: 1305-1308.

Bassing CH, Chua KF, Sekiguchi J, Suh H, Whitlow SR, Fleming JC, *et al*. Increased ionizing radiation sensitivity and genomic instability in the absence of histone H2AX. Proc Natl Acad Sci USA 2002; 99(12): 8173-8178.

Boose G, Stopper H. Genotoxicity of several clinically used topoisomerase II inhibitors. Toxicol Lett 2000; 116: 7-16.

Bursch W, Ellinger A, Kienzl H, Torok L, Pandey S, Sikorska M, *et al*. Active cell death induced by the anti-estrogens tamoxifen and ICI 164 384 in human mammary carcinoma cells (MCF-7) in culture: the role of autophagy. Carcinogenesis 1996; 17(8): 1595-1607.

Chinnaiyan AM, O'Rourke K, Tewari M, Dixit VM. FADD, a novel death domain-containing protein, interacts with the death domain of Fas and initiates apoptosis. Cell 1995; 81(4): 505-512.

Corcoran GB, Fix L, Jones DP, Moslen MT, Nicotera P, Oberhammer FA, Buttyan R. Apoptosis: Molecular control point in toxicity. Toxicol Appl Pharmacol 1994; 128: 169-181.

Cunha KS, Reguly ML, Graf U, Helena H. Taxanes: the genetic toxicity of paclitaxel and docetaxel in somatic cells of *Drosophila melanogaster*. Mutagenesis 2001; 16: 79-84.

Green DR, Reed JC. Mitochondria and Apoptosis. Science 1998; 281: 1309-1312.

Griffin C, McNulty J, Hamm C, Pandey S. Pancratistatin: a novel highly selective anti-cancer agent that induces apoptosis by activation of membrane-Fas-receptor associated caspase-3. *Trends in Cell Apoptosis Research.* NovaScience Publishers, Inc. 2007. Pgs. 93-110.

Hu W, Kavanagh JJ. Anticancer therapy targeting the apoptotic pathway. Lancet Oncol 2003; 4: 721-729.

Huang X, Okafuji M, Traganos F, Luther E, Holden E, Darzynkiewicz Z. Assessment of histone H2AX phosphorylation induced by DNA topoisomerase I and II inhibitors topotecan and Mitoxantron and by the DNA cross-linking agent cisplatin. Cytometry 2004; 58A: 99-110.

Jaattela M. Programmed cell death: many ways for cells to die decently. Ann Med 2002; 34: 480-488.

Kazi A, Hill R, Long TE, Kuhn DJ, Turos E, Dou QP. Novel *N*-thiolated β-lactam antibiotics selectively induce apoptosis in human tumor and transformed, but not normal or nontransformed, cells. Biochem Pharmacol 2004; 67: 365-374.

Kerr JF, Wyllie AH, Currie AR. Apoptosis: a basic biological phenomenon with wide-

ranging implications in tissue kinetics. Br J Cancer 1972; 26: 239-257.

Khan P, Abbas S, Petit B, Caffrey R, Megram V, McGown A. Development and validation of a high-performance liquid chromatographic assay using solid-phase extraction for the novel antitumor agent pancratistatin in human plasma. J Chromatogr B Biomed Sci Appl 1999; 726(1-2): 249-254.

Kim S, Ko H, Kim E, Kim D. Stereocontrolled total synthesis of pancratistatin. Org Lett 2002; 4(8): 1343-1345.

Luduena RF, Roach MC, Prasad V, Pettit GR. Biochem Pharmacol 1992; 43: 539.

Martin NMB. DNA repair inhibition and cancer therapy. J Photochem Photobiol B 1992; 63: 162-170.

McNulty J, Mao J, Gibe R, Mo R, Wolf S, Pettit GR, *et al*. Studies directed towards the refinement of the Pancratistatin cytotoxic pharmacophore. Bioorg Med Chem Lett 2001; 11: 169-172.

Naderi J, Hung M, Pandey S. Oxidative stress-induced apoptosis in dividing fibroblasts involves activation of p38 MAP kinase and over-expression of Bax: Resistance of quiescent cells to oxidative stress. Apoptosis 2003; 8: 91-100.

Pettit GR, Pettit GR III, Backhaus RA, Boyd MR, Meerow, AW. Antineoplastic Agents 256. Cell Growth Inhibitory Isocarbostyrils from *Hymenocallis*. J Nat Prod 1993; 56: 1682.

Rothkamm K, Löbrich M. Evidence for a lack of DNA double-strand break repair in human cells exposed to very low x-ray doses. Proc Natl Acad Sci USA 2003; 100(9): 5057-5062.

Siraki AG, Pourahmad J, Chan TS, Khon S, O'Brien PJ. Endogenous and endobiotic reactive oxygen species formation by isolated hepatocytes. Free Radical Biol Med 2002; 32: 2-10.

Souza-Fagundes EM, Brumatti G, Martins-Filho OA, Correa-Oliveira R, Zani CL, Amarante-Mendes GP. Myriadenolide, a labdane diterpene isolated from *Alomia myriadenia* (asteraceae) induces depolarization of mitochondrial membranes and apoptosis associated with activation of caspases-8, -9 and -3 in Jurkat and THP-1 cells. Exp Cell Res 2003; 290: 420-426.

CHAPTER 3

Pancratistatin induces apoptosis in clinical leukemia samples with minimal effect on non-cancerous peripheral blood mononuclear cells

BACKGROUND

Chemotherapy for acute myeloid leukemia, despite earnest attempts, has not significantly changed in the last 30 years. Treatment continues to be based on the cytotoxic chemotherapies of anthracyclines and cytarabine. The natural compound, pancratistatin, extracted from the *Hymenocallis littoralis*, has broad-range efficacy against several cancer cell lines at 1 μM, with minimal effect on non-cancerous cell lines of the same origin (McLachlan *et al,* 2005; Siedlakowski *et al,* 2007). Pancratistatin treatment causes phosphatidyl-serine flipping, caspase-3 activation, generation of reactive oxygen species (ROS), and loss of mitochondrial membrane potential, which leads to apoptosis in cultured T-cell (Jurkat) leukemia cells (Kekre *et al,* 2005). Although pancratistatin is a non-genotoxic drug, its target has not yet been elucidated (Kekre *et al,* 2005; Dumont *et al,* 2007). The efficacy of pancratistatin in inducing apoptosis selectively in cultured (commercial) cancer cell lines is well established, though its effect on leukemia cells obtained from patients has not been tested.

In this study, clinical leukemia and non-cancerous peripheral blood mononuclear cells (ncPBMCs) were treated with pancratistatin to determine its selectivity and efficacy to induce apoptosis *ex vivo*. Activity of pancratistatin was compared to that of the widely used chemotherapeutic, paclitaxel, against cancer cells. Peripheral blood samples from patients with a diagnosis of acute myeloid leukemia (AML; n=11), acute lymphoid leukemia (ALL; n=1), chronic myelogenous leukemia (CML; n=1), chronic myelomonocytic leukemia (CMML; n=1) and Mantle cell lymphoma (n=1) were obtained. The majority of samples were taken at diagnosis, that is, in chemo-näive patients. Of the 15 patients, 5 did not go into remission with induction chemotherapy. The median duration of remission was 3 months. Our pre-clinical results demonstrate that pancratistatin is effective against all types of leukemia tested and does not induce apoptosis in non-cancerous mononuclear cells.

METHODS

Cell culture

Human T-cell (Jurkat) leukemia cells were purchased from ATCC and maintained in RPMI 1640 medium supplemented with 10% fetal bovine serum and 10 μM gentamycin in an incubator set at 37°C and 5% CO_2 in air. Peripheral blood was obtained from leukemia patients at the Windsor Regional Cancer Centre (WRCC, Windsor Regional Hospital REB #04-043 and 04-044) upon written, informed consent and from healthy non-smoking volunteers aged 25-50 y (University of Windsor REB #04-147). Whole blood samples were collected in BD Vacutainer™ Cell Preparation Tubes, and mononuclear cells were separated by density gradient centrifugation. The isolated cells were maintained in RPMI 1640 media supplemented and maintained in the same way as the Jurkat cultures. Cells were treated within 3 h of collection with 1 μM pancratistatin or 500 nM paclitaxel for up to 48 h.

Apoptosis assays

Apoptotic cells were detected by microscopy with cell-permeable Hoechst 33342 dye (Molecular Probes, Eugene OR) or by flow cytometry with Annexin-V AlexaFluor-488 (Sigma-Aldrich, Missisauga, ON) using established protocols (Siedlakowski *et al,* 2007). Briefly, cells were treated with 1 μM pancratistatin for either 24 or 48 h, or with 500 nM paclitaxel for 24 h. For flow cytometry, cells were washed twice in room temperature PBS, resuspended in Annexin-V binding buffer and incubated with AlexaFluor-488 (1:50) for 15 min. They were washed in calcium-binding buffer and a minimum of 20,000 were analyzed on a Beckman Coulter Cytomics FC500 flow cytometer. To achieve the highest cell number per sample, propidium iodide was not used in this study. For microscopy, 5 min incubation with 10 μM Hoechst 33342 dye was added to the Annexin-V binding step. Brightly stained, condensed nuclei were visible with Hoechst dye, characteristic of apoptotic cells, as is phosphatidylserine externalization detected by Annexin-V binding. Images were captured on an inverted fluorescence microscope (Leica DM IRB, Germany). The percentage of apoptotic cells was calculated from a minimum of 5 fields with >100 cells/field. Statistical analysis by unpaired t-test, where † represents $p<0.05$; significantly different between means of untreated and pancratistatin treated leukemia samples.

RESULTS

Pancratistatin induces apoptosis in cultured leukemia cells

From previous experiments on the effects of pancratistatin on cultured Jurkat cells (T-cell leukemia), the majority of cells were apoptotic after 24 h (Kekre *et al,* 2005). Pancratistatin rapidly induced apoptosis in >80% of Jurkat cells in the present study, whereas paclitaxel induced cell death in ~25% of cells, as determined by flow cytometry using Annexin-V AlexaFluor 488 (Figure 1A).

Pancratistatin induces apoptosis in clinical leukemia samples

Table 1 gives details of each patient's age, leukemia type and percent blasts at diagnosis, alongside their response to pancratistatin treatment *ex vivo*. Nine of the 15 samples showed an increase in apoptosis of 40% greater than untreated PBMCs of the same patient after exposure to pancratistatin, as determined by Hoechst staining (Table 1). This result was confirmed by detection of Annexin-V AlexaFluor 488 binding by flow cytometry (Figure 1B). Figure 2 shows the efficacy of pancratistatin on both cultured leukemia (Jurkat) cells and patient-obtained leukemia PBMCs as observed by Hoechst staining and Annexin-V binding.

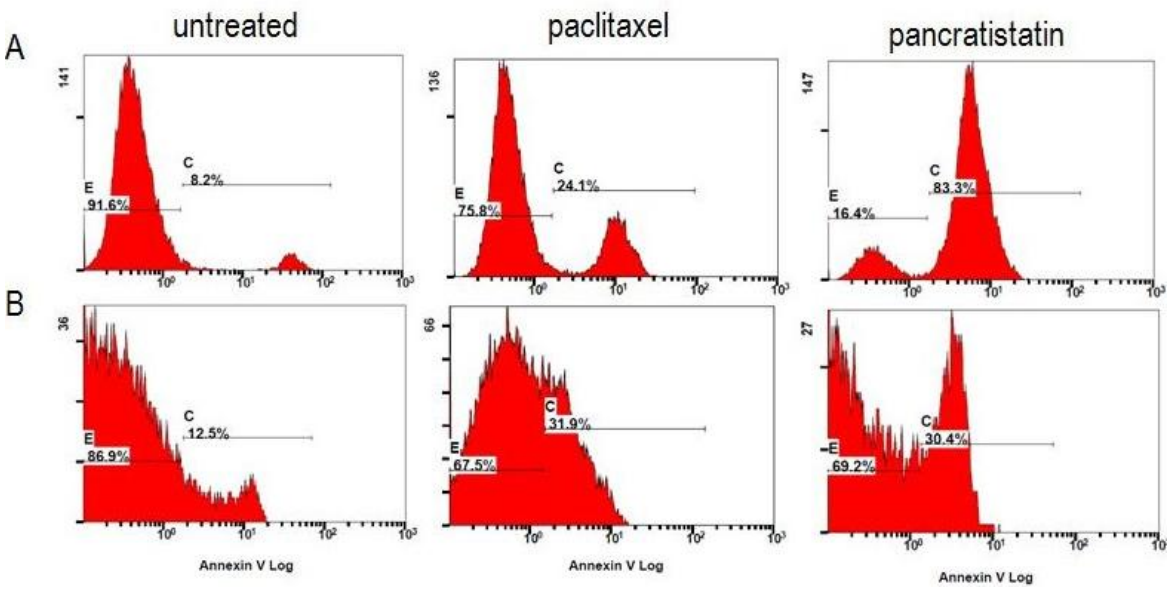

Figure 1. Detection of apoptosis in cells treated for 24 h with paclitaxel or pancratistatin. Flow cytometry with Annexin-V AlexaFluor 488 was used to detect apoptosis in Jurkat cells (**A**) and patient-obtained leukemic PBMCs (**B**) that were untreated, treated with 500 nM paclitaxel or treated with 1 µM pancratistatin for 24 h. The leukemic PBMCs were obtained from a chemo-näive female patient (65 y) diagnosed with AML – M1. Flipping of phosphatidylserine from the inner to the outer leaflet of the plasma membrane, which binds to Annexin-V in the presence of calcium, is a characteristic feature of apoptosis. A minimum of 20 000 events were measured for each sample on a Beckman Coulter Cytomics FC500 flow cytometer. Relative event number is displayed on the Y-axis, and relative fluorescence intensity is displayed on the X-axis.

Patient #	Age	Clinical Diagnosis	% Blasts	Clinical Response	Exposure	% Apoptosis
13	47	AML	44%	censored	48h	37.3 ± 7.7
9	45	AML	84%	censored	48h	63.9 ± 4.2
11	68	AML – M2	n/a	CR	48h	46.8 ± 12.2
2	81	AML – M2	20%	NR	24h	33.5 ± 7.7
8	74	AML – M2	60%	NR	48h	48.6 ± 6.7
1	60	AML – M3	85%	censored	24h	64.9 ± 4.2
10	57	AML – M3	43%	PR	48h	70.8 ± 5.9
5	23	AML – M5a	70%	NR	24h	30.6 ± 1.6
3	53	AMoL – M5a	96%	CR	24h	46.5 ± 7.9
14	71	AML – M0, relapsed	52%	relapsed	48h	45.3 ± 11.3
15	65	AML – MDS, relapsed	48%	CR	48h	37.3 ± 8.5
6	66	ALL – L3	34%	NR	48h	61.8 ± 9.8
4	73	CML	9%	censored	24h	63.9 ± 2.2
7	62	CMML – M4	32%	NR	48h	17.7 ± 2.7
12	80	Mantel cell lymphoma	0%	censored	48h	35.2 ± 6.6

Table 1. Clinical features, disease state, response in the clinic and *in vitro* of patient-obtained leukemia treated with pancratistatin. Apoptosis percentage values are corrected for the percentage of apoptosis observed in untreated samples of the same patient. All diagnoses are 1st occurrence unless otherwise stated. Patients were diagnosed in the clinic with: Acute Myeloid Leukemia (AML), subtyped as M0 – M7 or MDS (myelodysplastic syndrome); Acute Monocytic Leukemia (AMoL); Acute Lymphoblastic Leukemia (ALL), subtyped as Burkitt's (L3); Chronic Myelogenous Leukemia (CML); or Chronic Myelomonocytic Leukemia (CMML). Response to chemotherapy administered in the clinic is indicated as complete response (CR), partial response (PR), no response (NR), relapsed or censored.

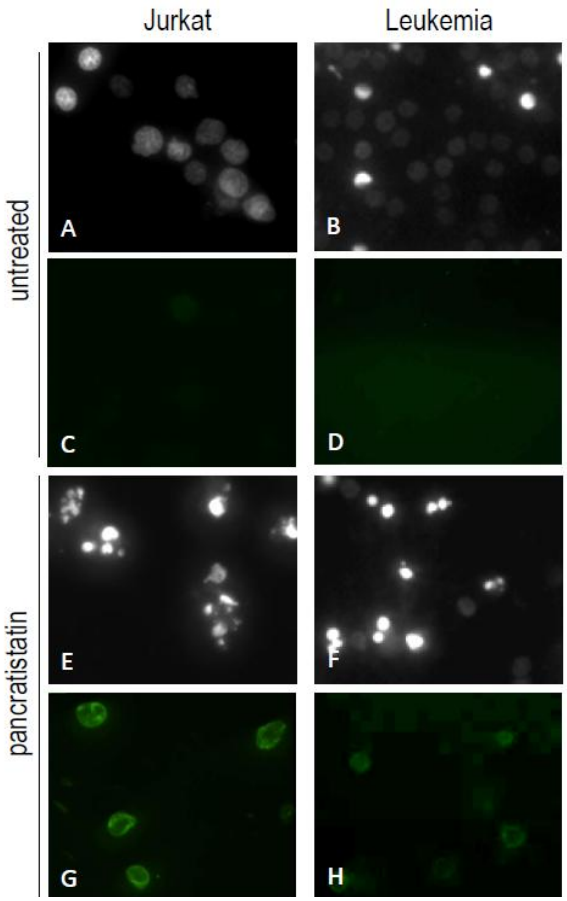

Figure 2. Response of clinical leukemia and cultured Jurkat cells to treatment with pancratistatin. The apoptotic effect of 24 h exposure to 1 µM pancratistatin was observed by microscopy using cell-permeable Hoechst dye. Compared to the nuclear morphology of untreated cells (A, B), treatment with pancratistatin resulted in apoptosis characterized by condensed, brightly stained nuclei in Jurkat (E) and patient obtained leukemic PBMCs (F). Annexin-V binding, another characteristic feature of apoptosis, was minimal in untreated cells (C, D) in contrast to the binding observed after pancratistatin treatment (G, H). Hoechst and Annexin-V images are not of the same field.

Pancratistatin is non-toxic to non-cancerous PBMCs

To determine if the apoptosis-inducing effect of pancratistatin is selective for cancer cells, PBMCs isolated from blood samples from healthy volunteers (n=8) were treated with 1 μM pancratistatin for up to 48 h. Interestingly, pancratistatin did not enhance apoptosis in these cells as in leukemic PBMC isolates, as determined by flow cytometry analysis using Annexin-V binding and nuclear morphology after Hoechst staining (Figure 3A, 3B). The cancer-selective apoptosis-inducing activity of pancratistatin was a trend that was observed in all samples obtained (Figure 4). These data demonstrate that pancratistatin is selectively toxic to cancer cells *ex vivo*, irrespective of leukemia type, with an insignificant effect on non-cancerous PBMC isolates.

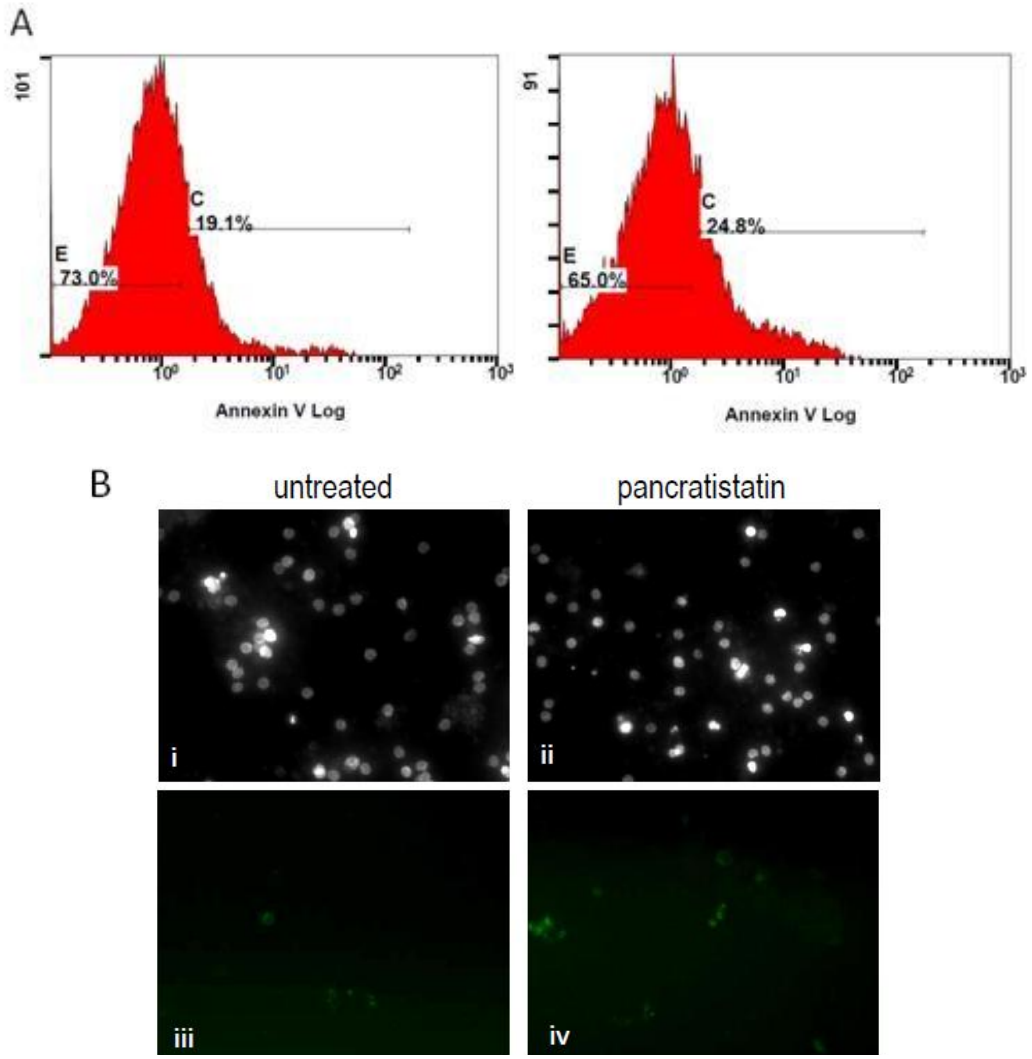

Figure 3. Non-cancerous peripheral blood mono-nucleated cells (PBMCs) are relatively unaffected by pancratistatin. (**A**) Flow cytometry analysis using Annexin-V AlexaFluor 488 was performed on PBMCs that were untreated (left panel) or treated with 1 µM pancratistatin (right panel) for 48 h. A minimum of 20 000 events were measured for each sample on a Beckman Coulter Cytomics FC500 flow cytometer. Relative event number is displayed on the Y-axis, and relative fluorescence intensity is displayed on the X-axis. (**B**) Hoechst staining and Annexin-V binding depicts the selective activity of pancratistatin; there is minimal difference in nuclear morphology (i, ii) and amount of externalized phosphatidylserine (iii, iv) between untreated and treated non-cancerous PBMCs.

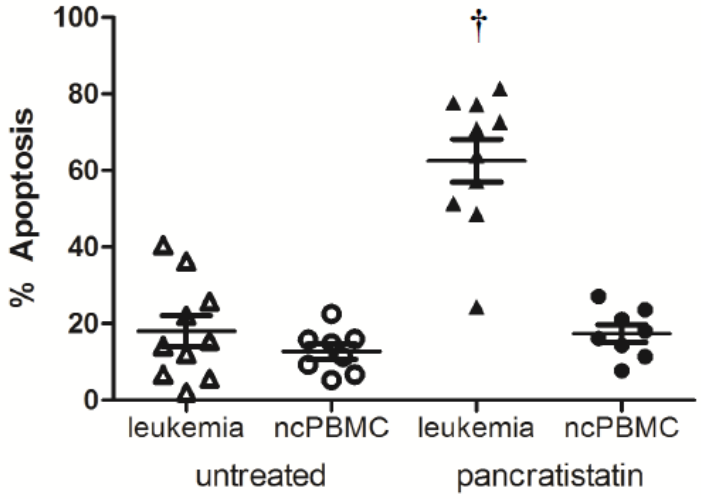

Figure 4. Comparative effect of 48 h pancratistatin treatment. Leukemia samples (n=10) and non-cancerous PBMCs (n=8) treated for 48 h with pancratistatin were stained with Hoechst dye and counted manually (a minimum of 5 fields with 100 cells per field); percent apoptosis was calculated per total cell number. Statistical analysis was performed (unpaired t-test, two-tailed p value); † represents $p<0.05$ between untreated and pancratistatin treated leukemia samples.

DISCUSSION

We report the novel finding that pancratistatin has selective apoptosis-inducing activity *ex vivo* at a low dose in a random sampling (n=15) of patient-obtained leukemias. In contrast, pancratistatin has no effect on non-cancerous peripheral blood mononuclear cells (n=8). Cellular subtypes in the PBMC samples may have differing sensitivities to pancratistatin and separation of these populations is needed to clarify this point, but requires much greater numbers. However, our results indicate that PBMCs collected from healthy volunteers of various ages were unaffected by pancratistatin. It is therefore unlikely that pancratistatin is toxic to a particular subtype of non-cancerous PBMC samples. The efficacy and selectivity of pancratistatin against clinical leukemia is based on two characteristic features of apoptosis, namely nuclear morphology and lipid rearrangement within the plasma membrane. Our results suggest that pancratistatin could be a novel way to treat leukemia and may not cause adverse effects common to intravenous chemotherapy (Gerber, 2008). Paclitaxel has been used to treat many types of cancer, including leukemia, for over a decade; but it causes harsh side effects often associated with chemotherapy (Sonnichsen, 1994). In contrast, pancratistatin is more effective against cancer cells than paclitaxel and has no significant effect on non-cancerous PBMC samples.

The mechanism of action and biochemical target of pancratistatin is currently being studied. Due to its broad-range effectiveness, we hypothesize that pancratistatin may selectively target cancer cell mitochondria, as opposed to a specific kinase or signalling protein. We have previously shown that pancratistatin causes mitochondrial membrane potential collapse and permeabilization, leading to reactive oxygen species (ROS) generation, cytochrome *c* leakage, caspase-3 activation, and apoptosis (Kekre *et al,* 2005; Siedlakowski *et al,* 2007; Griffin *et al,* 2007). Recent reports indicate that some leukemia cells have increased basal levels of ROS, suggesting increased susceptibility to oxidative stress, which can lead to mitochondrial permeabilization and subsequent apoptosis (Wang *et al,* 2008). It has also been reported that cancer cell mitochondria are dysfunctional and more susceptible to attack compared to non-cancerous cell mitochondria, which presents an opportunity for the development of new chemotherapeutics, especially for leukemia (Vondrácek *et al,* 2006). Liu and colleagues reported that Lycorine, also an *Amaryllidaceae* alkaloid, induces caspase-dependent apoptosis in leukemia cells by down-regulating the anti-apoptotic protein, Mcl-1 (Liu *et al,*

2009). It is possible that pancratistatin is also targeting a protein that regulates the balance of apoptosis/survival, which could explain the broad-range efficacy of this compound against cancer cells *in vitro*. This is supported by our evaluation of pancratistatin on patient-obtained leukemia cells *ex vivo* at a low dose (1 μM).

CONCLUSIONS

Our results show that pancratistatin is an effective and selective anti-cancer agent with potential for advancement to clinical trials (Kornienko and Evidente, 2008). Targeted therapies are the holy grail of systemic cancer therapy; the ideal drug should kill cancer cells without harming non-cancerous cells. This is an exciting development in the treatment of AML, for which treatment regimens used over the last 30 years have not significantly improved survival.

REFERENCES

Dumont P, Ingrassia L, Rouzeau S, Ribaucour F, Thomas S, Roland I, Darro F, Lefranc F, Kiss R: The Amaryllidaceae isocarbostyril narciclasine induces apoptosis by activation of the death receptor and/or mitochondrial pathways in cancer cells but not in normal fibroblasts. Neoplasia 2007; 9(9): 766-776.

Gerber DE: Targeted therapies: a new generation of cancer treatments. Amer Fam Physician 2008; 77(3): 311-319.

Griffin C, Sharda N, Sood D, Nair J, McNulty J, Pandey S: Selective cytotoxicity of pancratistatin-related natural Amaryllidaceae alkaloids: evaluation of the activity of two new compounds. Cancer Cell Int 2007; 7: 10.

Kekre N, Griffin C, McNulty J, Pandey S: Pancratistatin causes early activation of caspase-3 and flipping of phosphatidyl serine followed by rapid apoptosis specifically in human lymphoma cells. Cancer Chemother Pharmacol 2005; 56(1): 29-38.

Kornienko A, Evidente A: Chemistry, biology, and medicinal potential of narciclasine and its congeners. Chemistry Reviews 2008; 108(6): 1982-2014.

Liu X, Jiang J, Jiao X, Wu Y, Lin J, Cai Y: Lycorine induces apoptosis and down-regulation of Mcl-1 in human leukemia cells. Cancer Lett 2009; 274(1): 16-24.

McLachlan A, Kekre N, McNulty J, Pandey S: Pancratistatin: a natural anti-cancer compound that targets mitochondria specifically in cancer cells to induce apoptosis. Apoptosis 2005; 10: 619-630.

Siedlakowski P, McLachlan-Burgess A, Griffin C, Tirumalai SS, McNulty J, Pandey S: Synergy of Pancratistatin and Tamoxifen on breast cancer cells in inducing apoptosis by targeting mitochondria. Cancer Biol Ther 2007; 7(3): 376-384.

Sonnichsen DS, Relling MV: Clinical pharmacokinetics of paclitaxel. Clin Pharmacokinet 1994; 27(4): 256-269.

Vondrácek J, Soucek K, Sheard MA, Chramostová K, Andrysík Z, Hofmanová J, Kozubík A: Dimethyl sulfoxide potentiates death receptor-mediated apoptosis in the human myeloid leukemia U937 cell line through enhancement of mitochondrial membrane depolarization. Leukemia Res 2006; 30(1): 81-89.

Wang J, Li L, Cang H, Shi G, Yi J: NADPH oxidase-derived reactive oxygen species are responsible for the high susceptibility to arsenic cytotoxicity in acute promyelocytic leukemia cells. Leukemia Res 2008; 32(3): 429-436.

CHAPTER 4

Selective cytotoxicity of pancratistatin-related natural *amaryllidaceae* alkaloids: evaluation of the activity of two new compounds

BACKGROUND

The initial report by Pettit and colleagues in 1993 demonstrated that Pancratistatin (PST) a natural compound isolated from the Hawaiian spider lily (*Hymenocallis littoralis*) displayed potent cytotoxicity against human tumor cell lines (Pettit *et al,* 1993). They also noted that in the NCI "disease oriented" *in vitro* anti-tumor screen against 60 cell lines representing lung, colon, ovarian, renal, brain, melanoma and myelocytic leukemia, the pattern of activity of PST against various tumor types was distinct from that of other known anti-tumor drug classes. Recently, we demonstrated the selective toxicity of PST to cancer cells and the sparing of normal cells at micromolar doses (Kekre *et al,* 2005). In addition we have demonstrated that PST acts by affecting mitochondrial function and inducing apoptosis in malignant cell lines (McLachlan *et al,* 2005).

A systematic synthetic approach has been used to determine the minimum cytotoxic pharmacophore and is known to comprise the *trans*-fused b/c-ring system containing the 2, 3, 4-triol unit in the C-ring (McNulty *et al,* 2001; Rinner *et al,* 2004; McNulty *et al,* 2005). It has also been noted that the 2, 3-diol derivatives have significant activity (McNulty *et al,* 2001), indicating that the C3-hydroxyl is a moderating influence. The C-7 phenolic and C-1 hydroxyl functions are not essential (Pettit *et al,* 2004; Pettit *et al,* 2006).

The aim of present work was to further evaluate the structure-activity relationships of two other AMD alkaloids, AMD4 and AMD5 (Figure 1). Both these compounds lack the multiple hydroxyl groups but instead have a methoxy group that varies in orientation between AMD4 (α) and AMD5 (β). Our results indicated that like PST, AMD5 has the capability of selectively inducing apoptosis in cancer cells while sparing normal cells, albeit at a concentration 10-fold higher.

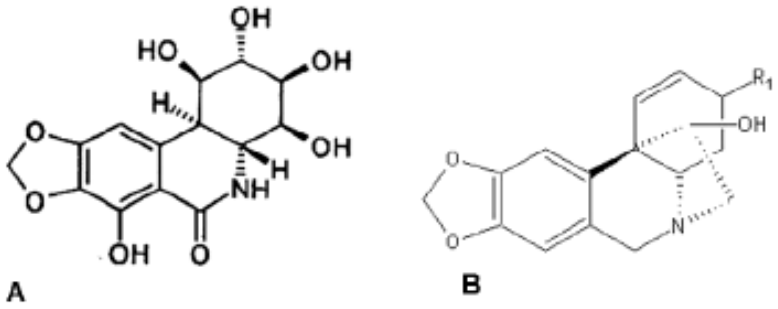

Figure 1. Chemical structure of native Pancratistatin (A) and of *Amaryllidaceae* alkaloids AMD4 and AMD5 (B). The phenanthridone skeleton is a conserved feature in alkaloids of the *Amaryllidaceae* family. The *Amaryllidaceae* compounds have a methoxy group that varies in orientation between AMD4 (α) and AMD5 (β).

METHODS

Cell culture

Human T-cell leukemia (Jurkat) cells were obtained from ATCC, Manassas, VA. These cells were maintained in RPMI 1640 medium supplemented with 10% fetal bovine serum (FBS) and 10 µM gentamycin (Life Technologies, Mississauga, ON) in an incubator set at 37°C, 5% CO_2 and 95% humidity. Human nucleated blood cells were isolated from whole blood taken from a healthy non-smoking male (University of Windsor REB #04-147). The whole blood sample was collected in a BD Vacutainer™ CPT (Cell Preparation Tube) obtained from Becton Dickinson, Franklin Lakes, NJ, and centrifuged at 500 x *g* for 30 min at 25ºC. The upper layer consisting of mononuclear cells, platelets and plasma was collected and maintained in RPMI 1640 media supplemented with 10% FBS and 10 µM gentamycin (Life Technologies) in the same incubator as Jurkat cells.

Cell treatment

Cells were grown and treated with either AMD4 or AMD5 alkaloids at various concentrations and time-points. AMD4 and AMD5 (99.5% pure) were derived as detailed by Pettit and colleagues (Pettit *et al,* 1993).

Cellular viability assay

Cells were grown to 70% confluence and treated with AMD4 and AMD5 at a final concentration of 10 µM. The cells were then stained with the cell permeable dye Hoechst 33342 (Molecular Probes, Eugene, OR) at 10 µM final concentration and incubated for 10 min at 25ºC. Brightly stained, condensed nuclei are characteristic features of apoptotic cells, as visualized with a fluorescent microscope (Leica DM IRB, Germany). Images were captured at 10X and 40X objectives; the percentage of apoptotic cells was calculated from the total number of cells with Microsoft® Excel 6.0 software and pictures were compiled using Adobe® Photoshop 7.0 software. A minimum of 5 fields of at least 100 cells per field was counted. Statistical significance was determined using STATISTICA® software.

Annexin-V binding assay

Jurkat cells were treated with 10 µM AMD4 and AMD5 for 24 hours. The Annexin-V binding assay was conducted according to the manufacturer's protocol using

a kit purchased from Molecular Probes, Eugene, OR. Briefly, cells were washed with phosphate-buffered saline (PBS) and re-suspended in Annexin-V binding buffer (10 mM HEPES/NaOH pH 7.5, 140 mM NaCl, 2.5 mM $CaCl_2$), containing Annexin-V Alexa Fluor® 488 conjugate (1:50) for 15 min at 25ºC; pictures were taken with a fluorescent microscope (Leica DM IRB, Germany) at 40X objective and compiled using Adobe® Photoshop 7.0 software.

TUNEL assay

After treating Jurkat cells with AMD4 and AMD5 at indicated times the TUNEL Assay was performed as per manufacturer's protocol (Molecular Probes, Eugene, OR) and a previously published method (McLachlan *et al,* 2005), to detect DNA damage. Cells were fixed by suspending them in 70% (v/v) ethanol and stored at -20^{o}C overnight. The sample was then incubated with DNA-labelling solution (10 µL reaction buffer, 0.75 µL TdT enzyme, 8 µL BrdUTP, 31.25 µL of dH2O) for 1 h at 25ºC. Each sample was then exposed to an antibody solution consisting of 5 µL Alexa Fluor® 488 labeled anti-BrdU antibody with 95 µL rinse solution and allowed to react for 20 min; pictures were taken at 20X objective using a fluorescent microscope (Leica DM IRB, Germany).

Caspase-3 assay

The caspase-3 assay was carried out using a previously published method (Kekre *et al,* 2005). Briefly, Jurkat or normal lymphocyte cellular lysates were collected and incubated with the fluorogenic substrate DEVD-AFC (MP Biomedicals, Aurora, OH) in DEVD buffer (0.1 M HEPES, pH 7.4, 2 mM DTT, 0.1% CHAPS, 1% sucrose) and allowed to incubate at 37ºC for 45 min. Fluorescence was measured at 400 nm excitation and 505 nm emission using the Spectra Max Gemini XS (Molecular Devices, Sunnyvale, CA). Caspase-3 activity was calculated per microgram of protein, and expressed as a percentage of control activity. Protein concentration was determined utilizing the BioRad protein assay reagent (BioRad, Mississauga, ON, Canada) with bovine serum albumin as a standard. Microsoft® Excel 6.0 software was used for data representation; statistical significance was determined using STATISTICA® software.

Mito-Casp assay

The Mito-Casp assay was performed as per manufacturer's protocol using a kit purchased from Cell Technology Inc., Mountain View, CA. Briefly, cells were treated with either alkaloid at 10 µM concentration for the desired times and washed twice in PBS. Cells were re-suspended in PBS according to protocol and incubated with both MMP dye and caspase reagent at a 1:30 dilution for 60 min at 37°C in darkness. Following incubation, the cell pellet was collected and re-suspended in wash buffer; fluorescence was measured from a 96-well micro-titre plate at 549 nm excitation and 574 nm emission using the Spectra Max Gemini XS (Molecular Devices, Sunnyvale, CA). Loss of MMP was presented as a loss in relative fluorescence units per 10 000 cells. Microsoft® Excel 6.0 software was used for data representation; statistical significance was determined using STATISTICA® software.

RESULTS

Amaryllidaceae alkaloids induce apoptosis in Jurkat cells

Jurkat cells were incubated with different concentrations of AMD4 and AMD5 for up to 72 h. The degree of apoptosis resulting from treatment was observed by Hoechst staining where condensed, brightly stained nuclei indicated apoptotic cell death. The number of apoptotic nuclei was expressed as a percentage of the total number of cells in a dose-dependent manner; alkaloid AMD5 at a concentration of 10 µM incited apoptosis in over 40% of Jurkat cells after 48 h and was the working concentration used for further experiments (Figure 2, 3A). In contrast to this finding, alkaloid AMD4 had a minimal effect on cancer cell viability under similar treatment conditions. To compliment Hoechst staining, the Annexin-V assay was carried out at several time-points in order to monitor phosphatidylserine flipping to the outer leaflet of the plasma membrane, a characteristic apoptotic event. As previously reported, Annexin-V staining is specific to apoptotic cells, and background staining is low in unaffected cells (Kekre *et al,* 2005). Jurkat cells incubated with 10 µM AMD5 resulted in a high incidence of phosphatidylserine flip; approximately 45% of Jurkat cells were observed to be labelled with Annexin-V-FITC (Figure 3B).

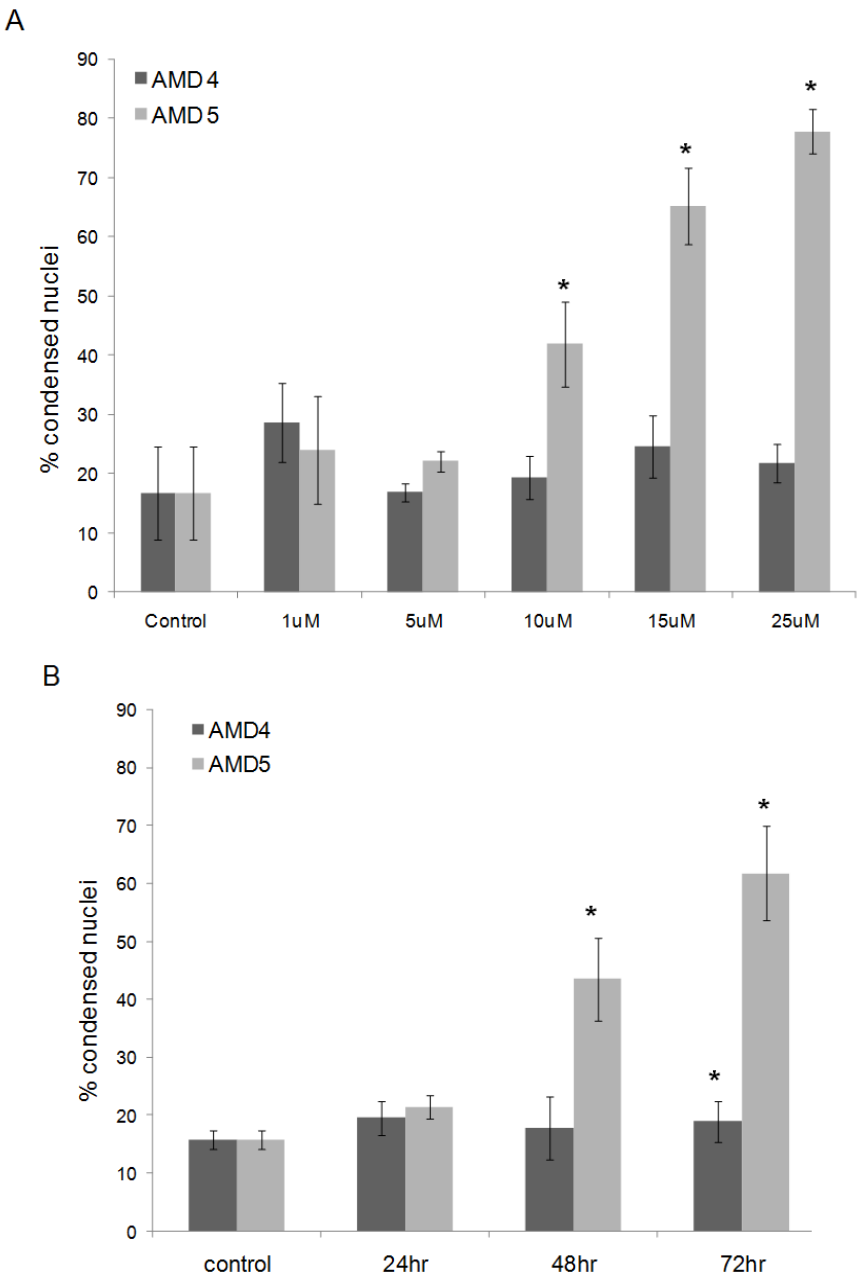

Figure 2. ***Amaryllidaceae*** **alkaloids induce apoptosis in Jurkat cells.** Cells were stained with cell-permeable Hoechst 33342 dye; the number of brightly stained and condensed nuclei were counted over the total number of cells visible and displayed as a percentage. A minimum of 5 fields with at least 100 cells per field were counted. (**A**) Dose-response curve for Jurkat cells treated with increasing concentration of AMD4 or AMD5 for 48 h. *Columns*, mean (n=5); *bars*, SD; *, $P < 0.05$, significantly different from control by paired *t*-test. (**B**) Time-response curve for Jurkat cells treated with 10 μM of AMD4 or AMD5. *Columns*, mean (n=5); *bars*, SD; *, $P < 0.05$, significantly different from control by paired *t*-test.

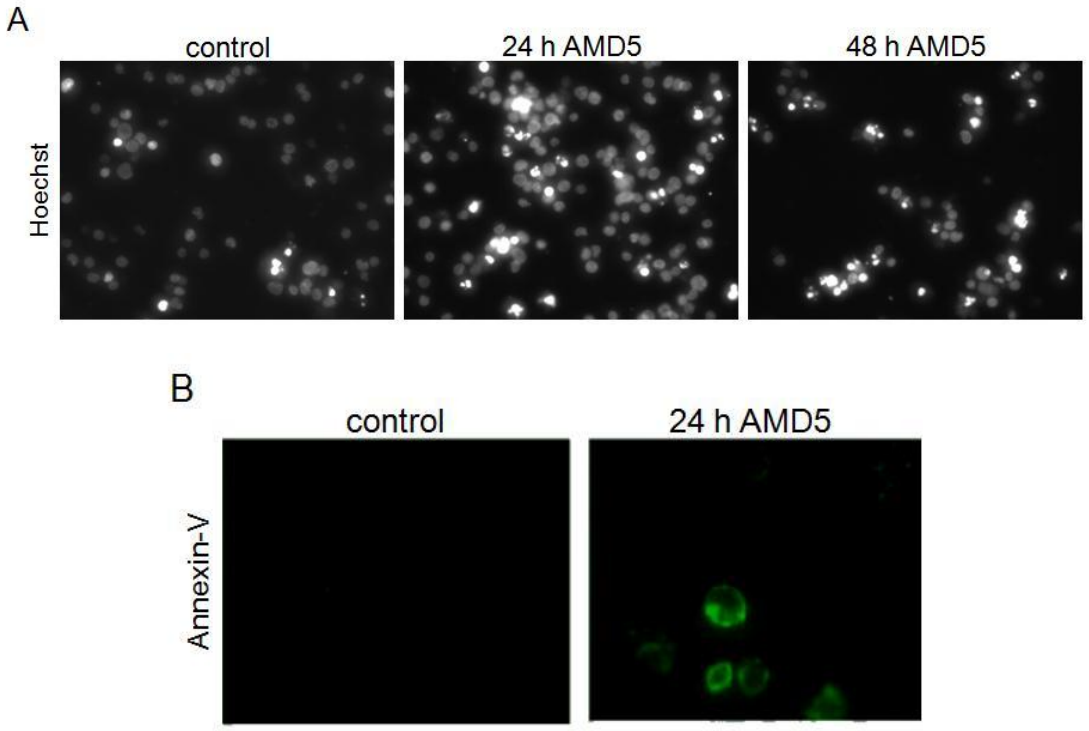

Figure 3. Effect of 10 µM AMD5 after 24 or 48 h on Jurkat cells. (**A**) Jurkat cells were stained with cell-permeable Hoechst 33342 dye to observe apoptotic nuclear morphology. Apoptotic nuclei are brightly stained and condensed compared to healthy nuclei. (**B**) Jurkat cells were incubated with Annexin-V 488 Alexa-Fluor conjugate to observe phosphatidyl-serine flipping from the inner to the outer leaflet of the plasma membrane, a characteristic event of apoptosis. Magnification: 400×

DNA fragmentation observed in Jurkat cells treated with *Amaryllidaceae* alkaloids

The TUNEL (terminal transferase dUTP nick end labeling) assay was used to measure the extent of DNA fragmentation that occurs following treatment with alkaloid AMD5. Cells were grown and treated at 10 µM final concentration for 24 h. At this time-point, approximately 20% of cells displayed characteristic apoptotic morphology with Hoechst staining. As shown in Figure 4, extensive DNA fragmentation was visible by fluorescence microscopy in cells treated with AMD5; this corresponds with the increase in apoptotic morphology at 48 h of treatment with this alkaloid.

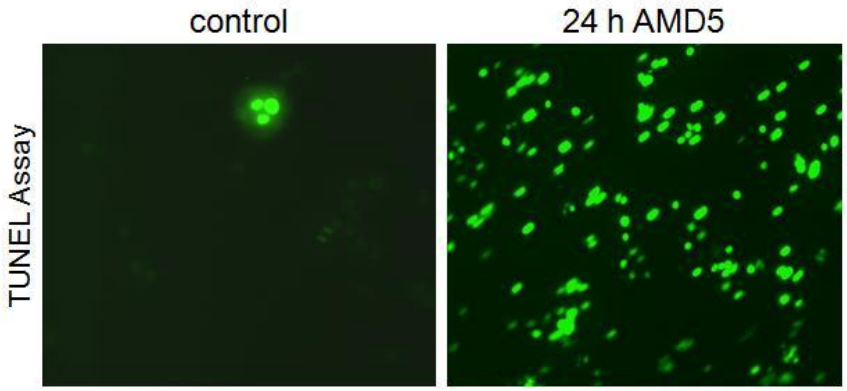

Figure 4. TUNEL assay on Jurkat cells treated with AMD5 at 10 μM for 24 h. Treated Jurkat cells were fixed and immuno-stained with anti-BrdU antibody to observe DNA damage. The level of staining indicates the degree of DNA damage induced by treatment, where positively stained cells are in the final stages of apoptosis. Magnification: 200×

***Amaryllidaceae* alkaloid AMD5 causes early activation of caspase-3; disruption of the mitochondrial membrane potential delayed**

The role of caspases as molecular mediators of apoptosis was examined after treatment up to 48 h with these alkaloids. A slight increase in caspase-3 activation was observed after 6 h in Jurkat cells treated with AMD4; however, a more drastic increase of 3-fold over control was incited after a 3 h treatment with AMD5 (Figure 5A). This assay detects activation of caspases-3, -6 and -7 (executioner caspases) and also measures a change in mitochondrial membrane potential. Our results show that after 48 h the mitochondrial membrane potential has destabilized in correspondence with an increased number of apoptotic cells (Figure 5B). Destabilization of the mitochondrial membrane potential indicates leakage of cytotoxic mitochondrial contents into the cytoplasm, initiating the cell death process.

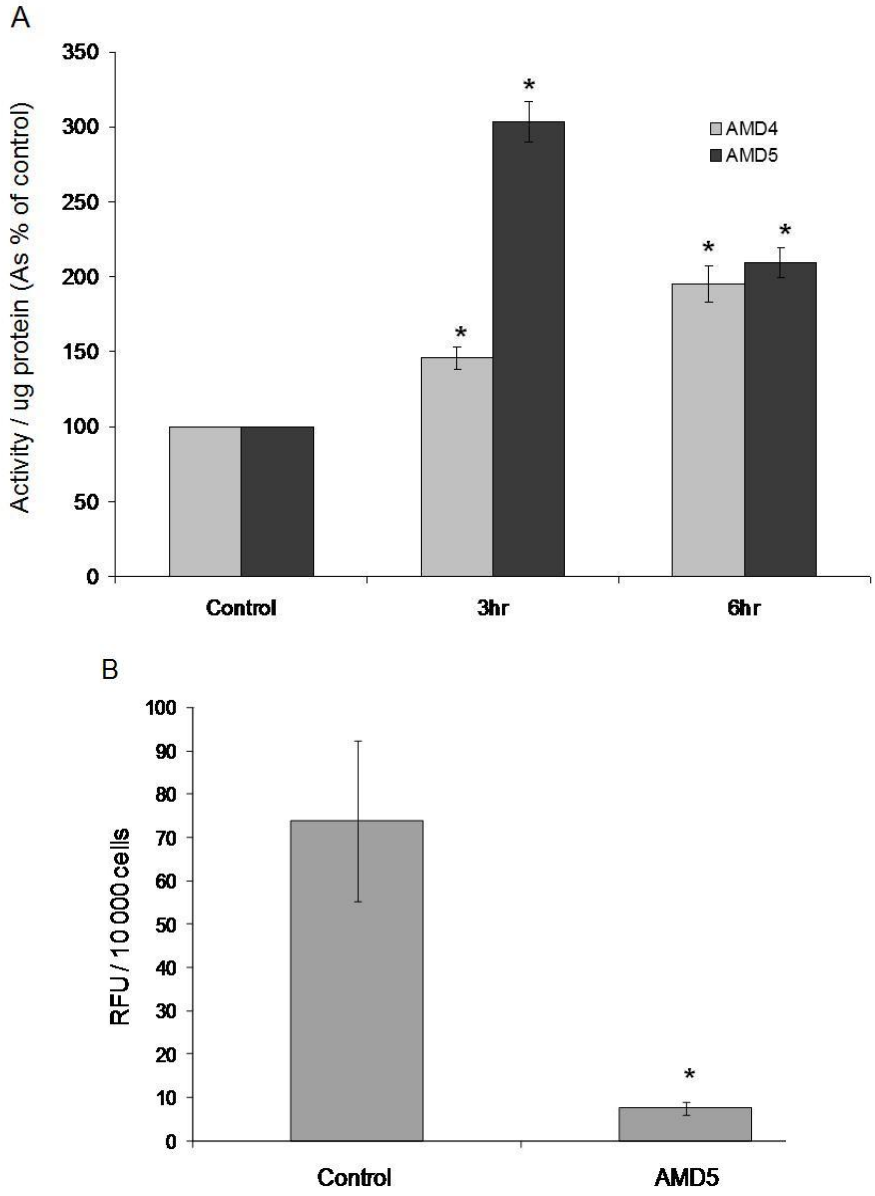

Figure 5. Effect of AMD5 on caspase activity and mitochondrial function. (**A**) Jurkat cells were treated with 10 μM AMD4 or AMD5 for 3 and 6 h and assayed for caspase activity levels. The level of caspase-3 activity was calculated per microgram of protein and then displayed as a percent increase in fluorescence from caspase-3 activity in untreated (control) cells. *Columns*, mean (n=3); *bars*, SD; *, $p<0.05$ significantly different from control by paired t-test. (**B**) Jurkat cells were treated with 10 μM AMD5 for 48 h and monitored with the Mito-Casp Assay. A mitochondrial membrane potential (MMP) sensitive dye was used to measure loss of MMP indicated by a loss of fluorescence. *Columns*, mean (n=3); *bars*, SD; *, $p<0.05$ significantly different from control by paired t-test.

Normal nucleated blood cells are unaffected by treatment with *Amaryllidaceae* alkaloid AMD5

Mononuclear cells from peripheral venous blood were purified from whole blood obtained from a healthy volunteer. Cells were then treated with 10 µM AMD5 for 48 h, and stained with Hoechst dye to observe apoptotic morphology. As shown in Figure 6, this alkaloid had minimal effect on the viability of normal nucleated blood cells in comparison to untreated cells. This result suggests that AMD5 may be less toxic to healthy cells at a dosage capable of inducing apoptosis in approximately 45% of cancerous Jurkat cells after 48 h. As the effect of AMD4 against Jurkat cells was minimal, this alkaloid was not tested against normal nucleated blood cells for specificity.

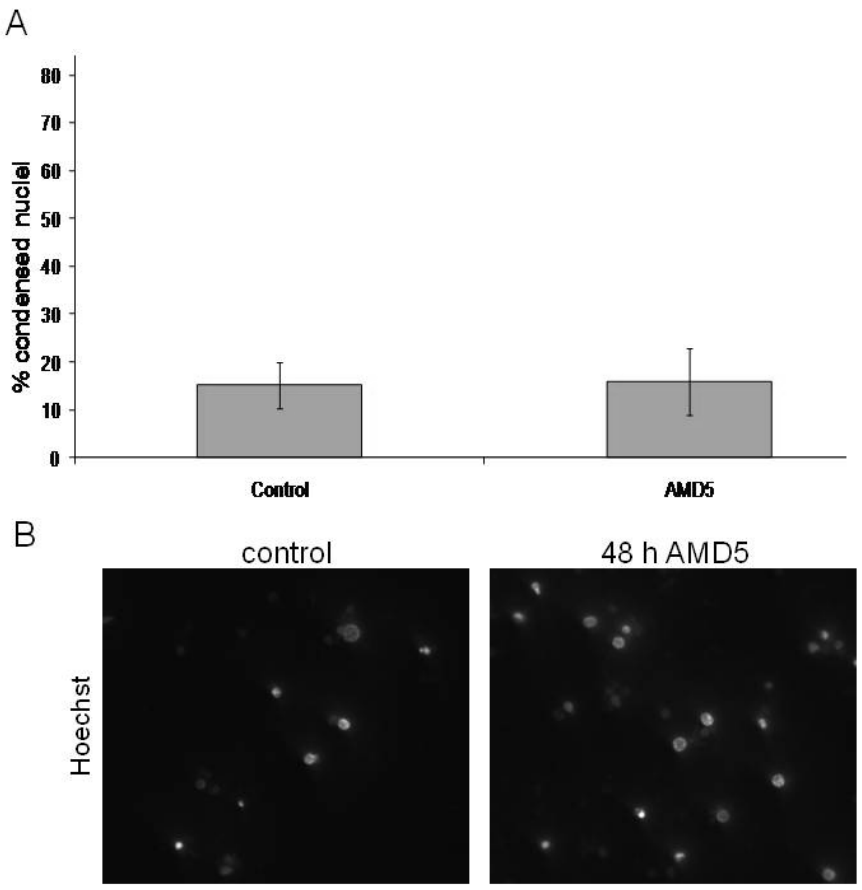

Figure 6. Effect of AMD5 on non-cancerous blood cells. (**A**) Degree of apoptosis in healthy peripheral mono-nucleated blood cells (PMBCs) treated with 10 μM AMD5 for 48 h. Cell permeable Hoechst 33342 dye was used to observe apoptotic nuclear morphology. The percentage of nuclei with apoptotic morphology was calculated by the number of brightly stained condensed nuclei over the total number of nuclei visible. A minimum of 5 fields with at least 100 cells per field were counted. Columns, mean (n=5); *bars*, SD. (**B**) Non-cancerous PBMCs were treated with 10 μM of AMD5 for 48 h and stained with Hoechst dye to observe apoptotic nuclear morphology. Magnification: 200×.

DISCUSSION

Here we observe that AMD5, a natural alkaloid from the *Amaryllidaceae* family, is capable of inducing apoptosis in more than 40% of Jurkat cells at a 10 µM concentration after 48 h treatment. In addition, this alkaloid was observed to have low toxicity to healthy mono-nucleated blood cells after 48 h treatment. This result suggests that crinane-type *Amaryllidaceae* alkaloids may possess anti-cancer activity similar to the lycorane derivatives related to PST. PST has been shown to be a highly specific anti-cancer agent, able to induce apoptosis in over 90% of Jurkat cells in only 24 h at 1 µM final concentration (Kekre *et al,* 2005; Griffin *et al,* 2007; Pandey *et al,* 2007). It appears that a correctly functionalized phenanthridone core may thus be a common minimal structural requirement for these cell specific anti-cancer agents. Although, AMD5 was found to be well tolerated in non-cancerous cell lines in a cell culture model, its effects on physiological parameters in animal models should be evaluated for pharmacokinetic studies to determine the adsorption, distribution, metabolism, excretion and toxic properties.

An early increase in caspase-3 activation upon treatment with AMD5 suggests that the extrinsic pathway of apoptosis may be stimulated by this alkaloid. Our study also found that mitochondrial membrane potential was disrupted after 48 h, when over 40% of cells had apoptotic nuclear morphology. There is substantial cross-talk between the extrinsic and intrinsic pathways of apoptosis, both of which lead to activation of caspase-3 downstream of cleavage and activation of initiator caspases. In comparison with AMD5, AMD4 had minimal effect against cancerous cells, which indicates that the position of the methoxy side-group is crucial. AMD5, with the β-methoxy configuration, may have a stronger interaction with a critical protein versus AMD4, whose functional group is in the alpha configuration. This difference may account for our finding that AMD5 is more efficient at inducing apoptosis in Jurkat cells than AMD4. It must be noted that the addition of an oxymethyl group has been shown to alter the activity of natural alkaloids (Gastpar *et al,* 1998). For example, researchers have observed increased cytotoxic activity of 8-methoxycaffeine compared to the parent compound (Russo *et al,* 1991). Nonetheless, the impact of the configuration of methoxy group and its varied effect on the activity of these AMD alkaloids is a novel and interesting observation.

CONCLUSIONS

A correctly functionalized phenanthridone skeleton present in natural *Amaryllidaceae* alkaloids may be a significant common element for selectivity against cancer cells. Importantly, the configuration of the methoxy-side groups is responsible for higher binding affinity to the target protein/s thus making for a more efficient anti-cancer agent.

REFERENCES

Gastpar R, Goldbrunner M, Marko D, von Angerer E. Methoxy-substituted 3-formyl-2-phenylindoles inhibit tubulin polymerization. J Med Chem 1998; 41(25): 4965-4972.

Griffin C, McNulty J, Hamm C, Pandey S. Pancratistatin: a novel highly selective anti-cancer agent that induces apoptosis by the activation of membrane-Fas-receptor associated caspase-3. Trends in Cell Apoptosis Research. NovaScience Publishers, Inc. 2007. Pgs 93-110.

Kekre N, Griffin C, McNulty J, Pandey S. Pancratistatin causes early activation of caspase-3 and the flipping of phosphatidyl serine followed by rapid apoptosis specifically in human lymphoma cells. Can Chemother Pharmacol 2005; 56: 29-38.

McLachlan A, Kekre N, McNulty J, Pandey S. Pancratistatin: a natural anti-cancer compound that targets mitochondria specifically in cancer cells to induce apoptosis. Apoptosis 2005; 10(3): 619-630.

McNulty J, Larichev V, Pandey S: A synthesis of 3-deoxydihydrolycoricidine: refinement of a structurally minimum Pancratistatin pharmacophore. Bioorg Med Chem Lett 2005; 15(23): 5315-5318.

McNulty J, Mao J, Gibe R, Mo R, Wolf S, Pettit GR, Herald DL, Boyd MR: Studies directed towards the refinement of the Pancratistatin cytotoxic pharmacophore. Bioorg Med Chem Lett 2001; 11(2): 169-172.

Pandey S, Somayajulu M, McLachlan A, Gueorguieva D, Griffin C. The Cutting Edge: Apoptosis and Cell Therapy. Artificial cell, Cell engineering & Therapy. Woodhead Publishers, Ltd. 2007. Pgs 117-136.

Pettit GR, Eastham SA, Melody N, Orr B, Herald DL, McGregor J, Knight C, Doubek DL, Pettit GR 3rd, Garner LC, Bell JA. Isolation and structural modification of 7-deoxynarciclasine and 7-deoxy-trans-dihydronarciclasine. J Nat Prod 2006; 69(1): 7-13.

Pettit GR, Melody N, Herald DL. Antineoplastic agents. 511. Direct phosphorylation of phenpanstatin and pancratistatin. J Nat Prod 2004; 67(3): 322-327.

Pettit GR, Pettit GR III, Backhaus RA, Boyd MR, Meerow AW: Antineoplastic Agents 256. Cell Growth Inhibitory Isocarbostyrils from Hymenocallis. J Nat Prod 1993; 56: 1682.

Rinner U, Hillebrenner HL, Adams DR, Hudlicky T, Pettit GR. Synthesis and biological activity of some structural modifications of pancratistatin. Bioorg Med Chem Lett 2004; 14: 2911–2915.

Russo P, Poggi L, Parodi S, Pedrini AM, Kohn KW, Pommier Y. Production of protein-associated DNA breaks by 8-methoxycaffeine, caffeine and 8-chlorocaffeine in isolated nuclei from L1210 cells: comparison with those produced by topoisomerase II inhibitors. Carcinogenesis 1991; 12(10): 1781-1790.

CHAPTER 5

Pancratistatin selectively targets cancer cell mitochondria and reduces growth of human colon tumor xenografts

BACKGROUND

Colorectal cancer is the third most diagnosed cancer worldwide and has a mortality rate of nearly 1 in 2 (Weekes *et al,* 2009). Current adjuvant chemotherapy of metastasized colorectal cancer includes DNA machinery-targeting drugs irinotecan, oxaliplatin, leucovorin and/or 5-fluorouracil (Weekes *et al,* 2009). More than 50% of chemotherapy agents currently in use are natural products or derived directly from natural sources, and recently there has been increasing interest in natural products as potential sources for novel therapeutics (Newman and Cragg, 2007; Deorukhkar *et al,* 2007). The findings presented in this article suggest that the natural alkaloid pancratistatin may act directly on the mitochondria to induce apoptosis selectively in human colorectal adenocarcinoma cells.

Pancratistatin is an *Amaryllidaceae* alkaloid isolated from the bulb of the *H. littoralis* species of spider lily. Numerous *Amaryllidaceae* alkaloids have been isolated and have diverse bioactivities; a few with potential medicinal properties (Kornienko and Evidente, 2008). We have recently shown that Pancratistatin induces apoptosis in several cancer cell lines and in *ex vivo* models of leukemia, with minimal effect on the growth and survival of non-cancerous counterpart cells (Chatterjee *et al,* 2011; Griffin *et al,* 2010; Kekre *et al,* 2005). We have previously reported that pancratistatin promotes reactive oxygen species (ROS) generation and mitochondrial depolarization leading to apoptosis in breast carcinoma cells independent of estrogen receptor status (McLachlan *et al,* 2005; Siedlakowski *et al,* 2008).

Apoptosis is a cell death program that can be induced by either the extrinsic or intrinsic pathways, although extensive cross-talk exists between them (Ravizza *et al,* 2004). Classical genotoxic chemotherapeutic agents cause intrinsic apoptosis by inducing extreme stress to the DNA and its repair mechanisms, but are also toxic to non-cancerous cells (Dy *et al,* 2008). Development of targeted therapeutics has lead to increased selectivity, albeit these options are often effective against only a small subset of cancers. Recently, a number of naturally derived mitochondria-directed small molecules, referred to as *mitocans*, have shown promise as selective anti-cancer agents (Ralph *et al,* 2010; Wang *et al,* 2010). Mitochondrial perturbation, either directly by small molecules or indirectly by activation of pro-apoptotic proteins, causes release of cytotoxic components such as cytochrome *c*, which leads to caspase activation, and ultimately apoptosis (Armstrong, 2006). Mitochondria-targeted compounds may be able to induce

apoptosis independent of p53 – a frequently mutated tumor suppressor in human carcinomas (Fantin and Leder, 2006).

In response to cellular stress, multifunctional p53 transcription factor induces the intrinsic pathway of apoptosis by activating specific pro-apoptotic BH3-only proteins of the Bcl-2 family (Green and Kroemer, 2009). Activated BH3-only proteins further activate multi-domain pro-apoptotic proteins Bax and/or Bak, which localize to the mitochondria and form oligomers that cause mitochondrial outer membrane permeabilization, leading to apoptosis (Wang *et al,* 2010). In this way, p53 plays a very important role as a potent tumor suppressor protein. Loss-of-function mutations in p53 correlate to aggressive, chemo-resistant tumors, especially in patients with colorectal cancer (Ravizza *et al,* 2004). In this study, the p53-negative HT-29 colorectal adenocarinoma cell line was compared to the wild-type p53 HCT116 colorectal carcinoma cell line to determine the efficacy of pancratistatin in both systems (Ravizza *et al,* 2004).

Here we report the novel finding that pancratistatin induces apoptosis in HT29 and HCT116 colon carcinoma cell lines *in vitro* and reduces growth of HT-29 xenografts *in vivo*. This study suggests that cell death induced by pancratistatin may be dependent on a component of the mitochondrial respiratory chain (MRC). For the first time we show that pancratistatin significantly reduces growth of p53-mutant HT-29 xenografts in nude mice and importantly, pancratistatin does not cause cell death in non-cancerous CCD-18Co colon fibroblasts. Our findings suggest that pancratistatin selectively targets cancer cell mitochondria to induce apoptosis, with minimal toxicity to non-cancerous cells.

METHODS

Chemicals

Media, gentamycin, Hoechst 33342 dye, JC-1 dye, Annexin-V AlexaFluor 488, and the TUNEL assay kit (Cat# A23210) were purchased from Invitrogen (GIBCO), Burlington, ON. Cell proliferation reagent WST-1 was purchased from Roche (Mississauga, ON). A water-soluble formulation of Coenzyme Q10 (ws-CoQ_{10}) was developed and provided by Dr. M. Sikorska at the National Research Council of Canada (US patents #6,045,826,6,191,172 B1 and 6,632,443). Benzyloxycarbonyl-Val-Ala-Asp(Ome)-fluoromethylketone (z-VAD-fmk) was used as a general caspase inhibitor, purchased from EMD BioSciences, Inc (Gibbstown, NJ). Anti-β-actin and anti-SDH-A antibodies were purchased from Santa Cruz Biotechnology, Inc (Santa Cruz, CA). Anti-cytochrome *c*, anti-AIF and anti-EndoG antibodies were purchased from AbCam (Cambridge, MA). Anti-Bcl-2 family antibodies were purchased from Sigma (Mississauga, ON). Anti-phosphohistone (Ser139) antibody (H2AX) was purchased from Upstate Chemicals (Billerica, MA). Bradford reagent was obtained from BioRad, Mississauga, ON. Pancratistatin (Figure 1A) was isolated from *H. littoralis* as previously described (McNulty *et al,* 2001) and provided by Dr. J. McNulty. All other chemicals were purchased from Sigma-Aldrich (Oakville, ON).

Cell lines, culture conditions, and assessment of apoptosis

Normal colon fibroblasts (CCD-18Co) and human colorectal adenocarcinoma (HT-29, HCT116) cells were purchased from American Type Culture Collection (Manassas, VA). Cells were passaged for fewer than 6 months and no authentication of cell lines was performed by the authors. HT-29 and HCT116 cells were grown in McCoy's 5A media and CCD-18Co cells were grown in Eagle's MEM; both supplemented as recommended by ATCC. Parental stock glioblastoma (U87MG) and the counterpart mtDNA-depleted cell line (U87MG ρ^0) were a generous gift from Dr. M. Sikorska at NRC, Ottawa, ON (Sandhu *et al,* 2005). These cells were grown in MEM supplemented with 10% FBS and 10 μM gentamycin. Human neuroblastoma (SH-SY5Y) cells transfected with single-domain antibodies against Bax protein were established and maintained as previously described (Gueorguieva *et al,* 2006). All cells were maintained at 5% CO_2 and 37°C. Cells were treated as indicated with 1 μM pancratistatin, predetermined as the effective concentration (Kekre *et al,* 2005; Pandey *et al,* 2005).

Nuclear morphology was evaluated by fluorescence microscopy after staining with Hoechst 33342 dye. Percent condensed nuclei (indicative of apoptosis) was calculated as [(number of cells with condensed, brightly stained nuclei / total number of cells)*100] with a minimum 5 fields with 100 cells/field counted.

Cytotoxicity assays

Cytotoxicity was measured using the WST-1 colorimetric assay following the manufacturer's protocol. Briefly, cells were seeded at 2 000 – 5 000 cells/well in 96-well tissue culture plates, allowed to adhere overnight and treated as indicated. Cells were then incubated with WST-1 for 4 h at 37°C. Absorbance was measured at 450 nm on a VICTOR^3 microplate reader. Absorbance is directly proportional to the number of living cells in culture. Percent viability was calculated based on average absorbance of untreated cells. To monitor the effect of pancratistatin on cell growth, cells were counted using the Trypan Blue Exclusion assay.

Mitochondrial functionality assays

Mitochondrial membrane potential (MMP) was observed using cell permeable JC-1 dye (1 µM) as previously described (McLachlan *et al,* 2005). To detect generation of reactive oxygen species (ROS) cells were treated with pancratistatin for the indicated time, trypsinized and incubated with H_2DCFDA (1 µM) for 45 min at 37°C in an opaque 96-well plate. Fluorescence was measured at Ex. 513 nm and Em. 530 nm using a SpectraMax GeminiXPS spectrofluorometer. Change in ROS generation was calculated as the fold difference from control (RFU) per 10^3 cells; cells were counted using the Trypan Blue Exclusion assay. Cytotoxicity and ROS generation was used to analyze the effect of anti-oxidants on pancratistatin treatment. Cells were co-treated with pancratistatin (1 µM) and either N-acetyl cysteine (5 mM) or ws- CoQ_{10} (50 µg/ml) for 48 or 72 h.

Mitochondrial isolation and western blotting

Cells treated with pancratistatin were washed with ice-cold PBS and the pellet was re-suspended in cold mitochondrial isolation buffer (75 mM sucrose, 20 mM HEPES, 225 mM mannitol, 0.5 mM EDTA, pH 7.2) and then disrupted by homogenization. Non-lysed cells/nuclei were pelleted by centrifugation at 500 x *g* for 15 min at 4°C. The

supernatant was further centrifuged at 4°C and 10 000 x *g* for 10 min, twice. The resulting pellet was designated as the mitochondrial fraction and the supernatant as the cytosolic fraction. Protein samples (20 µg) were separated by SDS-PAGE, transferred to nitrocellulose and probed with the indicated primary antibody (1:1000) overnight at 4°C. Membranes were then incubated with peroxidase-conjugated secondary antibody (1:1000) for 1 h at 25°C and visualized using enhanced chemiluminescence reagent. Equal loading of the protein samples was confirmed by parallel western blots for β-actin or SDH-A. Images were digitized and band intensity was quantified using NIH Image *J* software.

β-Tubulin polymerization activity assay

To determine whether pancratistatin affects the rate of β-tubulin polymerization / depolymerization compared to known polymerizing agent paclitaxel, the HTS-Tubulin Polymerization Assay kit (Cat. # BK004, Cytoskeleton Inc., Denver, CO) was utilized as described by the manufacturer and elsewhere (Li *et al,* 2009). Microtubule assembly was monitored by spectrophotometry as a change in absorbance at 340 nm every minute for 60 min at 37°C using a SpectraMax M5^e microplate reader.

Histone H2AX phosphorylation

To detect double-strand DNA breaks, cells were grown on cover-slips and treated with pancratistatin for 6 hrs then processed for immunohistochemical analysis of histone H2AX phosphorylation on Ser-139, as previously described (Kekre *et al,* 2005).

***In vivo* xenograft models**

Six-week old male homozygous CD-1 nude mice (25 – 30 g) were obtained from Charles River Laboratories, St. Constant, QC. Animals were housed in constant laboratory conditions of a 12 h light/dark cycle at 21°C in accordance with institutional animal protocols (University of Windsor Research Ethics Board - AUPP05). Prior to injection, HT-29 cells were washed with PBS and centrifuged at 500 x *g* for 5 min; cell pellets were suspended in aliquots of 200 µl PBS (4 x 10^6 cells per mouse). The cell suspension was injected s.c. in the right hind flank of each mouse. Tumors were allowed to grow to ~50 mm^3 and thereafter animals were randomized into treatment groups of 6 mice each (day 14 of study). Animals were treated intra-tumor (I.T.) with vehicle (5 µl

Me_2SO in PBS) or pancratistatin (3 mg/kg) twice a week for 5 weeks (Gabrielsen *et al,* 1992; Shah *et al,* 2009). Tumors were assessed at each treatment by measuring length and width using standard calipers; tumor volume was calculated using the formula [π/6 x length x width^2]. In parallel, tumor-free mice were treated intra-peritoneally (I.P.) twice a week for 2 months with vehicle or pancratistatin for toxicity studies. All animals were assessed for weight-loss twice weekly for the duration of the experiment.

Hematoxylin & Eosin staining and immunohistochemical analysis

One week after the last treatment, the tumor, liver and kidneys were collected from all animals and fixed in 10% formalin in PBS for up to 24 h, then moved to 70% ethanol. Sections of 8 µm thickness were sliced from paraffin-embedded tissues and placed on Superfrost/Plus microscope slides (Fisher Scientific, Ottawa, ON) for histopathological (H&E) and immunohistochemical (TUNEL) analysis. Slides were deparaffinized and hydrated for terminal deoxynucleotide transferase dUTP nick end labeling (TUNEL) assay.

RESULTS

Pancratistatin selectively induces cell death in colon cancer cells

We determined the effect of pancratistatin (refer to Figure 1A for chemical structure) on the viability of HT29 and HCT116 human colorectal adenocarcinoma cells, and non-cancerous human colon fibroblast CCD-18Co cells. Nuclear morphology of HT-29 and HCT116 cells after 72 h of pancratistatin exposure revealed brightly stained condensed nuclei characteristic of cells undergoing apoptosis, in contrast to CCD-18Co nuclear morphology, which was unchanged (Figure 1B). Viability of both colon cancer cell lines was significantly reduced after 72 h exposure to pancratistatin in a concentration-dependent manner, with an IC_{50} of ~100 nmol/L for both cell types (Figure 1C). By comparison, 100 nmol/L pancratistatin was significantly less toxic to non-cancerous CCD-18Co, and the IC_{50} for this non-cancerous cell line was determined to be 10 μmol/L (Figure 1C). We have previously reported the selective anti-cancer activity of pancratistatin using human cancerous and non-cancerous breast cell lines, and human leukemic and non-cancerous peripheral blood mononuclear cells (6, 9). As shown in Figure 1D, growth of HT-29 cells was dramatically reduced when treated with pancratistatin, especially when pancratistatin was added again after 72 h initial exposure. Moreover, HT29 cells remaining after 144 h pancratistatin single treatment were unable to proliferate when given fresh drug-free media and cultured for up to 72 h (Figure 1D). A similar effect was also observed in HCT116 cells (Supplementary Figure 1). These results indicated that pancratistatin decreased survival of human colorectal carcinoma cells, irrespective of p53-status, with minimal toxicity to non-cancerous colon fibroblasts.

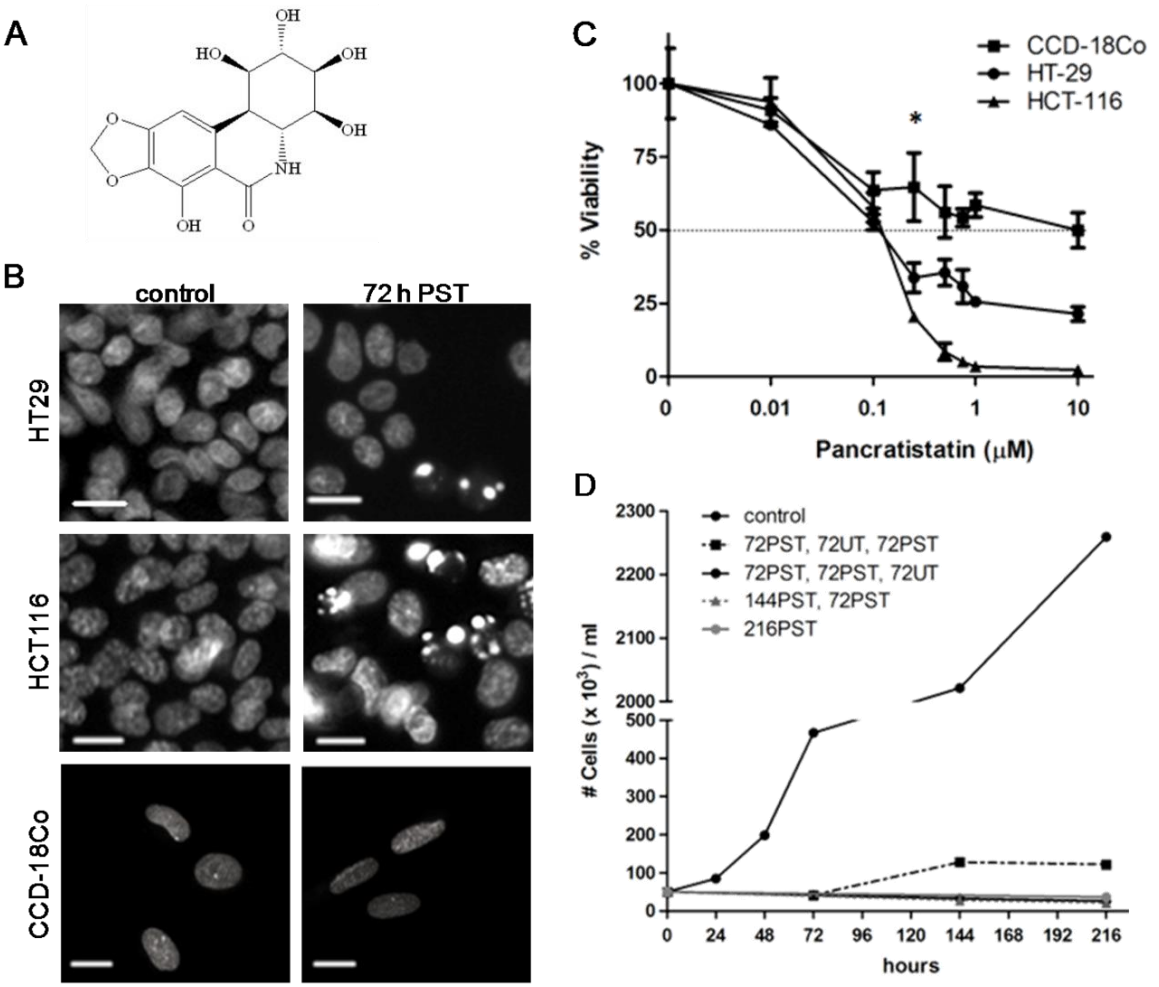

Figure 1. Pancratistatin selectively affects colon carcinoma cells. (**A**) Chemical structure of pancratistatin. (**B**) Representative nuclear morphology of HT-29, HCT116 and CCD-18Co cells stained with Hoechst dye after 72 h with 1 µM pancratistatin (PST) or control (Me_2SO). Scale bars represent 20 µm. (**C**) HT-29, HCT116 and CCD-18Co cells were treated with control (Me_2SO) or the indicated doses of pancratistatin for 72 h. Cytotoxicity was measured by the WST-1 colorimetric assay. *Data points*, mean (n=3); *bars*, SD. *, $P < 0.05$, significantly different between cell lines by two-tailed, paired *t*-test. (**D**) HT-29 cells treated for the indicated times with control (Me_2SO) or 1 µM pancratistatin (PST). Cell number was determined by Trypan blue dye exclusion assay. Cells cultured with fresh drug-free media (UT) after exposure to PST for the indicated time were unable to proliferate. *Data points*, mean (n=3); bars, SD.

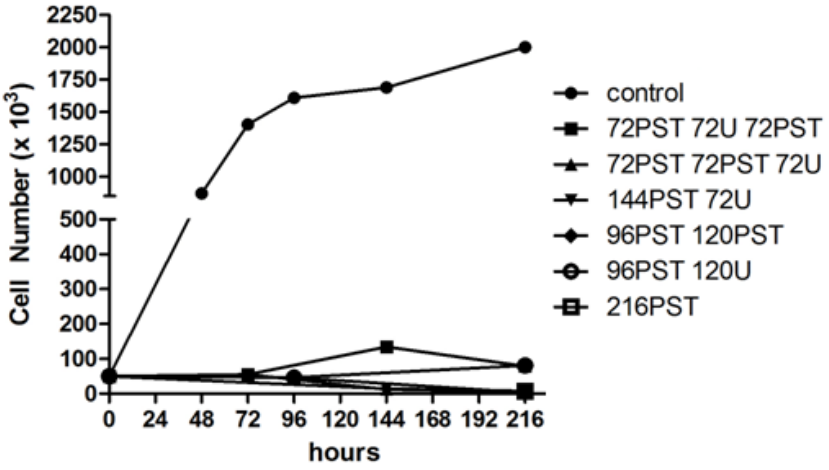

Supplementary Figure 1. Cell growth of HCT116 determined by Trypan blue exclusion assay. HCT116 cells were treated for the indicated times with control (Me_2SO) or 1 µM pancratistatin (PST) and cell number was determined by Trypan blue dye exclusion assay. Cells cultured with fresh drug-free media (U) after exposure to PST for the indicated time were unable to proliferate. *Data points*, mean (n=3).

Pancratistatin destabilizes cancer cell mitochondria

Dissipation of the mitochondria membrane potential (MMP), increased generation of reactive oxygen species (ROS) and release of pro-apoptotic factors like cytochrome *c* are characteristic features of mitochondria-mediated apoptosis. Thus, we monitored the occurrence of these phenomena in HT-29, HCT116 and CCD-18Co cell lines following pancratistatin treatment. First, the effect of pancratistatin on MMP using JC-1 fluorescence microscopy was observed. HT-29 cells treated with pancratistatin had a reduction in JC-1 aggregation compared to Me_2SO-treated (control) cells, as observed by a decrease in fluorescence. HCT116 cells also displayed reduced aggregation of JC-1 dye compared to control, indicating loss of MMP. Importantly, there was no evidence of MMP collapse in non-cancerous CCD-18Co cells treated with the same concentration of pancratistatin for 96 h (Figure 2A). This finding suggested that pancratistatin specifically targets cancer-cell mitochondria to cause MMP collapse and subsequent cell death, without affecting the potential of non-cancerous mitochondria.

Next, we tested the degree of ROS generation in HT-29 and HCT116 cells following exposure to pancratistatin. Over-production of ROS can trigger intrinsically-mediated apoptosis and has recently been described as a powerful method to induce cancer cell death in a selective manner (Ralph *et al,* 2010). Indeed in both cell lines there was a significant increase in ROS production that correlated with increased pancratistatin-incubation time (Figure 2B). Lastly, we tested for the release of the pro-apoptotic protein cytochrome *c* from the mitochondria to the cytosol in pancratistatin treated HT-29 cells. In accordance with pancratistatin-mediated MMP collapse, western blot analysis showed release of cytochrome *c* into the cytosolic fraction of cells treated with pancratistatin compared to untreated control cells (Figure 2C). These results indicated that pancratistatin caused collapse of MMP that was associated with release of cytochrome *c* and increased ROS generation.

To determine the effect of anti-oxidants on pancratistatin-induced ROS generation and cell death, HT-29 cells were co-treated with pancratistatin and N-acetylcysteine (NAC) for 48 and 72 h. As expected, co-treatment with NAC reduced ROS generation by approximately 2-fold compared to pancratistatin alone; however, NAC failed to protect cells from pancratistatin-induced apoptosis (Figure 2D). To extend this finding, the effect on cell viability of co-treatment of pancratistatin with other potential antagonists was tested on HT-29 cells. Cells were treated with and without 1 μM

pancratistatin, and with and without antagonists of mitochondria-specific components. The effect of NAC and another anti-oxidant, water-soluble Coenzyme Q10 (Q10), along with inhibitors of mitochondrial respiratory chain (MRC) complex I, Rotenone, and complex III, Antimycin A was monitored after 72 h treatment. In addition, we tested the effect of co-treatment with mitochondrial permeability transition pore (MPTP) inhibitor Cyclosporin A. Incubation with each of these antagonists alone did not significantly decrease cell viability of HT-29 cells after 72 h. Pancratistatin treatment decreased cell viability to less than 40%, and this response was unaltered by co-treatment with Rotenone, NAC or Q10. Co-treatment with pancratistatin and cyclosporin A resulted in a nearly 80% decrease in cell viability compared to cyclosporin A alone. Interestingly, co-treatment of pancratistatin with complex III inhibitor Antimycin A increased cell viability by approximately 45% over pancratistatin treatment alone (Supplementary Figure 2). These results indicate that pancratistatin may be targeting complex III of the MRC in colon cancer cells to induce ROS production leading to cell death.

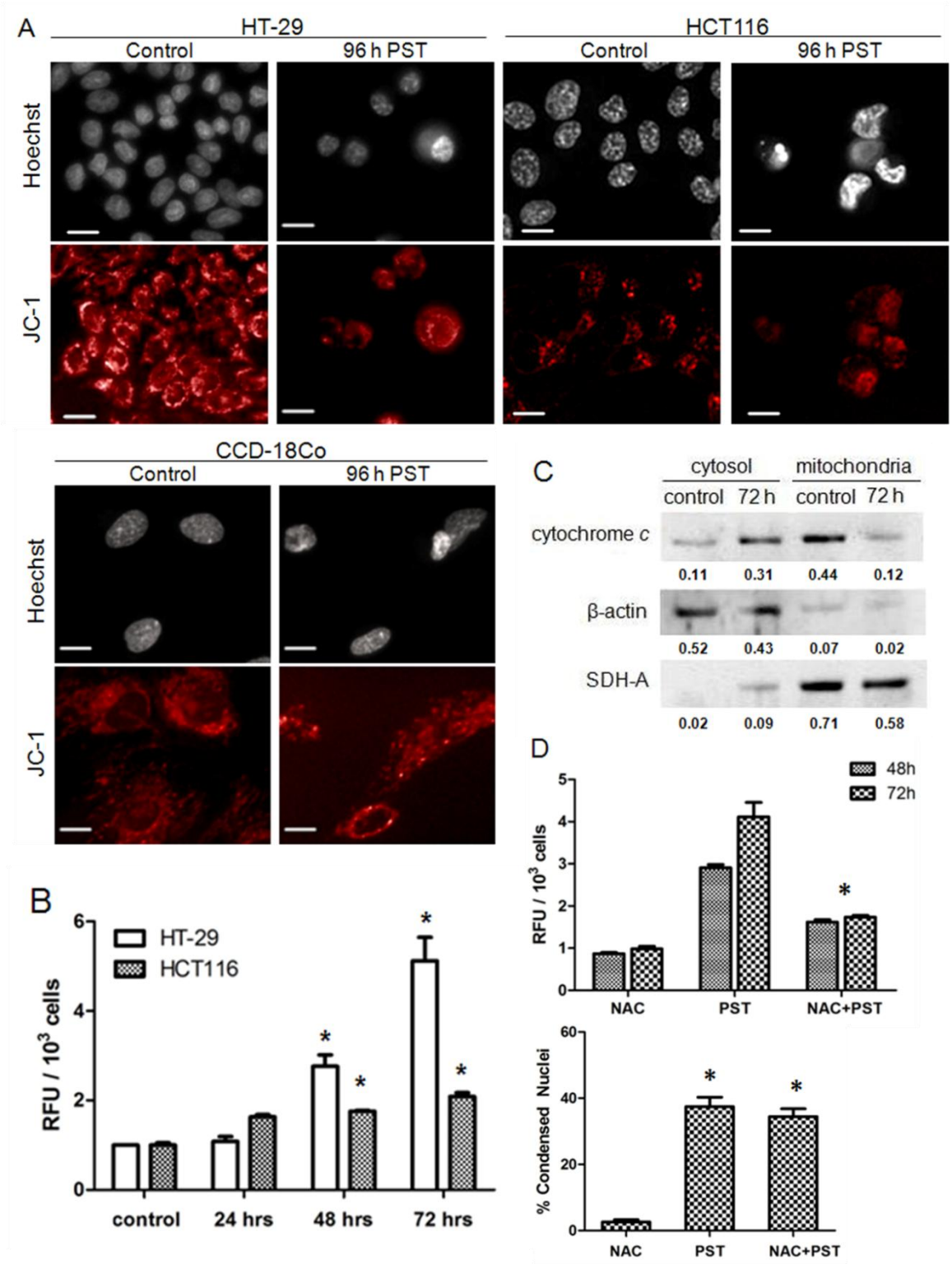
A
HT-29
HCT116
Control
96 h PST
Control
96 h PST
Hoechst
JC-1
CCD-18Co
Control
96 h PST
Hoechst
JC-1
B
HT-29
HCT116
RFU / 10^3 cells
control
24 hrs
48 hrs
72 hrs
C
cytosol
mitochondria
control
72 h
control
72 h
cytochrome c
0.11
0.31
0.44
0.12
β-actin
0.52
0.43
0.07
0.02
SDH-A
0.02
0.09
0.71
0.58
D
48h
72h
RFU / 10^3 cells
NAC
PST
NAC+PST
% Condensed Nuclei
NAC
PST
NAC+PST

Figure 2. Pancratistatin selectively affects mitochondrial function of colon cancer cells. (**A**) Representative fluorescence micrographs HT-29, HCT116 and CCD-18Co cells stained with Hoechst and JC-1 dye after 96 h with 1 µM pancratistatin (PST) or control (Me_2SO). Scale bars represent 15 µm. Pancratistatin induced MMP collapse in HT-29 and HCT116, but not in CCD-18Co cells. (**B**) Measurement of whole-cell ROS production in HT-29 and HCT116 cells after indicated length of exposure to control (Me_2SO) or 1 µM pancratistatin. Fluorescence generated by the oxidized product of H_2DCFDA is expressed as fold-difference of control per 10 000 cells in relative fluorescence units (RFU) and is indicative of cellular ROS levels. *Columns*, mean (n=3); *bars*, SD; *, $P < 0.05$, significantly different from control by one-tailed paired *t*-test. (**C**) HT-29 cells were treated with control (Me_2SO) or 1 µM pancratistatin for 72 h. Cytosolic and mitochondrial fractions were separated by SDS-PAGE followed by immunoblotting using specific antibodies against cytochrome *c*; antibodies against β-actin and succinate dehydrogenase-a (SDHA) were used as loading controls. Immunoblot images were digitized and the optical densities were quantified. (**D**) Measurement of whole-cell ROS production in HT-29 cells after 48 or 72 h exposure to 5 mM N-acetylcysteine (NAC) or 1 µM pancratistatin (PST) or co-treatment with both compounds. Fluorescence generated is expressed as fold-difference of control per 10 000 cells in relative fluorescence units (RFU). *Columns*, mean (n=3); *bars*, SD; *, $P < 0.05$, significantly different from pancratistatin treatment by one-tailed paired *t*-test. Quantification of condensed nuclei, characteristic to apoptotic cells, by Hoechst dye. HT-29 cells were treated with 5 mM NAC or 1 µM PST or co-treatment for 72 h and manually counted. A minimum 5 fields with 100 cells/field was counted. *Columns*, mean (n=5); *bars*, SD; *, $P < 0.05$, significantly different from NAC treatment by one-tailed paired *t*-test.

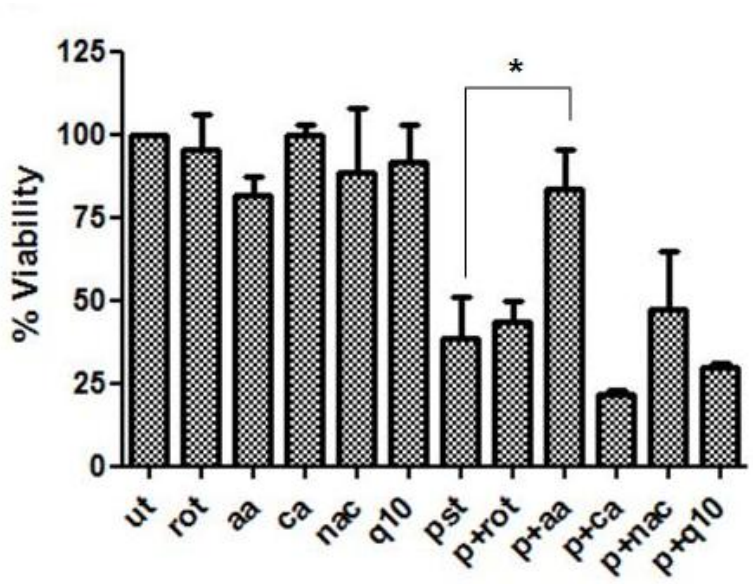

Supplementary Figure 2. Effect of co-treatment with pancratistatin and anti-oxidants or MRC inhibitors on HT29 cell viability. HT-29 cells were treated with 1 µM pancratistatin (pst, p) with and without various antagonists. The effect of treatment on cell viability was determined by WST-1 assay after 72 h. Antagonists studied: 10 µM Rotenone (rot), 5 µM Antimycin A (aa), 5 µM cyclosporin A (ca), 5 mM N-acetylcysteine (nac), 50 µg/ml water-soluble Coenzyme Q_{10} (q10). *Columns*, mean (n=6); *bars*, SD; *, $p<0.05$ significantly different between indicated treatments by one-tailed paired *t*-test.

Mitochondrial DNA-deficient ρ^0 cells are resistant to pancratistatin-induced apoptosis

To firmly establish that mitochondria are involved in pancratistatin-induced cell death, we used the Rho-0 (ρ^0) variant of U87MG glioblastoma cells in parallel with wild-type "parental" U87MG cells. Rho-0 cells depend on ATP derived from anaerobic glycolysis for survival; these cells lack the machinery required for oxidative phosphorylation and thus cannot generate ROS (Hu *et al,* 2000). We then aimed to determine whether pancratistatin can induce apoptosis in either the parental and ρ^0 U87MG cancer cells. As anticipated, we found that ρ^0 cells were resistant to 1 μM pancratistatin compared to wild-type cells, which had nuclear and cellular morphology characteristic of apoptosis (Figure 3A). Exposure to pancratistatin for 120 h resulted in a significant (50%) increase in apoptosis of wild-type cells over to ρ^0 cells (Figure 3B). This finding suggested that pancratistatin may target a component of mitochondrial respiratory chain (MRC) complexes to selectively induce apoptosis in cancer cells.

Bax inhibition does not attenuate pancratistatin-induced apoptosis

The Bcl-2 family of anti- and pro-apoptotic proteins is involved in the regulation of the intrinsic pathway of apoptosis. Activation of pro-apoptotic Bax protein leads to permeabilization of the mitochondrial outer membrane and subsequent cell death. To investigate if mitochondrial destabilization caused by pancratistatin is mediated by Bax, we utilized intracellularly expressed anti-Bax single-domain antibodies (sdAbs), also termed intra-bodies, previously established in our lab (Gueorguieva *et al,* 2006). Stable transfection with one of three anti-Bax intra-bodies (sdAb-1, -2, -4) into human neuroblastoma (SH-SY5Y) cells effectively blocks the pro-apoptotic function of Bax protein *in vivo*, and has been shown to prevent oxidative stress-induced apoptosis (Gueorguieva *et al,* 2006). As shown in figure 3C, Bax inhibition was unable to protect SH-SY5Y cells from pancratistatin-induced apoptosis. This novel finding suggested that pancratistatin acts independent of Bax function to induce cell death in cancer cells.

Furthermore, we studied the expression and localization of endogenous Bcl-2 family proteins in HT-29 and HCT116 cell lines. Interestingly, pancratistatin treatment caused increased mitochondrial localization of Bax protein in wild-type p53 HCT116 cells compared to control (Figure 3D). In contrast, pancratistatin caused no change in localization of Bax in p53-negative HT-29 cells, but instead caused increased expression

of the protein in the cytosol (Figure 3D). The significance of the differential response to pancratistatin treatment between cell lines is unknown at this time, and may be due to p53-mediated effects. In both cell lines, Bcl-2 protein was largely contained to the mitochondrial fraction, and pancratistatin treatment resulted in an increased proportion of cytosolic Bcl-2 significantly in HCT116 cells (Figure 3D). Taken together, these findings suggested that although pancratistatin may alter expression and localization of Bcl-2 family proteins, the pro-apoptotic function of Bax is not required for cell death induced by pancratistatin.

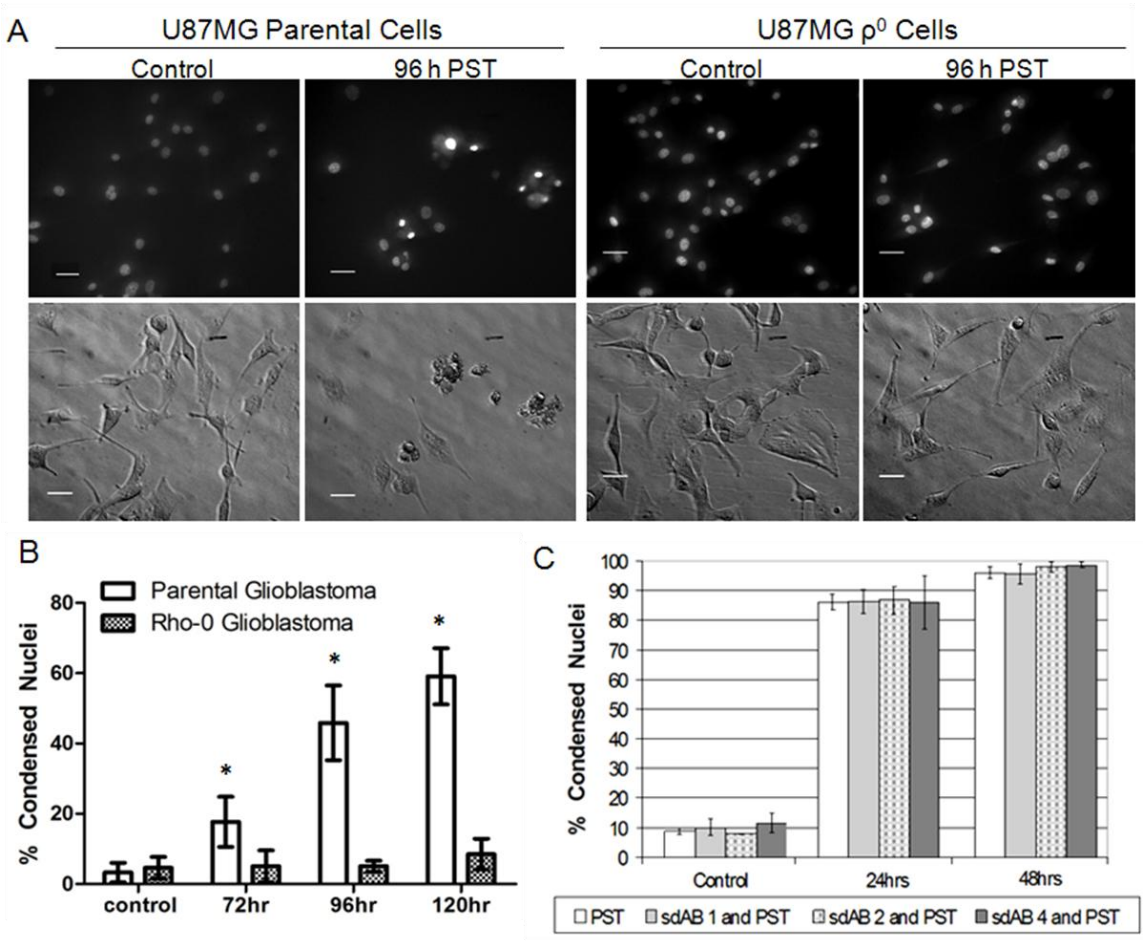
A
U87MG Parental Cells
U87MG ρ0 Cells
Control
96 h PST
Control
96 h PST
B
Parental Glioblastoma
Rho-0 Glioblastoma
% Condensed Nuclei
control
72hr
96hr
120hr
C
% Condensed Nuclei
Control
24hrs
48hrs
PST
sdAB 1 and PST
sdAB 2 and PST
sdAB 4 and PST
D
HCT116
HT29
control
72h PST
c
m
IB: Bax
IB: Bcl-2
IB: SDH-A
IB: β-actin
0.52 0.19 0.75 0.64
0.13 0.02 0.40 0.05
0.20 0.58 0.65 0.86
0.34 0.67 0.37 0.68
0.07 0.59 0.04 0.60
0.08 0.48 0.16 0.41
0.51 0.28 0.56 0.11
0.70 0.58 0.65 0.22

Figure 3. Pancratistatin activity is mitochondria-dependent. (**A**) Representative nuclear and cellular morphology of parental and ρ^0 (Rho-0) glioblastoma U87MG cells stained with Hoechst dye after 96 h with 1 µM pancratistatin (PST) or control (Me_2SO). Scale bars represent 15 µm. (**B**) Quantification of condensed brightly stained nuclei by Hoechst dye, characteristic of apoptotic cells. Parental and ρ^0 (Rho-0) glioblastoma U87MG cells were treated with control (Me_2SO) or 1 µM pancratistatin for 72, 96, or 120 h and manually counted. A minimum 5 fields with 100 cells / field was counted. *Columns*, mean (n=6); *bars*, SD; *, $P < 0.05$, significantly different from control by paired *t*-test. (**C**) Quantification of condensed, brightly stained nuclei by Hoechst dye, characteristic of apoptotic cells. Human neuroblastoma SH-SY5Y cells stably expressing intracellular anti-Bax intra-bodies (sdAB-1, sdAB-2 or sdAB-4), treated with control (Me_2SO) or 1 µM pancratistatin (PST) for 24 or 48 h and manually counted. *Columns*, mean (n=5); bars, SD. (**D**) HCT116 and HT-29 cells were treated with control (Me_2SO) or 1 µM pancratistatin for 72 h. Cytosolic and mitochondrial fractions were separated by SDS-PAGE followed by immunoblotting using specific antibodies against Bax or Bcl-2; antibodies against succinate dehydrogenase-a (SDHA) and β-actin were used as loading controls. Immunoblot images were digitized and the optical densities were quantified.

Pancratistatin induces apoptosis independent of caspase activation

To further characterize the mechanism of action of pancratistatin, we treated HT-29 cells in the presence of a cell permeable, irreversible pan-caspase-inhibitor (z-VAD-fmk) to determine whether pancratistatin-induced apoptosis is caspase-dependent. After 72 h exposure to pancratistatin in the presence or absence of z-VAD-fmk, cells were monitored for apoptotic nuclear morphology and viability using Hoechst dye and WST-1 assay. Unexpectedly, we found that pancratistatin effectively induced apoptotic nuclear morphology in HT-29 cells independent of caspase activity (Figure 4A). Indeed, pancratistatin retained the ability to significantly reduce cell viability of HT-29 cells when co-treated with a pan-caspase-inhibitor at various concentrations (Figure 4B). These results suggested that pancratistatin induced cell death independent of caspase activation. To further investigate this hypothesis, the effect of pancratistatin on caspase-independent pro-apoptotic proteins was analyzed. Figure 4C depicts the release of apoptosis-inducing factor (AIF) and endonuclease G (Endo G) to the cytosol following treatment with pancratistatin in HT-29 cells. Similar results were observed in HCT116 cells (not shown). These findings suggested that pancratistatin-induced cell death may occur via caspase independent mechanisms.

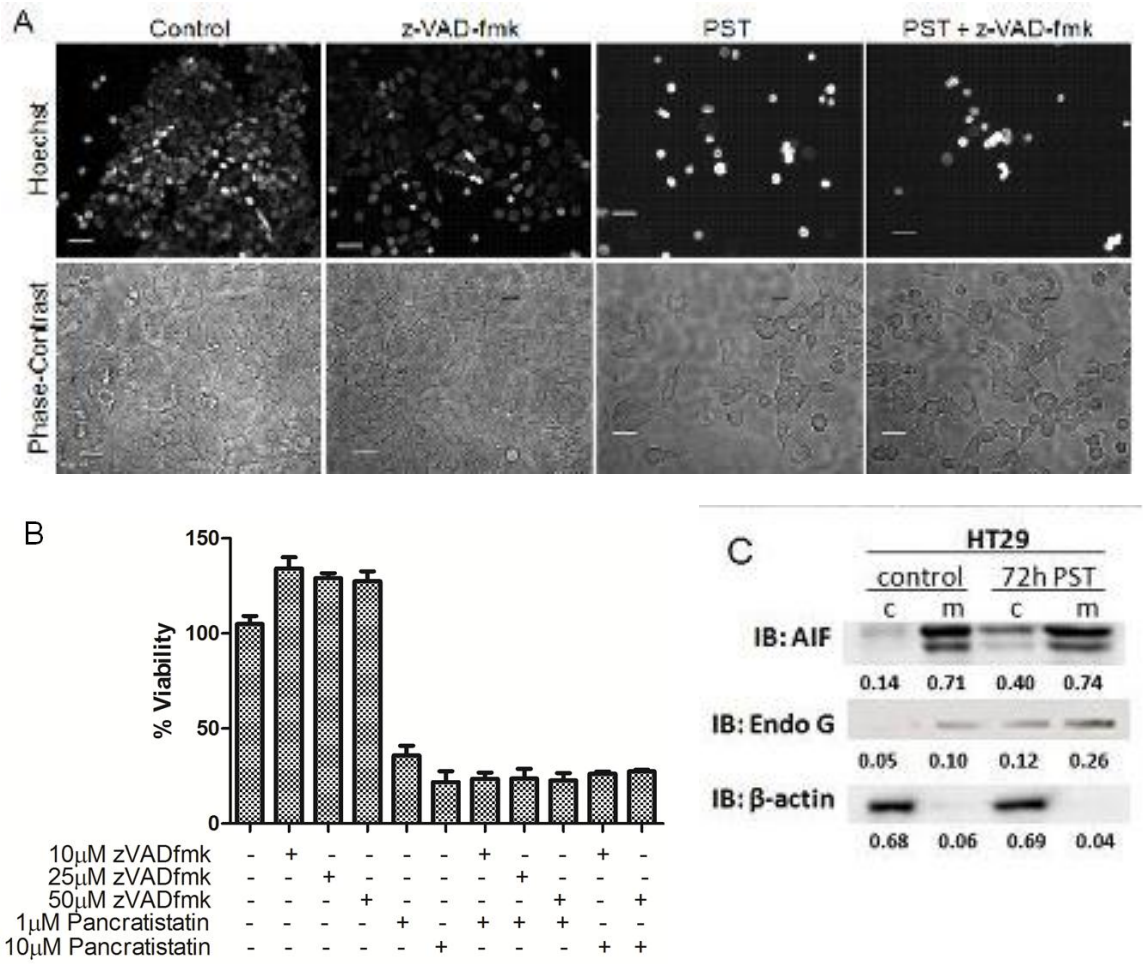

Figure 4. Pancratistatin induces cell death independent of caspase activation. (**A**) Representative images of nuclear and cellular morphology of HT-29 cells treated with a pan-caspase inhibitor and/or pancratistatin. Cells were treated with control (Me_2SO), 50 μM z-VAD-fmk, 1 μM pancratistatin (PST) or combination of 50 μM z-VAD-fmk and 1 μM PST for 96 h. Scale bars represent 15 μm. (**B**) HT-29 cells were treated with z-VAD-fmk and/or pancratistatin at indicated concentrations for 72 h. Effect of a pan-caspase inhibitor and pancratistatin or combination treatment on viability of cells was determined by WST-1 assay. *Columns*, mean (n=3); *bars*, SD; *, $P < 0.05$, significantly different from control by paired *t*-test. (**C**) HT-29 cells were treated with control (Me_2SO) or 1 μM pancratistatin for 72 h. Cytosolic and mitochondrial fractions were separated by SDS-PAGE followed by immunoblotting using specific antibodies against AIF and Endo G. Immunoblot images were digitized and the optical densities were quantified.

Pancratistatin does not interfere with microtubules or induce DNA damage as a primary mechanism of action

To determine if pancratistatin induces apoptosis in a manner similar to other plant alkaloids, namely the microtubule interfering compounds vincristine and paclitaxel, we tested the ability of pancratistatin to alter the polymerization rate of β-tubulin. In a direct comparison between pancratistatin and paclitaxel, we found that pancratistatin had no effect on β-tubulin polymerization rate compared to the expected rate increase caused by paclitaxel (Supplementary Figure 4A). This result indicated that pancratistatin does not interfere with microtubules to illicit a cell death response.

We have previously reported that, unlike genotoxic chemotherapeutics like etoposide, pancratistatin does not damage DNA as a primary mechanism of action, as evidenced by comet assay and histone H2AX phosphorylation (Kekre *et al,* 2005). Here we report a similar negative result that 6 h pancratistatin treatment did not cause double-strand DNA breaks in HT-29 and HCT116 cells. At this early time point there were no visible foci, which are representative of phosphorylation of histone H2AX in response to DNA damage (Supplementary Figure 4B). This result supported our earlier findings that pancratistatin is a non-genotoxic compound.

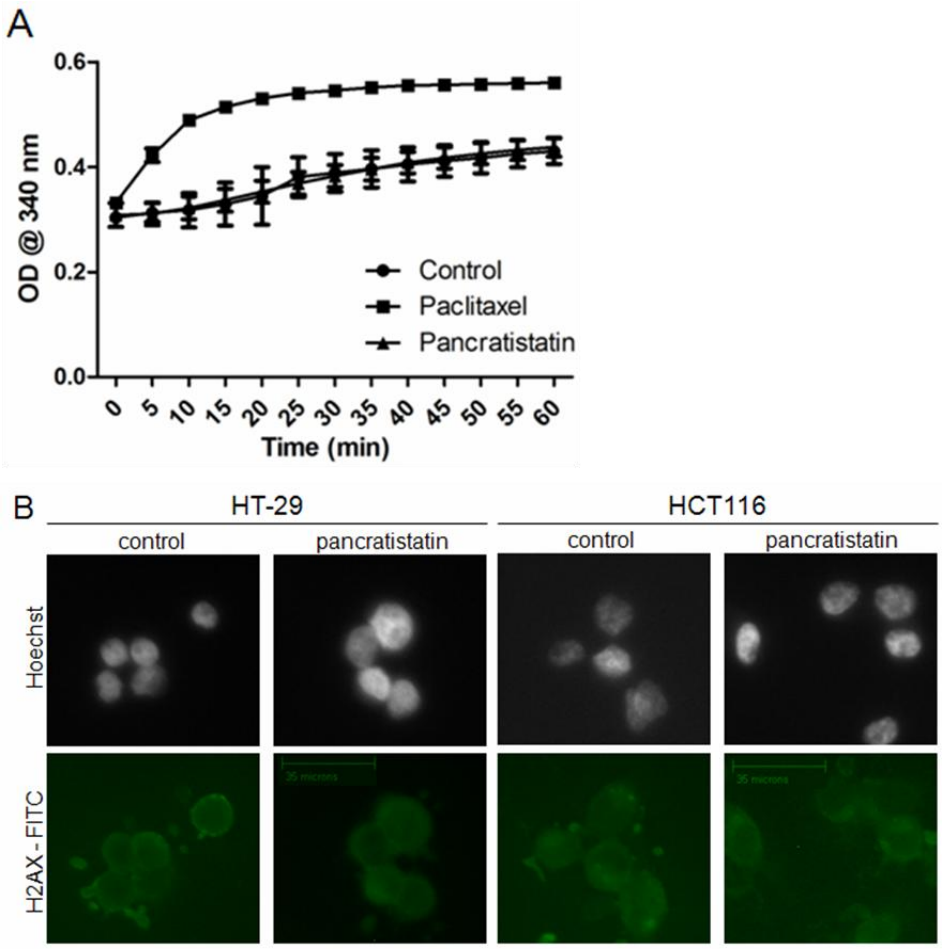

Supplementary Figure 4. Effect of pancratistatin on tubulin polymerization and DNA DSB formation. (**A**) Polymerization rate of purified bovine β-tubulin by control (general tubulin buffer), paclitaxel (10 µM) and pancratistatin (10 µM). Polymerization was started by incubating purified tubulin (4 mg/ml) with the indicated compound at 37°C, and absorbance readings at 340 nm were monitored for 60 min. *Data points*, mean (n=3); *bars*, SD. (**B**) Immuno-histochemical analysis of Histone H2AX phosphorylation with corresponding nuclear morphology by Hoechst staining of HT-29 and HCT116 cells treated with pancratistatin or control (Me_2SO) for 6 h. Scale bars represent 35 µm. There are only minimal visible foci, which are representative of double strand DNA breaks.

Pancratistatin administration reduces growth of HT-29 xenografts

To test the *in vivo* significance of our cellular observations, we determined the effect of pancratistatin administration on HT-29 xenograft growth in nude mice. Pancratistatin was administered intra-tumor (I.T.) twice a week at 3 mg/kg into animals bearing HT-29 xenografts. After 5 weeks of treatment, the average tumor volume in pancratistatin treated mice (18.0 ± 0.6 mm^3) was ~15-fold lower than the average tumor volume in control mice (249.5 ± 170.2 mm^3). Furthermore, after the 10 treatments there was a ~2.5-fold reduction in tumor volume in pancratistatin-treated animals compared to the average tumor volume in all animals (45.9 ± 5.4 mm^3) on day 1 of treatment (Figure 5B, 5C). These results indicated that pancratistatin significantly reduces growth of HT-29 xenografts in nude mice without causing any observable side effects. To determine if pancratistatin-mediated inhibition of HT-29 xenograft growth *in vivo* was accompanied by increased apoptosis, tumor tissues from control and pancratistatin-treated animals were processed for TUNEL assay. Compared to control, the pancratistatin-treated tumors had an increased amount of TUNEL positive cells, which corresponded with brighter DAPI staining (Figure 5D). The average body weight of control or pancratistatin-treated mice did not vary significantly throughout the study (Figure 5A). There were no observable signs of distress such as impaired movement, areas of redness or swelling or change in behaviour in pancratistatin-treated animals compared to control.

Intra-peritoneal administration of pancratistatin non-toxic to vital organs

To further assess whether pancratistatin had toxic effects on non-cancerous tissues, the liver and kidneys from animals treated with control or intra-peritoneal (I.P.) injection of pancratistatin were processed for histological analysis. H&E staining of the liver and kidneys revealed no gross morphological difference between treatment groups (Figure 6A). Tumor sections from control and pancratistatin-treated (I.T.) animals were also prepared for histological analysis by H&E staining. Figure 6B shows the difference in cellular morphology and tumor organization between the two groups. Together, our *in vivo* data indicated that pancratistatin significantly reduced tumor volume in HT-29 xenograft tumors by inducing apoptosis, without causing weight loss or obvious adverse effects to non-cancerous tissues.

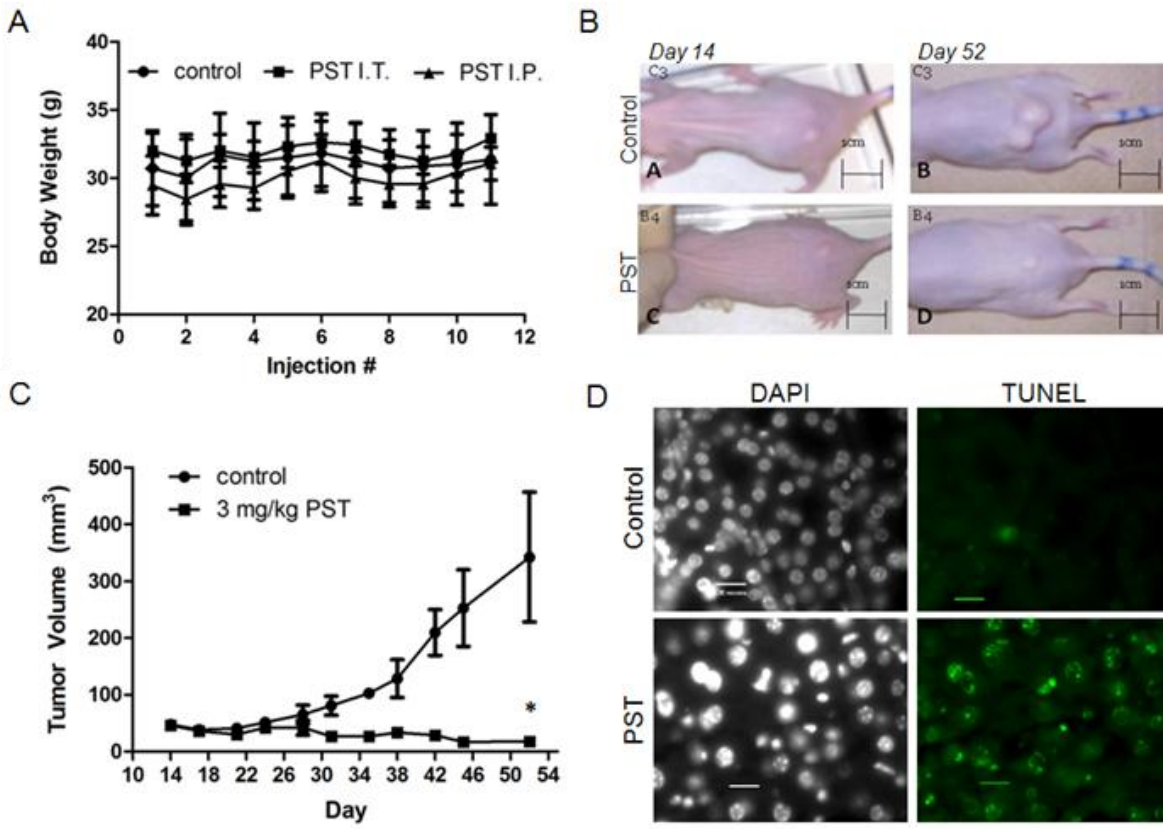

Figure 5. Pancratistatin reduces growth of and induces apoptosis in colon tumor xenografts. (**A**) Average body weights of control (5 µl Me_2SO in 200 µl PBS) and 3 mg/kg pancratistatin (PST)-treated (I.T. and I.P.) mice. The body weights of the control and PST-treated mice did not vary significantly throughout the study. *Data points*, mean (n=6); *bars*, SD. (**B**) Representative tumor size in CD-1 nude mice at day 1 of treatment (day 14 of study) and at time of sacrifice (day 52 of study). (**C**) Tumor growth curve showing efficacy of 3 mg/kg pancratistatin (PST) I.T. administration in reducing HT-29 tumor growth compared to control-treated animals. *Data points*, mean (n=6); *bars*, SD. *, $P < 0.05$, tumor volume of PST-treated mice significantly different between day 14 and day 52, and between control at day 52 of study, by paired *t*-test. (**D**) Histological analysis by TUNEL staining of tumors from control and 3 mg/kg PST-treated (I.T.) mice, with corresponding nuclear morphology by DAPI staining. Scale bars represent 35 µm.

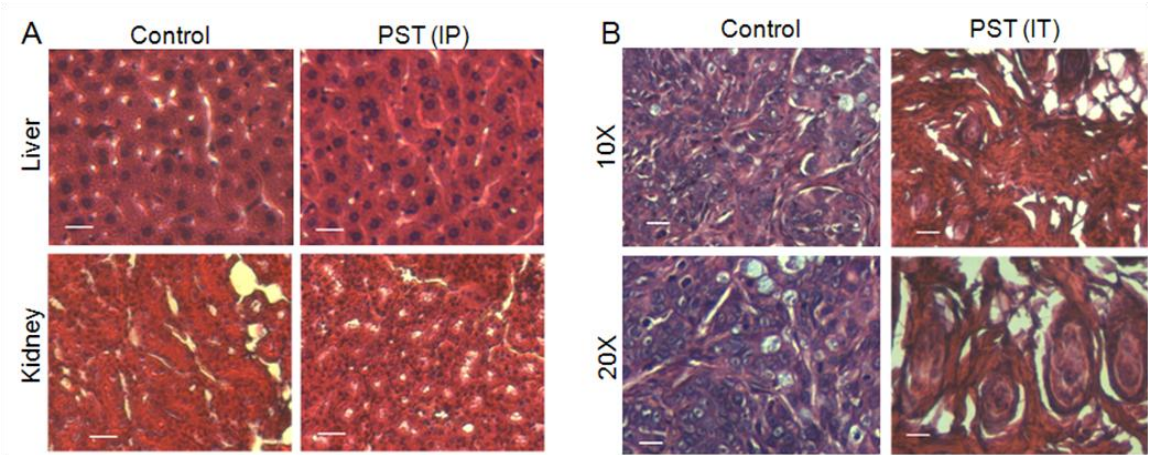

Figure 6. Histopathological analysis by H&E staining of pancratistatin treated tumors and non-cancerous tissues. (**A**) Representative images of liver and kidney from tumor-free mice treated intra-peritoneal (I.P.) with control (5 µl Me_2SO in 200 µl PBS) or 3 mg/kg pancratistatin (PST). Scale bars represent 35 µm. (**B**) Representative images of tumor sections from control and pancratistatin-treated (I.T.) animals. Scale bars represent 25 µm.

DISCUSSION

Induction of apoptosis by chemotherapeutic agents is often mediated through p53-dependent mechanisms; however, the majority of human carcinomas have p53 inactivation or mutations. The aim of this study was to investigate the potential anti-cancer activity of the natural alkaloid pancratistatin against p53-negative (HT-29) and wild-type p53 (HCT116) human colorectal carcinoma cell lines, and to delineate its mechanism of action. The present study revealed that pancratistatin has significant apoptotic activity against both cancer cell lines in culture and suppresses growth of HT-29 xenograft tumors. Interestingly, pancratistatin did not elicit an apoptotic response in non-cancerous human colon fibroblast (CCD-18Co) cells. This differential sensitivity to pancratistatin has been observed for other cancer cell lines and normal counterparts, both *in vitro* and *ex vivo* (Griffin *et al,* 2010; Griffin *et al,* 2011; McLachlan *et al,* 2005; Siedlakowski *et al,* 2008). We have previously shown that pancratistatin does not induce double-strand DNA breaks or comet formation at early time points compared to etoposide and paclitaxel in Human lymphoma cells (Kekre *et al,* 2005; Risinger *et al,* 2009). In this report, pancratistatin did not cause double-strand breaks in the DNA of HT-29 or HCT116 cells, nor did it affect microtubule assembly. Instead, pancratistatin-induced cell death was found to be mitochondria-dependent. Pancratistatin caused increased ROS production, collapse of mitochondrial membrane potential (MMP), and cytochrome *c* release. Furthermore, pancratistatin was found to act independent of p53, Bax and caspase activation, through the use of p53-negative HT-29 cells, mtDNA-depleted (ρ^0) cells, and caspase- and Bax-inhibition assays. Lastly, pancratistatin treatment caused significant growth reduction of HT-29 tumor xenografts with limited effects on non-cancerous tissues.

Collapse of the MMP and release of cytochrome *c* indicates that the intrinsic pathway of apoptosis is induced by pancratistatin. Once released, cytochrome *c* complexes with pro-caspase-9 and Apaf-1 to form the apoptosome, which activates caspase-3 resulting in apoptosis (Pradelli *et al,* 2010). Along with cytochrome *c*, other pro-apoptotic proteins are released including AIF and Endo G, which can trigger caspase-independent cell death (Constantinou *et al,* 2009; Pradelli *et al,* 2010). In this report we show that pancratistatin reduced viability of HT-29 cells in the presence of a general caspase-inhibitor, and also lead to the release of AIF and Endo G from the mitochondria of these cells (figure 4). Our hypothesis that this alkaloid targets the

mitochondria and triggers death upstream of caspase activation is bolstered by our result that caspase inhibitors cannot prevent pancratistatin-induced cell death. Complimentary to this study, we have previously reported that pancratistatin induces cell death in caspase-3-deficient estrogen-receptor positive MCF-7 breast cancer cells, and was also effective against estrogen-receptor negative Hs-578-T breast cancer cells (Siedlakowski *et al,* 2008).

A common mechanistic theme of *mitochondriotoxic* small molecules is that they act as antagonists of anti-apoptotic Bcl-2 family proteins, or are designed to mimic BH3-only proteins (Fantin and Leder, 2006; Fulda *et al,* 2010). In either case, the result is activation of Bax, which is responsible for mitochondrial outer membrane permeabilization (MOMP) (Pradelli *et al,* 2010). In this study, we utilized intracellularly expressed anti-Bax single-domain antibodies (intra-bodies) previously established in our lab to examine the effect of functional inactivation of Bax on pancratistatin activity (Gueorguieva *et al,* 2006). Interestingly, stable expression of anti-Bax intra-bodies did not attenuate pancratistatin-induced apoptosis in neuroblastoma cells, suggesting that pancratistatin is neither a Bcl-2 family protein antagonist nor a BH3-mimetic. In wild-type p53 colorectal carcinoma cells, pancratistatin induced mitochondrial-localization of Bax, where its pro-apoptotic function is activated; and increased the proportion of cytosolic Bcl-2, which inactivates the anti-apoptotic function of this protein. In contrast, Bax and Bcl-2 sub-cellular localization was largely unaffected by pancratistatin treatment in p53-negative HT-29 cells. These findings indicate that although pancratistatin alters the locale, and thus activity, of Bcl-2 family proteins, the pro-apoptotic member Bax is not a direct target of pancratistatin treatment and its function is indispensible for pancratistatin-induced cell death. Possible involvement of the functionally similar pro-apoptotic Bak protein however, cannot be ruled out, as it has been shown to compensate for Bax inhibition (Fantin and Leder, 2006).

Cancer cell mitochondria are prime targets for the development of selective anti-cancer agents, as they have manipulatable differences from normal cell mitochondria that can be exploited (Fulda *et al,* 2010; Modica-Napolitano *et al,* 2007). Unlike normal cell mitochondria, which utilize oxidative phosphorylation to generate ATP, cancer cells mainly depend on anaerobic glycolysis for energy (Warburg Theory) (Gogvadze *et al,* 2008). As a result, cancer cells have increased dependence on glucose and their mitochondria are typically hyperpolarized (DeBerardinis, 2008). Targeting components of

the mitochondrial respiratory chain (MRC) complexes, which are essentially dormant in cancer cells, should result in selective cancer cell death (Modica-Napolitano *et al,* 2007).

Compounds shown to inhibit MRC complex activity, such as the natural phytochemicals benzyl- and phenethyl-isothiocyanate, cause increased ROS production and MOMP specifically in cancer cells (Xiao *et al,* 2008). In this study, we show that pancratistatin treatment increased ROS production, collapse of MMP and release of cytochrome *c*, in colorectal cancer cells. In this study and in previous reports, we have shown that pancratistatin does not affect MMP nor lead to increased ROS production in non-cancerous cells (McLachlan *et al,* 2005). In an attempt to delineate the hierarchy of ROS production in pancratistatin-induced cell death, co-treatment with specific anti-oxidants or MRC complex inhibitors was performed. Our results demonstrate that the anti-oxidant N-acetylcyteine effectively quenched pancratistatin-induced ROS production, but it was unable to prevent cell death. Interestingly, co-treatment with the anti-oxidant CoQ_{10} did not alter the significant reduction in cell viability following pancratistatin treatment (Supplementary Figure 2B). These findings indicated that either pancratistatin does not directly compete with compounds, or that oxidative insult is not the primary cause of pancratistatin-induced cell death. Moreover, we report that mtDNA-deficient ρ^0 cancer cells resisted pancratistatin-induced cell death, which indicated that pancratistatin may be targeting a component of MRC complexes, as the parental cell line was sensitive to treatment (Sandhu *et al,* 2005; Xiao *et al,* 2008).

In response to cellular stress, Bax is activated either directly by p53 or indirectly by p53 mediated transcriptional regulation of BH3-only proteins Puma and Noxa (Gogvadze *et al,* 2008). A potent tumor suppressor, loss-of-function mutations of p53 correlates with chemo-resistant and aggressive tumors; *p53* mutation is considered to be an early step in the development of colon carcinoma (Bertholon *et al,* 2006). Here we report that pancratistatin effectively induced apoptosis and caspase-independent cell death in human colorectal adenocarcinoma (HT-29) cells that have a loss-of-function mutation of p53. Additionally, wild-type p53 colorectal carcinoma (HCT116) cells were proven sensitive to pancratistatin-induced apoptosis. Importantly, as proof-of-concept, we report that intra-tumor administration of pancratistatin caused a significant reduction in the growth of HT-29 xenograft tumors in nude mice. The concentration of pancratistatin used in this study (3 mg/kg) is below the previously determined maximum tolerated dose (Gabrielsen *et al,* 1992). There was no morbidity due to treatment, nor

was there drastic variation in activity level or significant weight loss/gain between control and treated animals, indicating low toxicity of pancratistatin *in vivo*. This observation correlated with histopathology analysis of the liver and kidneys from control and pancratistatin-treated animals having no gross morphological differences. The anti-tumor activity of pancratistatin was found to be more potent than the water-soluble sodium pancratistatin 3, 4-o-cyclic phosphate derivative, which was reported by Shnyder (2008) to have anti-tumor activity at a dose of 100 mg/kg (Shnyder *et al,* 2008). Other *Amaryllidaceae* alkaloids, including lycorine and narciclasine, have anti-tumor activity at doses that complement our findings (Liu *et al,* 2007; Ingrassia *et al,* 2009).

The minimal structural pharmacophore required for potent anti-cancer activity has been defined in the pancratistatin series of alkaloids based on a number of structure-activity correlations that have been conducted with both natural and synthetic analogues (Pettit *et al,* 1993; Rinner *et al,* 2004; McNulty *et al,* 2005; Pettit *et al,* 2009). The pharmacophore consists of the 2,3,4-triol structural element in ring-C. Although not requirements, the pharmacophoric element is moderated slightly by the incorporation of the C7 phenolic hydroxyl group and, interestingly, through the inclusion of a β–benzyloxy substituent on the C-1 position (Pettit *et al,*1993; Pettit *et al,* 2004). Since these features are not crucial, they highlight areas where further elaboration is possible on top of the intact pharmacophore. Fully functionalized seco-analogues of both the lactam and cyclitol rings are inactive, indicating that a fully intact tetracyclic core, having the correctly positioned hydroxyl groups in ring-C, is required (McNulty *et al,* 2008).

CONCLUSIONS

The results presented in this article show that pancratistatin selectively induces cell death and reduces growth of human colorectal adenocarcinoma cells in culture and *in vivo*. Pancratistatin effectively induces cell death independent of Bax and caspase-activation by targeting cancer cell mitochondria. We are currently working to further unravel the networks, interactions and pathways that pancratistatin employs to induce cell death in both p53 wild-type and mutated cell lines. Overall, mitochondriotoxic compounds show great promise as specific and potent anti-cancer agents.

REFERENCES

Armstrong JS. Mitochondria: a target for cancer therapy. Br J Pharmacol 2006; 147(3): 239-248.

Bertholon J, Wang Q, Galmarini CM, Puisieux A. Mutational targets in colorectal cancer cells with microsatellite instability. Fam Cancer 2006; 5(1): 29-34.

Chatterjee SJ, McNulty J, Pandey S. Sensitization of human melanoma cells by tamoxifen to apoptosis induction by pancratistatin, a nongenotoxic natural compound. Melanoma Res 2011. 2010 Mar 17 [Epub ahead of print].

Constantinou C, Papas KA, Constantinou AI. Caspase-independent pathways of programmed cell death: the unraveling of new targets of cancer therapy? Curr Cancer Drug Targets 2009; 9(6): 717-728.

DeBerardinis RJ. Is cancer a disease of abnormal cellular metabolism? New angles on an old idea. Genet Med 2008; 10(11): 767-777.

Deorukhkar A, Krishnan S, Sethi G, Aggarwal BB. Back to basics: how natural products can provide the basis for new therapeutics. Expert Opin Investig Drugs 2007; 16(11): 1753-1773.

Dy GK, Adjei AA. Systemic cancer therapy: evolution over the last 60 years. Cancer 2008; 113(7 Suppl): 1857-1887.

Fantin VR, Leder P. Mitochondriotoxic compounds for cancer therapy. Oncogene 2006; 25(34): 4787-4797.

Fulda S, Galluzzi L, Kroemer G. Targeting mitochondria for cancer therapy. Nat Rev Drug Discov 2010; 9(6): 447-464.

Gabrielsen B, Monath TP, Huggins JW, *et al*. Antiviral (RNA) activity of selected Amaryllidaceae isoquinoline constituents and synthesis of related substances. J Nat Prod 1992; 55(11): 1569-1581.

Gogvadze V, Orrenius S, Zhivotovsky B. Mitochondria in cancer cells: what is so special about them? Trends Cell Biol 2008; 18(4): 165-173.

Green DR, Kroemer G. Cytoplasmic functions of the tumor suppressor p53. Nature 2009; 458(7242): 1127-1130.

Griffin C, Hamm C, McNulty J, Pandey S. Pancratistatin induces apoptosis in clinical leukemia samples with minimal effect on non-cancerous peripheral blood mononuclear cells. Cancer Cell Int 2010; 10: 6.

Gueorguieva D, Li S, Walsh N, Mukerji A, Tanha J, Pandey S. Identification of single-domain, Bax-specific intrabodies that confer resistance to mammalian cells against oxidative-stress-induced apoptosis. FASEB J 2006; 20(14): 2636-2638.

Hu Y, Moraes CT, Savaraj N, Priebe W, Lampidis TJ. Rho(0) tumor cells: a model for studying whether mitochondria are targets for rhodamine 123, doxorubicin, and other drugs. Biochem Pharmacol 2000; 60(12): 1897-1905.

Ingrassia L, Lefranc F, Dewelle J, *et al*. Structure-activity relationship analysis of novel derivatives of narciclasine (an Amaryllidaceae isocarbostyril derivative) as potential anticancer agents. J Med Chem 2009; 52(4): 1100-1114.

Kekre N, Griffin C, McNulty J, Pandey S. Pancratistatin causes early activation of caspase-3 and the flipping of phosphatidyl serine followed by rapid apoptosis

specifically in human lymphoma cells. Cancer Chemother Pharmacol 2005; 56(1): 29-38.

Kornienko A, Evidente A. Chemistry, biology, and medicinal potential of narciclasine and its congeners. Chem Rev 2008; 108(6): 1982-2014.

Li H, Wu WK, Zheng Z, Che CT, Yu L, Li ZJ, *et al*. 2,3',4,4',5'-Pentamethoxy-trans-stilbene, a resveratrol derivative, is a potent inducer of apoptosis in colon cancer cells via targeting microtubules. Biochem Pharmacol 2009; 78(9): 1224-1232.

Liu J, Li Y, Tang LJ, Zhang GP, Hu WX. Treatment of lycorine on SCID mice model with human APL cells. Biomed Pharmacother 2007; 61(4): 229-234.

McLachlan A, Kekre N, McNulty J, Pandey S. Pancratistatin: a natural anti-cancer compound that targets mitochondria specifically in cancer cells to induce apoptosis. Apoptosis 2005; 10(3): 619-630.

McNulty J, Larichev V, Pandey S. A synthesis of 3-deoxydihydrolycoricidine: refinement of a structurally minimum pancratistatin pharmacophore. Bioorg Med Chem Lett 2005; 15: 5315-5318.

McNulty J, Mao J, Gibe R, *et al*. Studies directed towards the refinement of the pancratistatin cytotoxic pharmacophore. Bioorg Med Chem Lett 2001; 11(2): 169-172.

McNulty J, Nair JJ, Griffin C, Pandey S. Synthesis and biological evaluation of fully functionalized seco-pancratistatin analogues. J Nat Prod 2008; 71: 357-363.

Modica-Napolitano JS, Kulawiec M, Singh KK. Mitochondria and human cancer. Curr Mol Med 2007; 7(1): 121-131.

Newman DJ, Cragg GM. Natural products as sources of new drugs over the last 25 years. J Nat Prod 2007; 70(3): 461-477.

Pandey S, Kekre N, Naderi J, McNulty J. Induction of apoptotic cell death specifically in rat and human cancer cells by pancratistatin. Artif Cells Blood Substit Immobil Biotechnol 2005; 33(3): 279-295.

Pettit GR, Ducki S, Eastham SA, Melody N. Antineoplastic agents. 454. Synthesis of the strong cancer cell growth inhibitors trans-dihydronarciclasine and 7-deoxy-trans-dihydronarciclasine (1a). J Nat Prod 2009; 72: 1279-1282.

Pettit GR, Melody N, Herald DL. Antineoplastic agents. 511. Direct phosphorylation of phenpanstatin and pancratistatin. J Nat Prod 2004; 67: 322-327.

Pettit GR, Pettit GR III, Backhaus RA, Boyd MR, Meerow AW. Antineoplastic Agents, 256. Cell Growth Inhibitory Isocarbostyrils from Hymenocallis. J Nat Prod 1993; 56; 1682-1687.

Pradelli LA, Bénéteau M, Ricci JE. Mitochondrial control of caspase-dependent and -independent cell death. Cell Mol Life Sci 2010; 67(10): 1589-1597.

Ralph SJ, Rodríguez-Enríquez S, Neuzil J, Moreno-Sánchez R. Bioenergetic pathways in tumor mitochondria as targets for cancer therapy and the importance of the ROS-induced apoptotic trigger. Mol Aspects Med 2010; 31(1): 29-59.

Ravizza R, Gariboldi MB, Passarelli L, Monti E. Role of the p53/p21 system in the response of human colon carcinoma cells to Doxorubicin. BMC Cancer 2004; 4: 92.

Rinner U, Hillebrenner HL, Adams DR, Hudlicky T, Pettit GR. Synthesis and biological activity of some structural modifications of pancratistatin. Bioorg Med Chem Lett 2004; 14: 2911-2915.

Risinger AL, Giles FJ, Mooberry SL. Microtubule dynamics as a target in oncology. Cancer Treat Rev 2009; 35(3): 255-261.

Sandhu JK, Sodja C, McRae K, *et al*. Effects of nitric oxide donors on cybrids harbouring the mitochondrial myopathy, encephalopathy, lactic acidosis and stroke-like episodes (MELAS) A3243G mitochondrial DNA mutation. Biochem J 2005; 391(Pt 2): 191-202.

Shah MR, Kriedt CL, Lents NH, *et al*. Direct intra-tumoral injection of zinc-acetate halts tumor growth in a xenograft model of prostate cancer. Exp Clin Cancer Res 2009; 28: 84.

Shnyder SD, Cooper PA, Millington NJ, Gill JH, Bibby MC. Sodium pancratistatin 3,4-o-cyclic phosphate, a water-soluble synthetic derivative of pancratistatin, is highly effective in a human colon tumor model. J Nat Prod 2008; 71(3): 321-324.

Siedlakowski P, McLachlan-Burgess A, Griffin C, Tirumalai SS, McNulty J, Pandey S. Synergy of Pancratistatin and Tamoxifen on breast cancer cells in inducing apoptosis by targeting mitochondria. Cancer Biol Ther 2008; 7(3): 376-384.

Wang F, Ogasawara MA, Huang P. Small mitochondria-targeting molecules as anti-cancer agents. Mol Aspects Med 2010; 31(1): 75-92.

Weekes J, Lam AK, Sebesan S, Ho YH. Irinotecan therapy and molecular targets in colorectal cancer: a systemic review. World J Gastroenterol 2009; 15(29): 3597-3602.

Xiao D, Powolny AA, Singh SV. Benzyl isothiocyanate targets mitochondrial respiratory chain to trigger reactive oxygen species-dependent apoptosis in human breast cancer cells. J Biol Chem 2008; 283(44): 30151-30163.

CHAPTER 6

Pancratistatin induces apoptosis and autophagy in metastatic prostate cancer cells

BACKGROUND

Natural alkaloids of the *Amaryllidaceae* family of plants have been used in traditional medicine for centuries and have wide-ranging properties such as anti-viral, anti-bacterial and anti-neoplastic activity (Kornienko and Evidente, 2008). The phenanthridone alkaloid pancratistatin, isolated from the bulb tissues of *Hymenocallis littoralis* plants, has shown potential to be a potent anti-cancer agent with a notable therapeutic window, albeit with an elusive target (Griffin *et al,* 2011a). Our previous studies indicated that pancratistatin selectively and effectively induces apoptosis associated with mitochondrial destabilization and increased reactive oxygen species (ROS) production in human leukemia, melanoma and hormone-refractory breast carcinoma cells (Kekre *et al,* 2005; Chatterjee *et al,* 2011; Seidlakowski *et al,* 2007). We recently reported that pancratistatin-induced apoptosis occurs in a p53-independent manner and that cancer cell mitochondria are essential for the anti-cancer activity of pancratistatin (Griffin *et al,* 2011a).

The intrinsic pathway of apoptosis involves loss of mitochondrial membrane potential, rupture/opening of the outer mitochondrial membrane, and release of pro-apoptotic proteins to the cytosol (Ralph *et al,* 2010). Mitochondria-mediated apoptosis may be induced by increased reactive oxygen species (ROS) production, which is an indicator of cellular stress (Valko *et al,* 2007). Mitochondria, and more specifically mitochondrial respiratory chain (MRC) complexes I and III, are the primary sources of cellular ROS production (Valko *et al,* 2007). A review of recent literature reveals the potent anti-cancer properties of natural compounds that specifically target mitochondria or metabolic pathways, including resveratrol, betulinic acid and the vitamin E analog α-tocopheryl succinate (α-TOS) (Fulda *et al,* 2010; Liu *et al,* 2009; Neuzil *et al,* 2006). Alpha-TOS induces apoptosis in cancer cells via ROS generation by blocking MRC complex II activity (Dong *et al,* 2009). Additionally, Xiao and colleagues reported that isothiocyanates (constituents of cruciferous vegetables) generate excessive ROS by inhibiting oxidative phosphorylation, leading to mitochondrial-mediated apoptosis in prostate cancer cells (Xiao *et al,* 2010).

There are limited therapy options for hormone-refractory metastatic prostate carcinoma and patients often have poor prognosis. Recent studies have reported that a novel therapeutic strategy for advanced androgen-independent prostate cancer may be to target autophagy (DiPaola *et al,* 2008). Autophagy is a lysosomal process of self-

digestion, which is understood to be a survival mechanism employed by cells facing adverse environmental conditions, such as nutrient deprivation or hypoxia (Fimia and Piacentini, 2010). Ever the opportunists, tumor cells use the self-preservation facet of autophagy to overcome chemotherapeutic insult, thereby acquiring resistant phenotypes (Dalby *et al,* 2010). Thus a novel strategy for treatment is to combine standard chemotherapy with inhibition of autophagy, which may resensitize the resistant tumor cells (Qadir *et al,* 2008; Morselli *et al,* 2009). Conversely, several reports indicate that sustained autophagy actually results in programmed cell death type-II, or autophagic cell death, in cancer cells and that induction of autophagy may be a valid treatment tactic (Gibson, 2010; White *et al,* 2009).

The interplay between apoptosis and autophagy involves regulation of autophagy by classically defined anti-apoptotic proteins, such as Bcl-2 and Bcl-XL (Dalby *et al,* 2010). Another key regulator of apoptosis and autophagy processes is the tumor suppressor p53 (Olovnikov *et al,* 2009). Interestingly, in this report the two metastatic prostate cancer cell lines studied not only differ in their androgen sensitivity, but also in p53 status. DU145 cells are both androgen-refractory and contain functionally mutated p53 protein, and LNCaP cells maintain androgen sensitivity and wild-type p53 (Radhakrishnan *et al,* 2010). In this study, both cell lines were observed to undergo apoptosis induced by pancratistatin, which caused increased ROS production, and destabilization of the mitochondrial membrane potential. For the first time, we report the effect of pancratistatin on induction of autophagy, as well as the efficacy of pancratistatin against xenograft models of DU145 prostate tumors.

METHODS

Chemicals

Media, gentamycin, L-glutamine, amino acids, Hoechst 33342 dye, Tetramethyl Rhodamine Methyl Ester (TMRM) dye, and Annexin-V AlexaFluor 488 are products of Invitrogen (GIBCO). Caspase-3, -8 and -9 fluorometric substrates were purchased from MP Biomedicals. Cell proliferation reagent WST-1 was purchased from Roche. Anti-LC3 antibody was purchased from Abcam, and anti-β-actin antibody was purchased from SantaCruz Biotechnology. Pancratistatin (Figure 1A) was isolated from *H. littoralis* as previously described (McNulty *et al,* 2001) and provided by Dr. J. McNulty. All other chemicals were purchased from Sigma-Aldrich.

Cell culture

Androgen-sensitive human prostate LNCaP cells, which express wild-type p53, and androgen-refractory, p53 mutant DU145 cells were purchased from ATCC (Hu H *et al,* 2008). LNCaP cells were grown in RPMI media and DU145 cells were grown in DMEM; supplemented as recommended by ATCC. Human diploid fibroblast (AG09309) cells (NHF), purchased from the Coriell Institute for Medical Research, were grown in Earle's minimum essential medium supplemented with 15% (v/v) fetal bovine serum, 2 mM L-glutamine, 1.5 g/l sodium bicarbonate, essential and non-essential amino acids, vitamins, and gentamycin. All cultures were maintained at 5% CO_2 and 37 °C.

Cytotoxicity assays

Cytotoxicity was measured using the WST-1 colorimetric assay. Cells were seeded at 2 000 cells/well in 96-well tissue culture plates. After treatment with pancratistatin as indicated, cells were incubated with WST-1 according to manufacturer's protocol for 4 h at 37 °C. Absorbance was measured at 450 nm on a VICTOR^3 microplate reader. Absorbance is directly proportional to the number of living cells in culture. Each assay was performed in triplicate and the mean of three assays was calculated based on average absorbance of control-treated (Me_2SO) cells.

Assessment of apoptosis

Cells were treated as indicated and nuclear morphology was evaluated by fluorescence microscopy using cell-permeable Hoechst 33342 dye and an inverted

fluorescence microscope (Leica DM IRB, Germany). The percent of condensed nuclei (indicative of apoptosis) was calculated as: [(number of cells with condensed, brightly stained nuclei / total number of cells)*100] with a minimum 5 fields counted with 100 cells / field. To monitor phosphatidyl serine exposure, Annexin-V binding assay was performed. Cells were treated as indicated, trypsinized and washed 2X in room temperature PBS, then resuspended in Annexin-V binding buffer (10 mM HEPES/NaOH pH 7.5, 140 mM NaCl, 2.5 mM $CaCl_2$), containing Annexin-V AlexaFluor 488 conjugate (1:50) for 15 min at 25ºC; images were captured on an inverted fluorescence microscope (Leica DM IRB, Germany).

Trypan blue exclusion viability assay

Cell viability was assessed by Trypan Blue Exclusion after incubation of cells at increasing intervals with 1 µM pancratistatin. Cells were trypsinized and the cell pellet was resuspended in PBS. Cell suspension was diluted 1:1 with Trypan Blue Exclusion dye and cells were counted using a Fisher Hemocytometer. Data represents the mean of three assays calculated as percent Trypan Blue positive per total cells counted.

Mitochondrial functionality assays

Mitochondrial membrane potential (MMP) was observed using cell permeable TMRM dye (1 µM final concentration). Cells were grown on cover-slips and following treatment TMRM was added directly to the media and incubated for 30 min at 37°C in darkness; cell permeable Hoechst dye was added for the last 5 min of the incubation period, to observe nuclear morphology. To detect generation of reactive oxygen species (ROS) cells were treated with pancratistatin, trypsinized and counted using the Trypan Blue Exclusion assay prior to incubation with H_2DCFDA (1 µM) for 45 min at 37°C in an opaque 96-well plate. Fluorescence was measured at Ex. 513 nm and Em. 530 nm using a SpectraMax GeminiXPS spectrofluorometer. Change in ROS generation was calculated as the fold difference from control (RFU) and expressed per 10 000 cells.

Assessment of caspase activity

Caspase activity assays were carried out using a previously published method (Kekre *et al,* 2005). Briefly, cellular lysate was collected from LNCaP and DU145 cells and incubated with the desired fluorogenic substrate (caspase-3, DEVD-afc; caspase-8,

IETD-afc; caspase-9, LEHD-afc) in assay buffer (0.1 M HEPES, pH 7.4, 2 mM DTT, 0.1% CHAPS, 1% sucrose) and allowed to incubate at 37ºC for 45 min. Fluorescence was measured at 400nm excitation and 505nm emission using a SpectraMax Gemini XPS spectrofluorometer. Caspase activity was calculated per microgram of protein, and expressed as a percentage of control activity.

Wound-healing assay

Prostate cancer cells were seeded in 12-well plates and cultured to at least 95% confluence. Monolayer cells were scraped with a plastic 200 µL pipette tip, rinsed with warmed PBS and immediately cultured in fresh media with or without 1 µM pancratistatin. Phase-contrast microscopy was used to observe the wound-area at 0, 24 and 48 h after treatment. The relative migration distance (%) is equal to (A-B)/A*100, where A is the wound width before incubation, and B is the wound width after.

Monitoring autophagic vacuole formation

To detect the formation of autophagic vacuoles, cells were grown on cover-slips and treated as indicated. Monodansylcadaverine (MDC) was added directly to the media at 0.1 mM final concentration and incubated at 37ºC for 20 min in darkness; images were captured on an inverted fluorescence microscope (Leica DM IRB, Germany).

Western blot analysis

Cells treated with pancratistatin were mechanically lysed in ice-cold hypotonic buffer with protease inhibitors (10 mM Tris HCl (pH 7.2), 5 mM KCl, 1 mM $MgCl_2$, 1 mM EGTA, 1% Triton-X-100; 10 µM Leu-pep and Pep-A, 100 µM PMSF). Protein samples (20 µg) were separated by SDS-PAGE, transferred to nitrocellulose and probed with the indicated primary antibody (1:1000) overnight at 4°C. Membranes were then incubated with HRP-conjugated secondary antibody (1:1000) for 1 h at 25°C and visualized using enhanced chemiluminescence reagent. Equal loading of the protein samples was confirmed by parallel western blots for β-actin. Images were digitized and band intensity was quantified using NIH Image *J* software.

*In vivo x*enograft models

Six-week old male homozygous CD-1 nude mice (25 – 30 g) were obtained from Charles River Laboratories, St. Constant, QC. Animals were housed in constant laboratory conditions of a 12 h light/dark cycle at 21°C in accordance with institutional animal protocols (University of Windsor Research Ethics Board - AUPP05). Prior to injection, DU145 cells were washed with PBS and centrifuged at 500 x *g* for 5 min; cell pellets were suspended in aliquots of 200 µl PBS (4 x 10^6 cells per mouse). The cell suspension was injected s.c. in the right hind flank. Tumors were allowed to grow for 4 weeks and thereafter animals were randomized into two treatment groups (n=3). Animals were treated intra-tumor (IT) with vehicle (5 µl Me_2SO in PBS) or pancratistatin (3 mg/kg) 4 times over 3 weeks (Gabrielsen *et al,* 1992; Shah *et al,* 2009). Tumors were assessed at the end of the study by 2D digital volume extrapolation, using Image *J* software. Body weight of all animals was taken twice weekly during the study as a measure of overt toxicity. Intra-peritoneal injection of 3 mg/kg pancratistatin twice weekly for up to 2 months was previously shown to be non-toxic to liver and kidneys by histopathological analysis (Griffin *et al,* 2011).

Statistical analysis

Data were presented as the mean ± standard deviation and significance was determined by using Student's *t*-test or ANOVA, where appropriate. Values of $p<0.05$ (*) and $p<0.005$ (**) were considered significant.

RESULTS

Cytotoxic effect of pancratistatin on prostate cancer cells

To determine whether pancratistatin selectively affects prostate cancer cell viability, we tested this natural alkaloid on androgen-responsive LNCaP cells and androgen-refractory DU145 cells, as well as non-cancerous human fibroblast NHF cells. Cytotoxicity was assessed following exposure to increasing concentrations of pancratistatin over 72 h (Figure 1B). An EC_{50} value of approximately 100 nM resulted for both cancer cell lines. Treatment of NHF cells with pancratistatin for 72 h did not cause viability to drop below 50% (Figure 1B). To further test this result the Trypan Blue Exclusion assay was used, which confirmed that at 1 µM, pancratistatin selectively decreases viability of LNCaP and DU145 prostate cancer cells, but does not significantly increase cell death in non-cancerous NHF cells (Figure 1C). These results suggest that pancratistatin selectively reduces viability of cancer cells regardless of androgen sensitivity with an insignificant effect on non-cancerous cells.

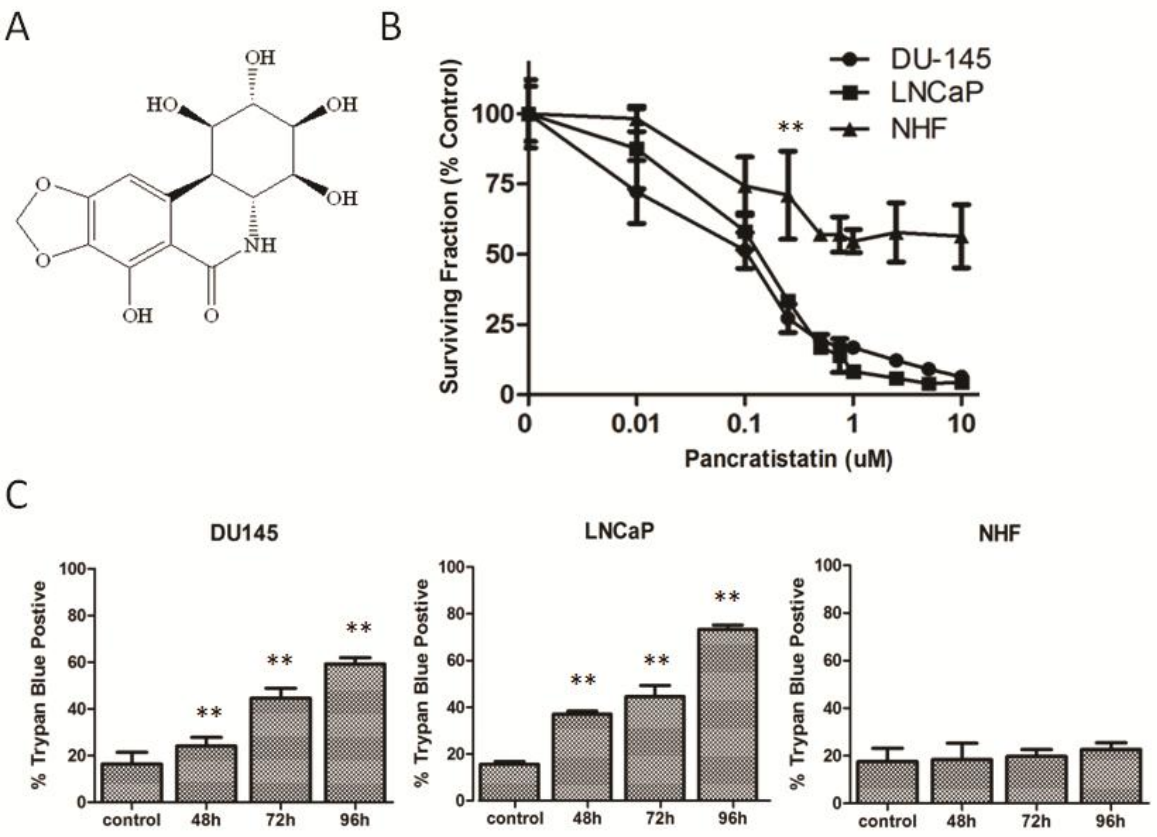

Figure 1. Pancratistatin selectively affects viability of prostate carcinoma cells. (**A**) Chemical structure of pancratistatin. (**B**) DU145, LNCaP and NHF cells were treated with control (Me_2SO) or the indicated doses of pancratistatin for 72 h. Cytotoxicity was measured by the WST-1 colorimetric assay. *Data points*, mean (n=3); *bars*, SD; **, $P < 0.005$, significantly different between cell lines by paired *t*-test. (**C**) DU145, LNCaP and NHF cells treated for the indicated times with control (Me_2SO) or 1 µM pancratistatin (PST). Cell viability was determined by Trypan blue dye exclusion assay. *Data points*, mean (n=3); *bars*, SD; **, $P < 0.005$, significantly different from control by one-way ANOVA.

Pancratistatin induces apoptosis in metastatic prostate cells

Pancratistatin has been shown to effectively induce apoptosis in breast cancer cells, independent of estrogen receptor status *in vitro*, and in acute and chronic forms of leukemia *ex vivo* (Siedlakowski *et al,* 2008; Griffin *et al,* 2010). To investigate whether the observed cytotoxicity of 1 µM pancratistatin on prostate cancer cells was due to induction of apoptosis, we performed Hoechst staining at 48 and 96 h of treatment. In both DU145 and LNCaP cell lines, there was an increased number of cells with brightly stained, condensed nuclei, characteristic to apoptotic cells (Figure 2A). Moreover, in both prostate cancer cell lines, there was a marked increase in Annexin-V positive cells, indicative of phosphatidyl serine exposure, a characteristic marker of apoptosis (refer to Appendix B, Figure 6). In line with previous reports (Griffin *et al,* 2011), pancratistatin did not affect nuclear morphology in non-cancerous cells (Figure 2A). Exposure to pancratistatin for increased lengths of time resulted in increased apoptotic morphology in cancer cells, with a 70% increase in apoptosis over control after 96 h in both prostate cancer cell lines. There was an insignificant change in the number of cells with apoptotic nuclear morphology in NHFs exposed to pancratistatin at all time points (Figure 2B). These findings indicate that pancratistatin induces apoptosis selectively in prostate carcinoma cells.

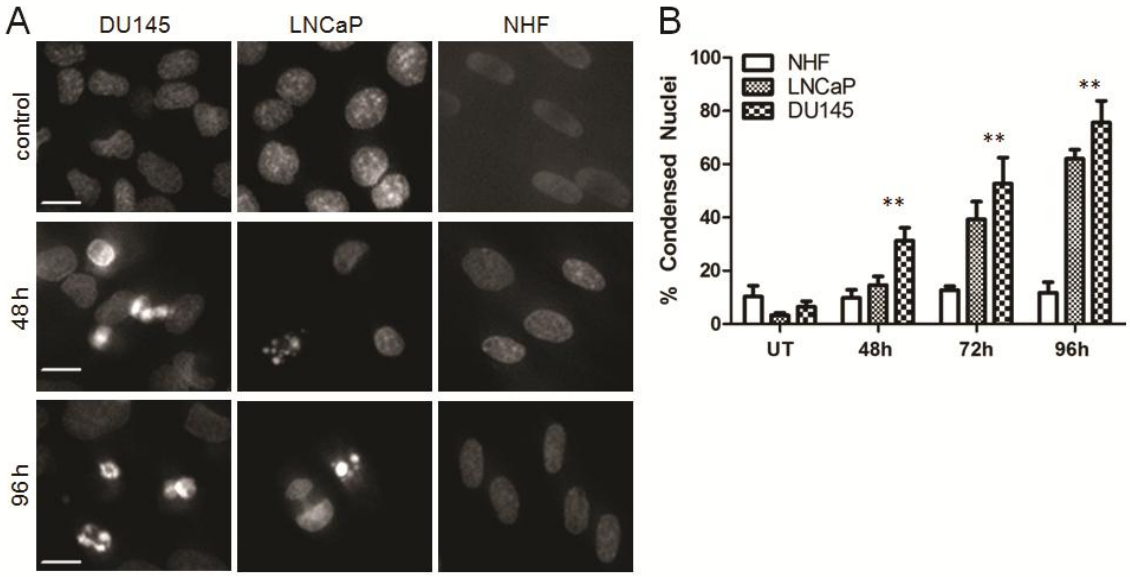

Figure 2. Pancratistatin induces apoptosis in prostate cancer cells. (**A**) Representative nuclear morphology of DU145, LNCaP and NHF cells stained with Hoechst dye after 72 h with 1 µM pancratistatin (PST) or control (Me_2SO). Scale bars represent 15 µm. (**B**) Quantification of condensed brightly stained nuclei by Hoechst dye, characteristic of apoptotic cells. DU145 (AR-) and LNCaP (AR+) cells were treated with control (Me_2SO) or 1 µM pancratistatin for 48-, 72-, or 96-h and stained with Hoechst. A minimum 5 fields with 100 cells/field was counted. *Columns*, mean (n=6); *bars*, SD; **, $P < 0.005$, significantly different from control by two-way ANOVA.

Inhibition of the wound-healing capacity of prostate cancer cells by pancratistatin

To evaluate the anti-migratory effect of pancratistatin on metastatic prostate cancer cells, we monitored the wound-healing capacity of DU145 prostate cancer cells. A scratch-wound was made in a sub-confluent cell monolayer and cells were allowed to migrate into the cell-free area for up to 48 h (Figure 3A). Pancratistatin treatment caused a 35% reduction in the ability of prostate cancer cells to migrate into the wound-area compared to control at 24 h, and a 50% reduction after 48 h (Figure 3B). This result presents the novel finding that pancratistatin affects the migration capacity of metastatic prostate cancer cells *in vitro*.

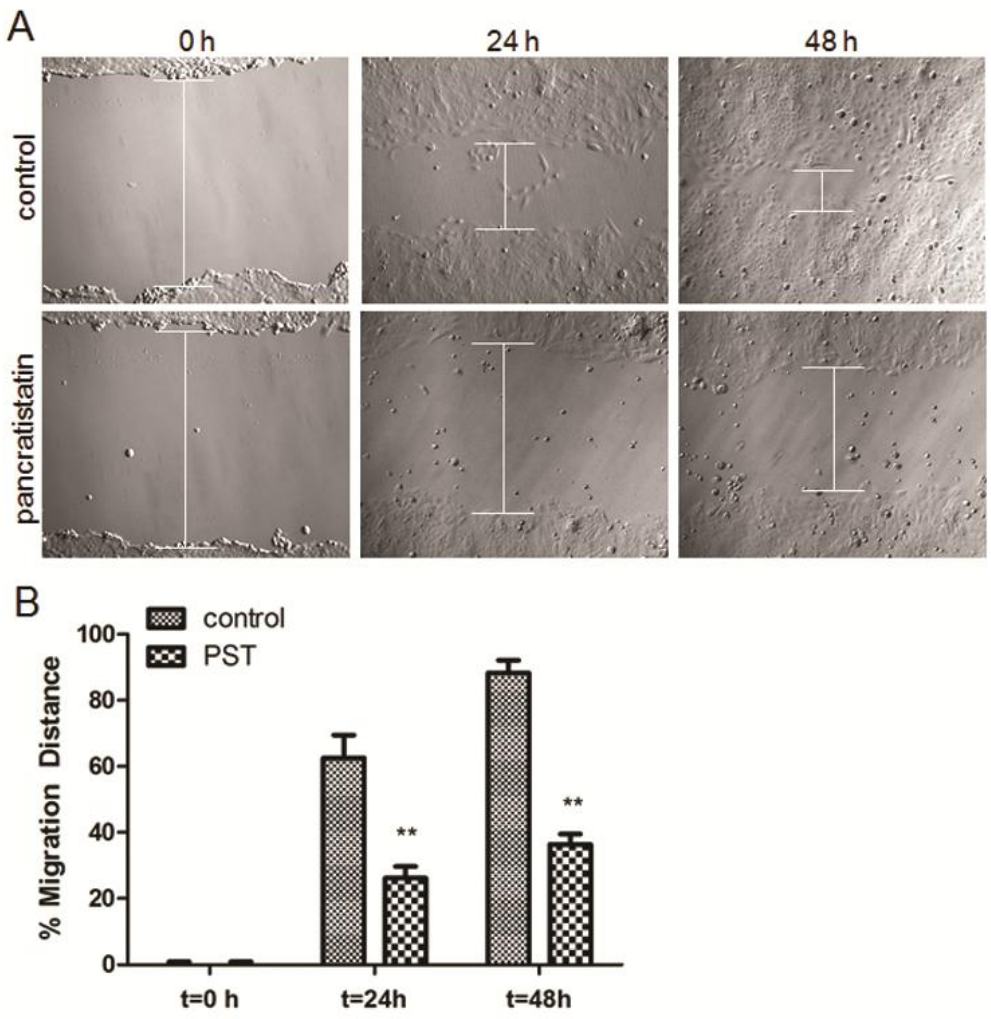

Figure 3. Pancratistatin reduces wound-healing capacity. (A) Wound healing capacity, indicative of migration potential, was decreased in DU145 cells after treatment with pancratistatin compared to control. Images represent data obtained from three independent experiments. **(B)** Quantification of wound-healing capacity. Percent migration distance was calculated in relation to the mean width of the wound at 0 h, as: [100*(A-B)/A)]; where A is the mean wound width at t = 0 h, and B is the mean wound width at the indicated treatment time. *Columns*, mean (n=5); *bars*, SD; **, $P < 0.005$, significantly different from control by two-way ANOVA.

Pancratistatin induces ROS production

Due to its selective anti-cancer activity we hypothesized that pancratistatin may be targeting the mitochondria of cancer cells, which have distinct properties and metabolic alterations from normal mitochondria (Fulda *et al,* 2010). Increasing reports indicate that mitochondrial-mediated ROS production activates apoptotic cell death in cancer cells more potently than in non-cancerous cells (Ralph *et al,* 2009; Wang *et al,* 2010). Here we report that pancratistatin treatment increased ROS production in metastatic prostate cancer cells and that longer treatment with pancratistatin corresponded with higher ROS levels, up to 72 h. As shown in figure 4A, ROS production in p53-mutant DU145 cells was significantly higher than control, with as much as 10-fold increase in ROS production after 72 h exposure to pancratistatin. Treatment with pancratistatin also increased ROS production in wild-type p53 LNCaP cells, albeit to a lesser extent than in DU145 cells, causing an approximate 5-fold increase over control after 72 h (Figure 4A). This result suggests pancratistatin induced ROS production in prostate cancer cells, which may be modulated by p53 function.

Loss of mitochondrial membrane potential results from exposure to pancratistatin

Pancratistatin has previously been shown to cause selective dissipation of mitochondrial membrane potential in melanoma and colorectal adenocarcinoma cells (Chatterjee *et al,* 2011; Griffin *et al,* 2011). To determine whether pancratistatin elicits a similar response in metastatic prostate cancer cells, mitochondrial membrane potential was monitored using TMRM dye following 72 h exposure to pancratistatin. Pancratistatin treatment resulted in near complete loss of TMRM puncta, which indicates collapse of the mitochondrial membrane potential, in both DU145 and LNCaP cells (Figure 4B). When paired with the observed increase in ROS production, this result suggests that pancratistatin induces mitochondrial-mediated apoptotic cell death.

Caspase activation following pancratistatin treatment

Regardless of whether the extrinsic or intrinsic pathway of apoptosis is induced, apoptotic cell death typically culminates with cleavage and activation of caspases. Mechanistically, caspase-9 is activated upstream of caspase-3, and downstream of mitochondrial membrane permeabilization, thus indicates that the intrinsic pathway of apoptosis is being induced. Caspase-8 becomes activated following death-receptor

stimulation, which is characteristic of extrinsically-mediated apoptotic cell death. To delineate the apoptosis pathway activated by pancratistatin, time-based caspase-activity profiling was performed. Pancratistatin treatment resulted in caspase-9 activation in prostate cancer cells; with 4-fold increase over control in LNCaP cells after only 24 h and approximately 5-fold increase in DU145 cells after 72 h (Figure 4C). Caspase-9 activation correlated with increased caspase-3 activation in LNCaP cells, resulting in 5-fold increased activity over control after 48 h treatment. Interestingly, activation of caspase-3 in androgen-refractory, p53-mutant DU145 cells was much less pronounced (less than 2-fold increase) after 72 h treatment with pancratistatin. Caspase-8 activity did not significantly increase in either cell line in response to pancratistatin exposure (Figure 4C). Taken together these findings indicate that pancratistatin leads to activation of caspases involved in the intrinsic pathway of apoptosis.

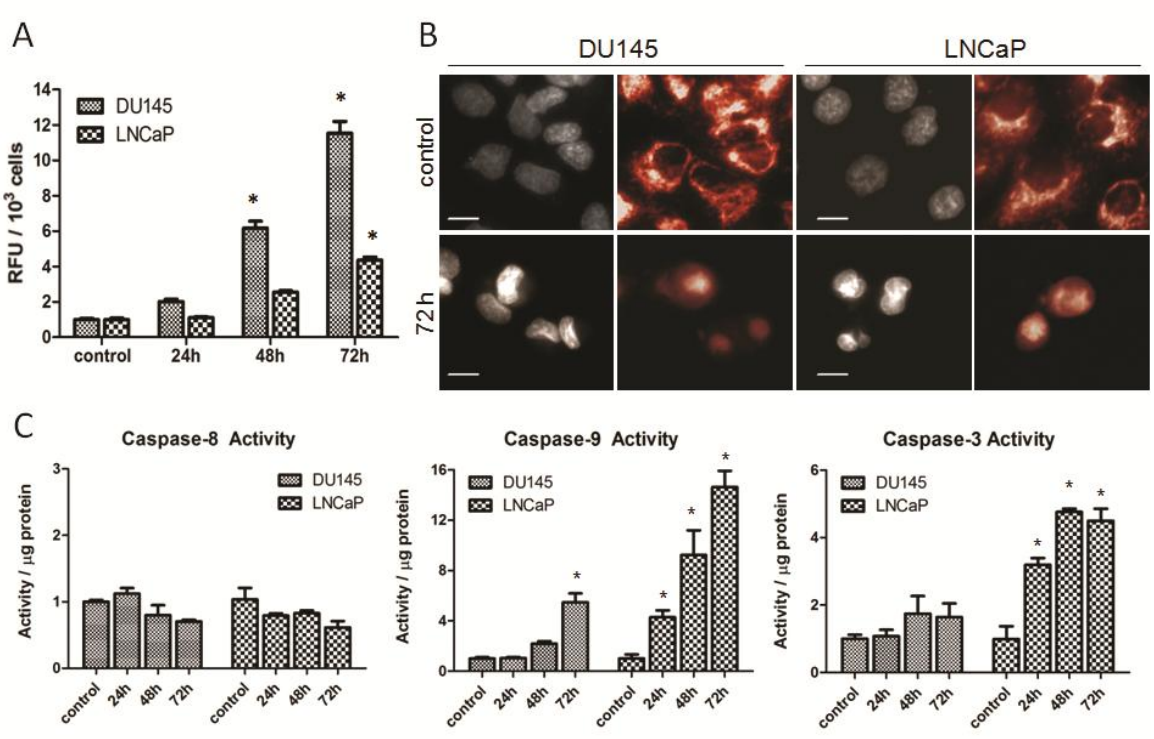

Figure 4. Pancratistatin selectively affects mitochondrial function of prostate cancer cells. (**A**) Measurement of whole-cell ROS production in DU145 and LNCaP cells after indicated length of exposure to control (Me_2SO) or 1 µM pancratistatin. Fluorescence generated by the oxidized product of H_2DCFDA is expressed as fold-difference of control per 10 000 cells in relative fluorescence units (RFU) and is indicative of cellular ROS levels. *Columns*, mean (n=3); bars, SD; *, $P < 0.05$, significantly different from control by paired *t*-test. (**B**) Representative fluorescence micrographs of DU145, LNCaP and NHF cells stained with Hoechst and TMRM dye after 72 h with 1 µM pancratistatin (PST) or control (Me_2SO). Scale bars represent 15 µm. Pancratistatin induced MMP collapse in DU145 and LNCaP cells. (**C**) Caspase-3, -8 and -9 activity was assayed in DU145 and LNCaP cells following treatment with control (Me_2SO) or 1 µM pancratistatin for the indicated time points. Cleavage of caspase-specific fluorogenic substrates (caspase-3, DEVD-afc; caspase-8, LEHD-afc; caspase-9, IETD-afc) indicates the level of caspase activity in the sample. Caspase activity was calculated relative to control and expressed as activity (RFU) per microgram protein. *Columns*, mean (n=3); bars, SD; *, $P < 0.05$, significantly different from control by paired *t*-test.

Pancratistatin induces autophagy in p53 mutant prostate cancer cells

Autophagy is a process of self-digestion induced in response to nutrient deprivation, and is used by tumor cells to survive adverse conditions in the tumor microenvironment. Sustained autophagy however, can be detrimental to a cell, resulting in autophagic cell death. To determine whether pancratistatin elicits an autophagy response in metastatic prostate cancer cells, DU145 and LNCaP cells were treated with 1 µM pancratistatin or 5 µM tamoxifen, a known inducer of autophagy. Compared to control-treated cells, there was an increase in autophagic vacuoles visualized by MDC staining in DU145 cells after 96 h with pancratistatin, but no observable change in LNCaP cells (Figure 5A). As anticipated, tamoxifen induced non-lethal autophagy in both cell lines, at both 24 and 96 h (Figure 5A). To further confirm pancratistatin-induced autophagy in DU145 cells, we analyzed the expression level of microtubule-associated protein1 light chain 3 (LC3), an important marker and effector of autophagy. Indeed, after 96 h exposure to pancratistatin or tamoxifen, there was increased expression of LC3 compared to control (Figure 5B). There was no observable increase in LC3 expression after 24 h pancratistatin treatment compared to control. These data indicate, for the first time, that pancratistatin induces an autophagic cell death response in androgen-independent prostate cancer cells.

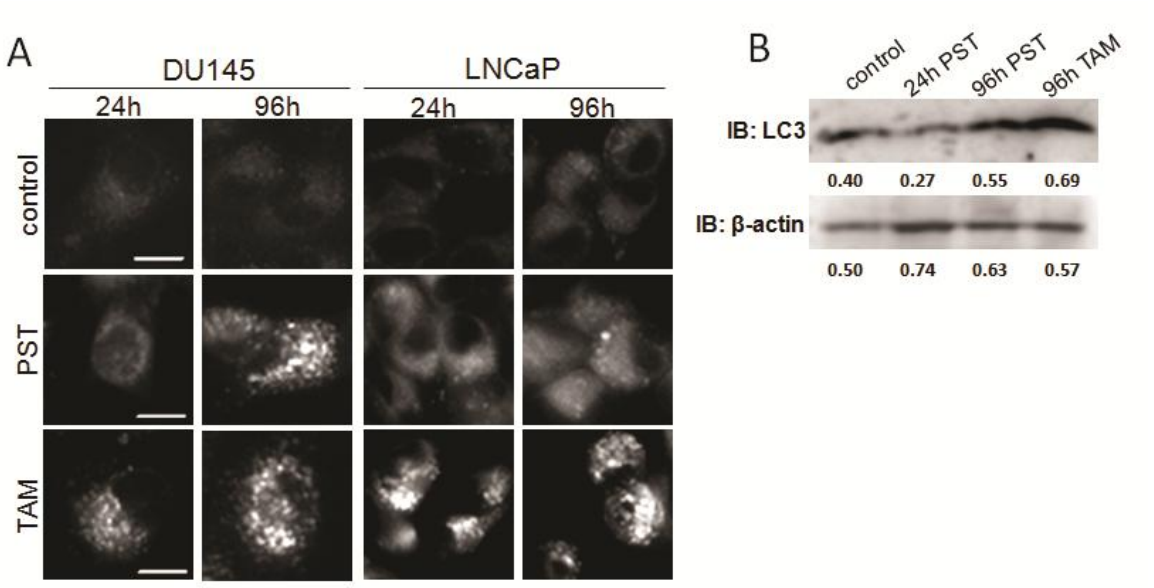

Figure 5. Pancratistatin induces autophagy in androgen-refractory prostate cancer cells. (A) Representative images of DU145 and LNCaP cells stained with MDC after 24- and 96-h with control (Me_2SO), 1 µM pancratistatin (PST) or 5 µM tamoxifen (TAM). Scale bars represent 15 µm. (**B**) DU145 cells were treated with control (Me_2SO), 1 µM pancratistatin (PST) for 24 and 96 h, or 5 µM tamoxifen (TAM) for 96 h. Post-nuclear lysate was separated by SDS-PAGE followed by immunoblotting using specific antibodies against LC-3 or β-actin. Immunoblot images were digitized and optical densities were quantified using NIH Image *J* software.

Anti-tumor effect of pancratistatin on prostate tumor xenografts

To assess the efficacy of pancratistatin *in vivo*, we tested its anti-tumor potential against human prostate tumor xenografts grown in immune-compromised mice. Pancratistatin (3 mg/kg) or vehicle (5 µl Me_2SO in PBS) was administered intra-tumor (IT) four times over three weeks in animals bearing DU145 xenografts. After the final treatment, the average tumor volume in pancratistatin-treated mice was approximately 50% smaller than that of vehicle-treated mice (Figure 6A, 6B). The average body weight of the animals did not vary significantly between treatment groups throughout the study (Figure 6C). Importantly, there were no observable signs of stress such as redness or swelling at the injection site or change in activity / behaviour of animals receiving pancratistatin compared to control. This finding suggests that pancratistatin has anti-tumor activity against human prostate cancer *in vivo*, and is well-tolerated by mice at the dosage tested.

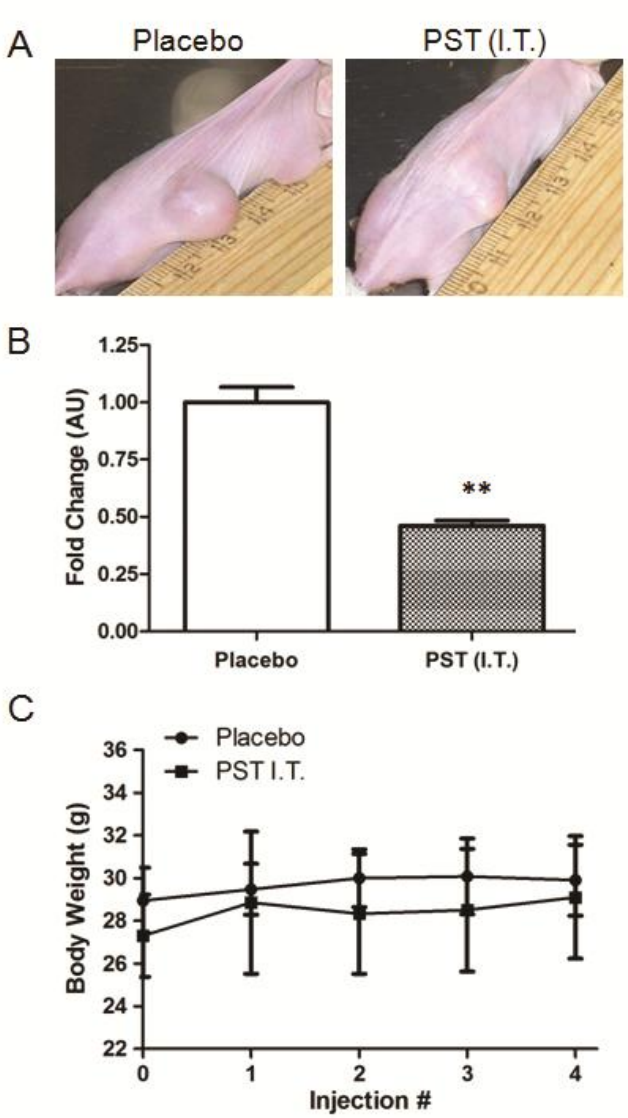

Figure 6. Pancratistatin reduces growth of human prostate tumor xenografts. (**A**) Representative images of DU145 tumor xenografts in control (Me_2SO) and 3 mg/kg pancratistatin (PST)-treated (IT) Nu/Nu immune-compromised mice. (**B**) Fold-difference of tumor volume between control and PST treated mice upon completion of the study. *Columns*, mean (n=3); bars, SD; **, $P < 0.005$, significantly different from control by paired *t*-test. (C) Average body weights of control (Me_2SO) and pancratistatin (PST)-treated (3 mg/kg, IT) mice. The body weights of control and PST-treated mice did not vary significantly throughout the study. *Data points*, mean (n=3); bars, SD.

DISCUSSION

Metastatic prostate cancer is typically androgen-refractory and treatment options are limited for advanced stages of the disease. It is proposed that resistance to chemotherapy, specifically endocrine therapy, is a result of cancer cell protection through evasion of apoptosis and/or induction of autophagy. Avoidance of apoptosis is considered one of the hallmarks of cancer, and stimulation of apoptosis is the primary aim of many anti-cancer drugs (Hanahan and Weinberg, 2000). In tumor cells, the process of autophagy is thought to promote survival in adverse conditions of the tumor microenvironment, including chemotherapeutic insult. Autophagy is a process of self-digestion used by cells in times of starvation, or in attempt to clear damaged proteins/organelles from the cell (Levine, 2007). Thus, inhibition of autophagy has become an attractive approach to modulate resistance of tumor cells to chemotherapy agents (White *et al,* 2009; Dalby *et al,* 2010).

The interplay between autophagy and apoptosis has garnered significant interest in the past few years, and it has come to light that proteins traditionally viewed as pro-apoptotic or anti-apoptotic are also important regulators of autophagy (Dalby *et al,* 2010; Olovnikova *et al,* 2009; Fimia and Piacentini, 2010). The quintessential tumor suppressor protein p53 may be viewed as a central player in both processes, as it is known to induce apoptosis and inhibit autophagy (Galluzzi *et al,* 2010; Green and Kroemer, 2009). In response to extensive DNA damage or other lethal stressors, pro-apoptotic proteins such as Bax and PUMA (p53-upregulated modulator of apoptosis) become activated by p53 and result in mitochondrial-mediated apoptosis (Green and Kroemer, 2009). Functional p53 also acts to inhibit autophagy either directly, through activation of DRAM (damage-regulated autophagy modulator), or indirectly through suppression of mTOR (mammalian target of Rapamycin) – the primary regulator of survival autophagy (Olovnikova *et al,* 2009).

It is suggested that over half of human cancers have functionally inactive p53 mutations (Green and Kroemer, 2009). Lack-of-function mutations of p53 allow tumor cells to escape apoptosis, use autophagy to protect against stressors, and survive on enhanced glycolysis. Mitochondria of cancer cells are purportedly more vulnerable to attack than non-cancerous cell mitochondria, due to their aberrant metabolic reprogramming (Fulda *et al,* 2010). Cancer cells, unlike normal cells, primarily use glycolysis for production of ATP, and largely bypass oxidative phosphorylation (a

phenomenon known as the Warburg effect). As a result, cancer cells over-produce lactate compared to their normal cell counterparts, contributing to acidification of the tumor microenvironment (Fulda *et al,* 2010). Another aspect worth consideration is that the rapid proliferation rate of cancer cells may result in improper lipid remodelling of mitochondrial membranes (as well as other organelles), making cancer cell mitochondria more susceptible to disruption (Alirol and Martinou, 2006). In this report, our findings suggest that pancratistatin directly targets the mitochondria and leads to p53-independent cell death.

Our results indicate that pancratistatin induces cell death with features characteristic to apoptosis, and elicits an autophagy response in metastatic prostate cancer cells. We suspect that pancratistatin is inducing autophagic cell death in prostate cancer cells, rather than protective autophagy, due to the decreased cell viability, collapsed mitochondrial membrane potential and increased ROS production that results from prolonged exposure (96 h) to pancratistatin. Importantly, as proof-of-concept, we report that intra-tumor administration of pancratistatin caused a significant reduction in the growth of DU145 xenograft tumors in immune-compromised mice. The concentration of pancratistatin used *in vivo* (3 mg/kg) is well under the previously determined maximum tolerated dose (Gabrielsen *et al,* 1992). There was no morbidity due to treatment, nor was there drastic variation in activity level or significant weight loss/gain between control and treated animals, indicating low toxicity of pancratistatin *in vivo*. This current observation correlated with previous histopathology analysis performed on vital organs from pancratistatin-treated animals, which had no gross morphological differences from vehicle-treated animals (Griffin *et al,* 2011). This proof-of-concept study indicated that pancratistatin causes significant growth reduction of DU145 xenograft tumors without deleterious side-effects.

CONCLUSIONS

In this study, we report for the first time that pancratistatin induced apoptotic cell death in metastatic prostate cancer cells independent of androgen sensitivity. In addition, pancratistatin was found to have anti-tumor activity on human prostate tumors *in vivo*. Pancratistatin treatment caused increased ROS production and is believed to selectively target cancer cell mitochondria. For the first time, pancratistatin was shown to incite autophagic cell death in p53-mutant metastatic prostate cancer cells. Taken together, these results demonstrate that pancratistatin is a potent and selective natural anti-cancer compound that may be an effective treatment option for metastatic prostate cancer, independent of p53-status and hormone-sensitivity.

REFERENCES

Alirol E, Martinou JC. Mitochondria and cancer: is there a morphological connection? Oncogene 2006; 25: 4706-4716.

Chatterjee SJ, McNulty J, Pandey S. Sensitization of human melanoma cells by tamoxifen to apoptosis induction by pancratistatin, a nongenotoxic natural compound. Melanoma Res 2011. 2010 Mar 17 [Epub ahead of print].

Dalby KN, Tekedereli I, Lopez-Berestein G, Ozpolat B. Targeting the prodeath and prosurvival functions of autophagy as novel therapeutic strategies in cancer. Autophagy 2010; 6(3): 322-329.

DiPaola RS, Dvorzhinski D, Thalasila A, *et al*. Therapeutic starvation and autophagy in prostate cancer: a new paradigm for targeting metabolism in cancer therapy. Prostate 2008; 68(16): 1743-1752.

Dong LF, Freeman R, Liu J, *et al*. Suppression of tumor growth in vivo by the mitocan alpha-tocopheryl succinate requires respiratory complex II. Clin Cancer Res 2009; 15(5): 1593-1600.

Fimia GM, Piacentini M. Regulation of autophagy in mammals and its interplay with apoptosis. Cell Mol Life Sci 2010; 67(10): 1581-1588.

Fulda S, Galluzzi L, Kroemer G. Targeting mitochondria for cancer therapy. Nat Rev Drug Discov 2010; 9: 447-464.

Gabrielsen B, Monath TP, Huggins JW, *et al*. Antiviral (RNA) activity of selected Amaryllidaceae isoquinoline constituents and synthesis of related substances. J Nat Prod 1992; 55(11): 1569-1581.

Galluzzi L, Morselli E, Kepp O, Vitale I, Pinti M, Kroemer G. Mitochondrial liaisons of p53. Antioxid Redox Signal 2010 Aug 16. [Epub ahead of print]

Gibson SB. A matter of balance between life and death: targeting reactive oxygen species (ROS)-induced autophagy for cancer therapy. Autophagy 2010; 6(7): 835-837.

Green DR, Kroemer G. Cytoplasmic functions of the tumor suppressor p53. Nature 2009; 458(7242): 1127-1130.

Griffin C, Hamm C, McNulty J, Pandey S. Pancratistatin induces apoptosis in clinical leukemia samples with minimal effect on non-cancerous peripheral blood mononuclear cells. Cancer Cell Int 2010; 10: 6.

Griffin C, Karnik A, McNulty J, Pandey S. Pancratistatin selectively targets cancer cell mitochondria and reduces growth of human colon tumor xenografts. Mol Can Ther 2011; 10(1): 57-68.

Hanahan D, Weinberg RA. The hallmarks of cancer. Cell 2000; 100(1): 57-70.

Hu H, Lee HJ, Jiang C, *et al*. Penta-1,2,3,4,6-O-galloyl-beta-D-glucose induces p53 and inhibits STAT3 in prostate cancer cells in vitro and suppresses prostate xenograft tumor growth in vivo. Mol Cancer Ther 2008; 7(9): 2681-2691.

Kekre N, Griffin C, McNulty J, Pandey S: Pancratistatin causes early activation of caspase-3 and the flipping of phosphatidyl serine followed by rapid apoptosis specifically in human lymphoma cells. Cancer Chemother Pharmacol 2005; 56: 29-38.

Kornienko A, Evidente A. Chemistry, Biology, and Medicinal Potential of Narciclasine and its Congeners. Chem Rev 2008; 108: 1982–2014.

Levine B. Cell biology: Autophagy and cancer. Nature Q&A 2007; 446: 745-747.

Liu EH, Qi LW, Wu Q, Peng YB, Li P. Anticancer agents derived from natural products. Mini Rev Med Chem 2009; 9(13): 1547-1555.

McNulty J, Mao J, Gibe R, *et al*. Studies directed towards the refinement of the pancratistatin cytotoxic pharmacophore. Bioorg Med Chem Lett 2001; 11(2): 169-172.

Morselli E, Galluzzi L, Kepp O, *et al*. Anti- and pro-tumor functions of autophagy. Biochim Biophys Acta 2009; 1793(9): 1524-1532.

Neuzil J, Wang XF, Dong LF, Low P, Ralph SJ. Molecular mechanism of 'mitocan'-induced apoptosis in cancer cells epitomizes the multiple roles of reactive oxygen species and Bcl-2 family proteins. FEBS Lett 2006; 580(22): 5125-5129.

Olovnikova IA, Kravchenkoa JE, Chumakov PM. Homeostatic functions of the p53 tumor suppressor: Regulation of energy metabolism and antioxidant defence. Sem Can Biol 2009; 19: 32–41.

Pradelli LA, Beneteau M, Ricci JE. Mitochondrial control of caspase-dependent and -independent cell death. Cell Mol Life Sci 2010; 67: 1589–1597.

Qadir MA, Kwok B, Dragowska WH, *et al*. Macroautophagy inhibition sensitizes tamoxifen-resistant breast cancer cells and enhances mitochondrial depolarization. Breast Cancer Res Treat 2008; 112: 389–403.

Radhakrishnan S, Miranda E, Ekblad M, *et al*. Efficacy of oncolytic mutants targeting pRb and p53 pathways is synergistically enhanced when combined with cytotoxic drugs in prostate cancer cells and tumor xenografts. Hum Gene Ther 2010; 21(10): 1311-1325.

Ralph SJ, Rodríguez-Enríquez S, Neuzil J, Moreno-Sánchez R. Bioenergetic pathways in tumor mitochondria as targets for cancer therapy and the importance of the ROS-induced apoptotic trigger. Mol Aspects Med 2010; 31(1): 29-59.

Shah MR, Kriedt CL, Lents NH, *et al*. Direct intra-tumoral injection of zinc-acetate halts tumor growth in a xenograft model of prostate cancer. Exp Clin Cancer Res 2009; 28: 84.

Siedlakowski P, McLachlan-Burgess A, Griffin C, Tirumalai SS, McNulty J, Pandey S. Synergy of Pancratistatin and Tamoxifen on breast cancer cells in inducing apoptosis by targeting mitochondria. Cancer Biol Ther 2008; 7(3): 376-384.

Valko M, Leibfritz D, Moncol J, Cronin MT, Mazur M, Telser J. Free radicals and antioxidants in normal physiological functions and human disease. Int J Biochem Cell Biol 2007; 39(1): 44-84.

Wang F, Ogasawara MA, Huang P. Small mitochondria-targeting molecules as anti-cancer agents. Mol Asp Med 2010; 31: 75–92.

White E, DiPaola RS. The double-edged sword of autophagy modulation in cancer. Clin Cancer Res 2009; 15(17): 5308-5316.

Xiao D, Powolny AA, Moura MB, *et al*. Phenethyl isothiocyanate inhibits oxidative phosphorylation to trigger reactive oxygen species-mediated death of human prostate cancer cells. J Biol Chem 2010; 285(34): 26558-26569.

CHAPTER 7

General Discussion

The aim of this work was to evaluate the anti-cancer activity of the natural alkaloid pancratistatin and to determine its mechanism of action. Pancratistatin, extracted from *H. littoralis*, is considered one of the most important biologically active metabolites of *Amaryllidaceae* plants, which have been used for the management of cancer in folk medicine for centuries (Kornienko and Evidente, 2008).

The current standard of care for cancer has room for improvement to say the least; the high fatality associated with metastatic disease has not changed dramatically in the last decade, despite major advances in molecular medicine (Jemal *et al,* 2010). Although based on observations made over half a century ago, the trend in cancer research over the last few years has shifted away from oncogene-interference tactics and towards exploiting the vulnerability of cancer cell mitochondria (Warburg, 1956; Bouchier-Hayes *et al,* 2005; Fulda *et al,* 2010). This is evident by the popularity of the new term “mitocan” in the literature, which is the moniker given to *mito*chondria-targeting *can*cer drugs (Neuzil *et al,* 2006). Cancer cell mitochondria are typically hyperpolarized, rely heavily on glycolysis, have deregulated mitochondrial respiration, an acidic microenvironment, and high intracellular ROS (Galluzzi *et al,* 2010; Khandrika *et al,* 2009; Mathupala *et al,* 2010). Ultimately, the fundamental role of mitochondria in cell death cannot be tamed; mitochondrial outer membrane permeabilization (MOMP) causes even the most oncogene-addicted tumor cell to succumb to apoptotic death (Green and Evan, 2002). Compounds that directly target the mitochondria to trigger MOMP act independently of upstream anti-apoptotic signalling pathways (such as those mediated by Bcl-2 proteins) that contribute to the chemo-resistance phenotype of many tumors (Fulda, 2010; Biasutto *et al,* 2010).

Recently, many natural products have been discovered that directly target cancer cell mitochondria, including alpha-tocopheryl succinate (α-TOS), methyl jasmonate, resveratrol and green tea polyphenols (Biasutto *et al,* 2010; Ralph and Neuzil, 2009). Alpha-tocopheryl succinate, a vitamin E analogue, is known to bind and inhibit complex II of the MRC and has also been shown to disrupt interaction of pro-apoptotic Bak with Bcl-2 and Bcl-XL, thus acting as a BH3-mimetic (Dong *et al,* 2009; Ralph and Neuzil, 2009). Studies with mtDNA-deficient cells proved that α-TOS targets a component of the MRC, which is similar to the findings presented in this work to delineate the target of pancratistatin. Methyl jasmonate, a plant stress hormone, induces opening of the

mitochondrial permeability transition pore (MPTP) by detaching hexokinase (HK) from VDAC on the mitochondrial membrane (Goldin *et al,* 2008). HK is bound to VDAC specifically in cancer cells to couple residual ATP to the rate-limiting step of glycolysis (Biasutto *et al,* 2010). The possible modulation of mitochondrial-associated HK by pancratistatin was studied in our laboratory, but there was no evidence of HK dissociation from VDAC following treatment with pancratistatin in cancer cells (*unpublished data*). The flavonoid polyphenols resveratrol and epigalocatechin gallate (EGCG), also reportedly target the mitochondria, albeit in different ways. Resveratrol acts at several different sites of the MRC, likely competing with coenzyme Q_{10}, and also blocks the F_1-ATPase (Ralph and Neuzil, 2009). EGCG, an anti-oxidant and chemopreventative, acts as a BH3-mimetic to prevent inhibition of Bax and Bak by Bcl-2 anti-apoptotic proteins (Deorukhkar *et al,* 2010; Ralph and Neuzil, 2009).

In this work, it was determined that pancratistatin effectively and selectively induces cell death in cancer cells in *in vitro*, *ex vivo* and *in vivo* models, by targeting the mitochondria (Griffin *et al,* 2010; Griffin *et al,* 2011a,b). Pancratistatin was found to cause increased ROS production, collapse of MMP, release of pro-apoptotic factors and caspase activation, in a p53-independent manner. Moreover, mt-DNA deficient cancer cells were insensitive to pancratistatin-induced cell death, suggesting that mt-DNA encoded components of the MRC are crucial for the anti-cancer activity of pancratistatin.

Pancratistatin has high potential for clinical development as a potent anti-cancer agent based on the 'therapeutic window' of selective activity observed *in vitro, ex vivo* and the significant anti-tumor affect *in vivo* (Griffin *et al,* 2010; Griffin *et al,* 2011a,b). Clinical use of pancratistatin as a single agent could prove efficient against multiple types of cancer. Natural compounds have the propensity to act on multiple sites, which may mirror effects achieved by combination of two (or more) targeted drugs, but with the toxicity of only one (Deorukhkar *et al,* 2010). Even so, combination therapy is the standard practice of current cancer treatment (Blagosklonny, 2005). Thus, pancratistatin, predicted to have low toxicity to non-cancerous tissues, in combination with standard or targeted therapies, will likely enhance the overall response to treatment. Combination of pancratistatin with other (low-toxicity) natural products may provide the best synergistic effect. Combination of pancratistatin with curcumin, a component of turmeric spice that has anti-inflammatory, anti-oxidant and anti-tumor activity, was shown to be more

effective than either agent alone against melanoma cells *in vitro* (Chatterjee *et al,* 2011). Effective treatment of cancer will likely be found in combination therapy with agents that have non-overlapping targets and/or with natural products that have broad-range activities.

Speculation of the target(s) of pancratistatin in attempt to explain its broad-range of activity against different types of human cancer is up for debate until definitively determined. It has been reported that some *Amaryllidaceae* alkaloids have anti-glycosidic (and hence anti-viral) activity due to the similarity of their oxygenation pattern to that of natural sugars (Gabrielsen *et al,* 1992; Hudlicky *et al,* 2002). Cancer cells rely heavily on glucose metabolism for their energy needs, and have been shown to upregulate the expression of glucose transporters (GLUT1 and/or GLUT3) on the plasma membrane (Macheda *et al,* 2009). It may be possible that cancer cells are actively importing metabolites other than glucose, such as pancratistatin, by GLUT1. GLUT1 is also reported to regulate the influx of vitamin C in tumor cells, indicating its capacity for transport of substrates other than glucose (KC *et al,* 2005). Another possible target of pancratistatin may be anti-apoptotic proteins of the Bcl-2 family. Pancratistatin has structural resemblance to the designer BH3 mimetic Gossypol, which has recently been shown to modulate the interaction between Bcl-2/Bcl-XL and Beclin-1 to stimulate autophagy in prostate cancer cells (Zhang *et al,* 2010). Other natural plant-based compounds, i.e., resveratrol and EGCG, and some *Amaryllidaceae* alkaloids have been shown to bind and inhibit anti-apoptotic Bcl-2 family proteins leading to activation of Bax/Bak, MOMP and apoptotic cell death (Ralph and Neuzil, 2009). It is therefore possible that pancratistatin may be modulating the anti-apoptotic effect of Bcl-2 proteins to contribute to cell death. Lastly, due to the common confusion of its name, pancratistatin is assumed to have cholesterol-lowering properties of common statins (e.g., Lipitor); however, its name is actually derived from the Latin for its natural source (*Pancratium littorale*) and for its plant-growth inhibitory activity (Gabrielsen *et al,* 1992). Interestingly enough it can be argued that pancratistatin has a skeletal structure that resembles that of cholesterol steroid hormones like estrogen. With this in mind, pancratistatin may act as a hormone antagonist, blocking physiological roles of estrogen such as growth stimulation and regulation of MRC components (Chen *et al,* 2009).

Based on current literature and the data presented in this work, the mechanism of action of pancratistatin is decidedly mitochondria-targeted. In some cancer cell lines, caspase activation was noted as the initiating event in pancratistatin-induced apoptosis. However, this hypothesis was revised after finding that caspase inhibition did not affect pancratistatin activity, and mt-DNA deficient cells were insensitive to pancratistatin-induced apoptosis. A common event in response to pancratistatin treatment was increased ROS generation. Recently, ROS generation was discounted as the primary cause of cell death, given that anti-oxidants were unable to protect cells from pancratistatin-induced apoptosis. At this time, our data indicate that pancratistatin targets a component of the mitochondrial respiratory chain to induce excess ROS production, which destabilizes the mitochondrial membrane potential to the extent that the outer mitochondrial membrane becomes permeable and releases cytotoxic factors to the cytosol. Compared to other natural compounds, pancratistatin may also contribute to cell death by indirect activation of pro-apoptotic Bcl-2 proteins, and/or interfering with anti-oxidant response mechanisms (Dong *et al,* 2009; Ralph and Neuzil, 2009). These possible alternate actions of pancratistatin may contribute to cell death even when co-treated with anti-oxidants. Additionally, ROS generation may trigger mitochondria-selective autophagy (mitophagy) (Kroemer *et al,* 2007). Although pancratistatin-induced ROS generation may incite mitophagy in attempt to clear away damaged organelles, our current hypothesis is that pancratistatin ultimately induces mitochondrial permeabilization, leading to cell death that cannot be reversed by autophagy.

The reported anti-cancer activity of other *Amaryllidaceae* alkaloids, including lycorine and narciclasine, strengthen our hypothesis and the significance of results presented in this work. Lycorine has been implicated in the down-regulation of anti-apoptotic Bcl-2 family member Mcl-1 (Liu *et al,* 2009). Our observation that pancratistatin induces an autophagic response in p53-mutant prostate cancer cells (detailed in Chapter 6) may be due in part to possible down-regulation of Bcl-2 proteins by pancratistatin. Decreased function of Bcl-2, an inhibitor of autophagy, would potentiate the activation of Beclin-1-mediated autophagy induction (Fimia and Piacentini, 2010). Pancratistatin did not increase levels of autophagy in p53-wild type prostate cancer cells, but these cells did undergo apoptotic cell death – indicating that pancratistatin targets a protein downstream of p53-regulatory jurisdiction.

Narciclasine, an *Amaryllidaceae* alkaloid with a structure that closely resembles pancratistatin, has also been shown to have potent anti-cancer properties with selective action against cancer cells (Dumont *et al,* 2007). More recently, Narciclasine was shown to have a growth-inhibitory effect in cellular and orthotopic tumor models of metastatic brain cancer at low (50 – 100 nM) concentrations (Van Goietsenoven *et al,* 2010). The authors report that narciclasine targets elongation factor 1A (eEF1A), a core component of protein synthesis machinery (Van Goietsenoven *et al,* 2010). In a related study by Ingrassia and colleagues, the stability of narciclasine was determined to be unaffected after 7 days in media at 37°C, and oral administration of narciclasine to rats (3 mg/kg, 5X/week for 3 weeks) did not significantly affect body weight or cause fatality (Ingrassia *et al,* 2009).

Recently, narciclasine was discovered to be a potent inhibitor of human cytochrome P450 3A4 (CYP3A4) activity, which is one of the most important enzymes in the oxidation and detoxification of xenobiotics (McNulty *et al,* 2010). The CYP3A subfamily comprises approximately one third of the cytochrome P450 enzyme pool in the liver, and the CYP3A4 isoenzyme accounts for ~60% of drugs metabolized (Nelson *et al,* 2004; Weinberg, 2007). Interestingly, the derivative dihydronarciclasine and native pancratistatin did not inhibit this enzyme, which indicates a critical function of the double bond at C-1 in narciclasine that is not present in the other two compounds (McNulty *et al,* 2009; McNulty *et al* 2010). Inhibition of CYP3A4 by narciclasine may lead to drug accumulation and hepatic toxicity, and insufficient detoxification of potential carcinogens by CYP3A4, which raises serious concerns for the clinical development of narciclasine (McNulty *et al,* 2010).

Another recent study revealed pancratistatin as a novel substrate of ATP-binding cassette transporter (ABCG2) protein (Deeken *et al,* 2009). ABCG2 is a membrane-associated protein believed to regulate oral availability and serve a protective role in hematopoietic stem cells (HSCs), the blood-brain barrier and the maternal-fetal barrier (Deeken *et al,* 2009). Interestingly, a thiosemicarbazone (NSC73306) was also discovered as a substrate of ABCG2, and is reportedly active against cancer cells that over-express functional P-glycoprotein, re-sensitizing these cells to chemotherapeutic agents (Wu *et al,* 2007). ABCG2 is widely expressed in hematopoietic stem cells as protection from potentially damaging xenobiotics, and it is possible that cancer stem cells, proposed to have the self-renewal capabilities of HSCs, may harbour intrinsic

chemotherapy resistance due to high expression of ABCG2 (Deeken *et al,* 2009). These novel findings suggest that pancratistatin interacts with ABCG2 in such a way as to facilitate activity against multi-drug resistant cancer cells, and does not inhibit the important drug metabolizing enzyme CPY3A4, perhaps enabling its detoxification and excretion.

Pancratistatin and plant alkaloids in general have low solubility in water (less than 0.4 mg/ml), which is an issue for pharmacokinetic analysis and clinical application (Beijnen *et al,* 1995; Gabrielsen *et al,* 1992). Multiple efforts to synthesize more soluble analogues that retain the anti-cancer activity of native pancratistatin, have lead to the development of water-soluble sodium pancratistatin 3,4-*O*-cyclic phosphate (Shnyder *et al,* 2008). Sodium pancratistatin 3,4-*O*-cyclic phosphate was shown to disrupt mitochondrial function in colon cancer cells and significantly reduce growth of human colon xenografts; however, these effects were achieved using the high concentration of 250 µM *in vitro*, and the (maximum tolerated) dose of 100 mg/kg *in vivo* (Shnyder *et al,* 2008). Compared to the native compound, the anti-cancer activity of this analogue is significantly lower, but it is vastly more soluble in water than pancratistatin.

The challenging issues of solubility and bioavailability of pancratistatin mirror the struggles that hindered clinical development of paclitaxel (Taxol), a natural product extracted from the bark of the Pacific Yew tree. Taxol, first discovered in 1964, was difficult to synthesize, could only be obtained from the natural source and was virtually insoluble in aqueous media (Chabner *et al,* 2005). Synthetic analogues with increased solubility and potent activity were developed, and in 1992 (nearly 30 years after its initial discovery) Taxol was FDA approved for use against ovarian cancer (Chabner *et al,* 2005). Recent advances in the development of synthetic derivatives of pancratistatin include an analogue with increased solubility but decreased potency, i.e., sodium pancratistatin 3,4-*O*-cyclic phosphate; and an analogue with comparable potency but similar insolubility, i.e., C-1 acetoxymethyl pancratistatin (see Chapter 1, figure 5).

It has been 24 years since the discovery of pancratistatin by Pettit and colleagues, and research efforts since then have elucidated the minimum active pharmacophore and provided clues as to its target and mechanism of action, demonstrating the high potential of pancratistatin for advancement to clinical trials (Pettit *et al,* 1986; McNulty *et al,* 2008; Griffin *et al,* 2011).

FUTURE DIRECTION

Due to the low bioavailability of the native compound from its natural source, pre-clinical development of pancratistatin should continue with focus on active synthetic derivatives, specifically C-1 acetoxymethyl pancratistatin. Future work on this project should involve detailed characterization of the protein target(s) and determination of the sub-cellular localization of pancratistatin and/or active synthetic derivatives. This may be achieved by synthesis of a radioactive C^{14}-labelled analogue and/or cross-linking of an analogue to agarose beads for analysis by affinity chromatography. Synthesis of a radio-labelled analogue of pancratistatin will allow study of the uptake, localization and efflux of the analogue, using both *in vitro and in vivo* models. Study of potential interacting partners of (synthetic derivatives of) pancratistatin will elucidate possible target proteins and give an indication of alternate effects. An active analogue may be cross-linked to agarose beads using a 4-6 carbon long linker chain, preferably attached at a variable region of the alkaloid (see Chapter 1, figure 5), which can then be analyzed by affinity chromatography, followed by identification of binding partners using MALDI–TOF mass spectrometry.

An alternate method to potentially identify the target(s) of pancratistatin is to compare the differential expression of proteins between responsive and non-responsive cancer cell lines by 2D-gel electrophoresis. This work has established that pancratistatin targets the mitochondria, and possibly specific components of the mitochondrial respiratory chain to induce cell death selectively in cancer cells. Previous studies in our laboratory revealed that pancratistatin was unable to induce cell death in non-small cell lung cancer cells (*unpublished data*). To better understand the mechanism of action of pancratistatin, it would be advantageous to compare the differential protein expression between this cancer cell line and a pancratistatin-sensitive cancer cell line.

Another important direction for the project is analysis of the *in vivo* effects of active synthetic derivatives of pancratistatin. Already, a preliminary study has tested intra-tumor (IT) administration of C-1 acetoxymethyl pancratistatin against human colon tumor xenografts, with promising results; however, IT administration does not accurately reflect clinical application. In the next animal study, intra-venous administration should be employed, as the ideal mode of oral feeding is not feasible due to low solubility of the alkaloid. Moreover, the route of administration will greatly affect the ADMET (absorption, distribution, metabolism, excretion, toxicity) properties, which are largely unknown at this

time. Pharmacokinetic and pharmacodynamic analysis is a critical step in the pre-clinical development of anti-cancer agents.

This work is has significantly contributed to understanding the mechanism of action of the natural anti-cancer alkaloid pancratistatin, and structure-activity relationship-based screening has lead to the synthesis of potent anti-cancer derivatives of pancratistatin. Importantly, these studies are the first to report the mitochondria-targeting activity of pancratistatin, to detail its effect on autophagy levels and to demonstrate the efficacy of pancratistatin in reducing growth of human colon and prostate tumors in animal models. Collectively, this work highlights the potential for advancement of (synthetic derivatives of) pancratistatin as an effective anti-cancer agent for clinical use in the fight against cancer.

REFERENCES

Beijnen JH, Flora KP, Halbert GW, Henrar RE, Slack JA. CRC/EORTC/NCI Joint Formulation Working Party: experiences in the formulation of investigational cytotoxic drugs. Br J Cancer 1995; 72(1): 210-218.

Biasutto L, Dong LF, Zoratti M, Neuzil J. Mitochondrially targeted anti-cancer agents. Mitochondrion 2010; 10: 670–681.

Blagosklonny MV. How cancer could be cured by 2015. Cell Cycle 2005; 4(2): 269-278.

Bouchier-Hayes L, Lartigue L, Newmeyer DD. Mitochondria: pharmacological manipulation of cell death. J Clin Invest 2005; 115(10): 2640-2647.

Chabner BA, Roberts TG. Timeline: Chemotherapy and the war on cancer. Nat Rev Cancer 2005; 5(1): 65-72.

Chatterjee SJ, McNulty J, Pandey S. Sensitization of human melanoma cells by tamoxifen to apoptosis induction by pancratistatin, a nongenotoxic natural compound. Melanoma Res 2011. 2010 Mar 17 [Epub ahead of print].

Chen JQ, Cammarata PR, Baines CP, Yager JD. Regulation of mitochondrial respiratory chain biogenesis by estrogens/estrogen receptors and physiological, pathological and pharmacological implications. Biochim Biophys Acta 2009; 1793(10): 1540-1570.

Deeken JF, Robey RW, Shukla S, *et al*. Identification of compounds that correlate with ABCG2 transporter function in the National Cancer Institute Anticancer Drug Screen. Mol Pharmacol 2009; 76(5): 946-956.

Deorukhkar A, Krishnan S, Sethi G, Aggarwal BB. Back to basics: how natural products can provide the basis for new therapeutics. Expert Opin Investig Drugs 2007; 16(11): 1753-1773.

Dong LF, Freeman R, Liu J, *et al*. Suppression of tumor growth in vivo by the mitocan alpha-tocopheryl succinate requires respiratory complex II. Clin Cancer Res 2009; 15(5): 1593-1600.

Dumont P, Ingrassia L, Rouzeau S, Ribaucour F, Thomas S, Roland I, *et al*. The Amaryllidaceae isocarbostyril narciclasine induces apoptosis by activation of the death receptor and/or mitochondrial pathways in cancer cells but not in normal fibroblasts. Neoplasia 2007; 9(9): 766-776.

Fimia GM, Piacentini M. Regulation of autophagy in mammals and its interplay with apoptosis. Cell Mol Life Sci 2010; 67: 1581–1588.

Fulda S, Galluzzi L, Kroemer G. Targeting mitochondria for cancer therapy. Nat Rev Drug Discov 2010; 9(6): 447-464.

Gabrielsen B, Monath TP, Huggins JW, *et al*. Antiviral (RNA) activity of selected Amaryllidaceae isoquinoline constituents and synthesis of related substances. J Nat Prod 1992; 55(11): 1569-1581.

Galluzzi L, Morselli E, Kepp O, *et al*. Mitochondrial gateways to cancer. Mol Aspects Med 2010; 31(1): 1-20.

Goldin N, Arzoine L, Heyfets A, *et al*. Methyl jasmonate binds to and detaches mitochondria-bound hexokinase. Oncogene 2008; 27(34): 4636-4643.

Green DR, Evan GI. A matter of life and death. Cancer Cell 2002; 1: 19-30.

Griffin C, Hamm C, McNulty J, Pandey S. Pancratistatin induces apoptosis in clinical leukemia samples with minimal effect on non-cancerous peripheral blood mononuclear cells. Cancer Cell Int 2010; 10: 6.

Griffin C, Karnik A, McNulty J, Pandey S. Pancratistatin selectively targets cancer cell mitochondria and reduces growth of human colon tumor xenografts. Mol Can Ther 2011a; 10(1): 57-68.

Griffin C, McNulty J, Pandey S. Pancratistatin induces apoptosis and autophagy in metastatic prostate cancer cells. 2011b [Submitted to Int J Oncol].

Hudlicky T, Rinner U, Gonzalez D, *et al*. Total synthesis and biological evaluation of Amaryllidaceae alkaloids: narciclasine, ent-7-deoxypancratistatin, regioisomer of 7-deoxypancratistatin, 10b-epi-deoxypancratistatin, and truncated derivatives. J Org Chem 2002; 67(25): 8726-8743.

Ingrassia L, Lefranc F, Dewelle J, *et al*. Structure-activity relationship analysis of novel derivatives of narciclasine (an Amaryllidaceae isocarbostyril derivative) as potential anticancer agents. J Med Chem 2009; 52(4): 1100-1114.

Jemal A, Siegel R, Xu J, Ward E. Cancer statistics, 2010. CA Cancer J Clin 2010; 60(5): 277-300.

KC S, Cárcamo JM, Golde DW. Vitamin C enters mitochondria via facilitative glucose transporter 1 (Glut1) and confers mitochondrial protection against oxidative injury. FASEB J 2005; 19(12): 1657-1667.

Khandrika L, Kumar B, Koul S, Maroni P, Koul HK. Oxidative stress in prostate cancer. Cancer Lett 2009; 282(2): 125-136.

Kornienko A, Evidente A. Chemistry, biology, and medicinal potential of narciclasine and its congeners. Chem Rev 2008; 108: 1982–2014.

Kroemer G, Galluzzi L, Brenner C. Mitochondrial membrane permeabilization in cell death. Physiol Rev 2007; 87: 99-163.

Liu XS, Jiang J, Jiao XY, Wu YE, Lin JH, Cai YM. Lycorine induces apoptosis and down-regulation of Mcl-1 in human leukemia cells. Cancer Lett 2009; 274(1): 16-24.

Macheda ML, Rogers S, Best JD. Molecular and cellular regulation of glucose transporter (GLUT) proteins in cancer. J Cell Physiol 2005; 202(3): 654-662.

Mathupala SP, Ko YH, Pedersen PL. The pivotal roles of mitochondria in cancer: Warburg and beyond and encouraging prospects for effective therapies. Biochim Biophys Acta 2010; 1797(6-7): 1225-1230.

McNulty J, Nair JJ, Griffin C, Pandey S. Synthesis and biological evaluation of fully functionalized seco-pancratistatin analogues. J Nat Prod 2008; 71(3): 357-363.

McNulty J, Nair JJ, Singh M, Crankshaw DJ, Holloway AC. Structure-activity studies on seco-pancratistatin analogs: potent inhibitors of human cytochrome P450 3A4. Bioorg Med Chem Lett 2009; 19(19): 5607-5612.

McNulty J, Thorat A, Vurgun N, *et al*. Human cytochrome P450 liability studies of trans-dihydronarciclasine: a readily available, potent, and selective cancer cell growth inhibitor. J Nat Prod 2010 Sept 21. [Pre-print]

Nelson DR, Zeldin DC, Hoffman SM, Maltais LJ, Wain HM, Nebert DW. Comparison of cytochrome P450 (CYP) genes from the mouse and human genomes, including

nomenclature recommendations for genes, pseudogenes and alternative-splice variants. Pharmacogenetics 2004; 14(1): 1-18.

Neuzil J, Wang XF, Dong LF, Low P, Ralph SJ. Molecular mechanism of 'mitocan'-induced apoptosis in cancer cells epitomizes the multiple roles of reactive oxygen species and Bcl-2 family proteins. FEBS Lett 2006; 580(22): 5125-5129.

Pettit GR, Gaddamidi V, Herald DL, *et al*. Antineoplastic agents, 120. Pancratium littorale. J Nat Prod 1986; 49(6): 995-1002.

Ralph SJ, Neuzil J. Mitochondria as targets for cancer therapy. Mol Nutr Food Res 2009; 53: 9-28.

Shnyder SD, Cooper PA, Millington NJ, Gill JH, Bibby MC. Sodium pancratistatin 3,4-o-cyclic phosphate, a water-soluble synthetic derivative of pancratistatin, is highly effective in a human colon tumor model. J Nat Prod 2008; 71(3): 321-324.

Van Goietsenoven G, Hutton J, Becker JP, Lallemand B, Robert F, Lefranc F, *et al*. Targeting of eEF1A with Amaryllidaceae isocarbostyrils as a strategy to combat melanomas. FASEB J 2010; 24(11): 4575-4584.

Warburg O. On respiratory impairment in cancer cells. Science 1956; 124: 269-270.

Weinberg RA. The biology of cancer. Garland Science Taylor & Francis Group, LLC, 2007. Pgs. 485-490.

Wu CP, Shukla S, Calcagno AM, Hall MD, Gottesman MM, Ambudkar SV. Evidence for dual mode of action of a thiosemicarbazone, NSC73306: a potent substrate of the multidrug resistance linked ABCG2 transporter. Mol Cancer Ther 2007; 6: 3287–3296.

Zhang XQ, Huang XF, Hu XB, *et al*. Apogossypolone, a novel inhibitor of antiapoptotic Bcl-2 family proteins, induces autophagy of PC-3 and LNCaP prostate cancer cells in vitro. Asian J Androl 2010; 12(5): 697-708.

APPENDIX A

COPYRIGHT TRANSFER FORMS

I. *Cancer Chemotherapy & Pharmacology (2005)*

Publication of Springer Science+Business Media

SPRINGER LICENSE
TERMS AND CONDITIONS

License Number	2545701331060
License date	Nov 10, 2010
Licensed content publisher	Springer
Licensed content publication	Cancer Chemotherapy and Pharmacology
Licensed content title	Pancratistatin causes early activation of caspase-3 and the flipping of phosphatidyl serine followed by rapid apoptosis specifically in human lymphoma cells
Licensed content author	Natasha Kekre
Licensed content date	Jul 1, 2005
Volume number	56
Issue number	1
Type of Use	Thesis/Dissertation
Portion	Full text
Number of copies	5
Author of this Springer article	Yes and you are a contributor of the new work
Title of your thesis / dissertation	Evaluation of the Selective Anti-cancer Activity of Natural and Synthetic Alkaloids
Expected completion date	Jan 2011
Estimated size(pages)	200
Terms and Conditions	

Limited License
With reference to your request to reprint in your thesis material on which Springer Science and Business Media control the copyright, permission is granted, free of charge, for the use indicated in your enquiry. Licenses are for one-time use only with a maximum distribution equal to the number that you identified in the licensing process. This License includes use in an electronic form, provided it is password protected or on the university's intranet, destined to microfilming by UMI and University repository. The material can only be used for the purpose of defending your thesis, and with a maximum of 100 extra copies in paper.

Although Springer holds copyright to the material and is entitled to negotiate on rights, this license is only valid, provided permission is also obtained from the (co) author (address is given with the article/chapter) and provided it concerns original material which does not carry references to other sources (if material in question appears with credit to another source, authorization from that source is required as well). Permission free of charge on this occasion does not prejudice any rights we might have to charge for reproduction of our copyrighted material in the future.

Altering/Modifying Material: Not Permitted
However figures and illustrations may be altered minimally to serve your work. Any other abbreviations, additions, deletions and/or any other alterations shall be made only with prior written authorization of the author(s) and/or Springer Science + Business Media.

Copyright Notice:
Please include the following copyright citation referencing the publication in which the material was originally published. Where wording is within brackets, please include verbatim. "With kind permission from Springer Science+Business Media: <book/journal title, chapter/article title, volume, year of publication, page, name(s) of author(s), figure number(s), and any original (first) copyright notice displayed with material>."

No Transfer of License
This license is personal to you and may not be sublicensed, assigned, or transferred by you to any other person without Springer Science + Business Media's written permission.

II. ***Cancer Cell International (2007, 2010)***

Open Access Publication of BioMed Central Ltd.

Anyone is free:

- to copy, distribute, and display the work;
- to make derivative works;
- to make commercial use of the work;

Under the following conditions: Attribution

- the original author must be given credit;
- for any reuse or distribution, it must be made clear to others what the license terms of this work are;
- any of these conditions can be waived if the authors gives permission.

III. ***Molecular Cancer Therapeutics (2011)***

Publication of the American Association for Cancer Research (AACR)

Authors of articles published in AACR Journals are permitted to use their article or parts of their article in the following ways **without requesting permission** from the AACR. All such uses must include **appropriate attribution** to the original AACR publication. Authors may:

1. reproduce parts of their article, including figures and tables, in books, reviews, or subsequent research articles they write;
2. use parts of their article in presentations, including figures downloaded into PowerPoint, which can be done directly from the journal's website;
3. post the accepted version of their article (after revisions resulting from peer review but before editing and formatting) on their institutional website, if this is required by their institution. The version on the institutional repository must contain a link to the final, published version of the article on the AACR journal website. The posted version may be released publicly (made open to anyone) 12 months after its publication in the journal;
4. **submit a copy of their article to his or her university in support of a doctoral thesis.**

IV. ***International Journal of Oncology (2011)***

Open Access; Spandidos Publications Ltd.

Anyone is free:

- to copy, distribute, and display the work;
- to make derivative works;
- to make commercial use of the work;

Under the following conditions: Attribution

- the original author must be given credit;
- for any reuse or distribution, it must be made clear to others what the license terms of this work are;
- any of these conditions can be waived if the authors gives permission.

APPENDIX B

UNPUBLISHED DATA

BACKGROUND

The results presented in this section of the thesis relate to the studies in chapters 2, 5 and 6 of this thesis, as indicated. These findings represent important experimental data obtained after publication.

METHODS

Chemicals

Media, gentamycin, Hoechst 33342 dye, Annexin-V AlexaFluor 488, and JC-1 dye were purchased from Invitrogen. Cell proliferation reagent WST-1 was purchased from Roche. A water-soluble formulation of Coenzyme Q10 (ws-CoQ_{10}) was developed and provided by Dr. M. Sikorska at NRC Ottawa (US patents #6,045,826,6,191,172 B1 and 6,632,443). Caspase-3 and -8 fluormetric substrates were purchased from MP Biomedicals. The PM-MTOX1 plate, redox dyes and serum-free media were purchased from BiOLOG, Inc. (Hayward, CA). Pancratistatin (PST) was isolated from *H. littoralis* and provided by Dr. J. McNulty. All other chemicals were purchased from Sigma-Aldrich.

Cell culture

Human colorectal adenocarcinoma (HT-29, HCT116) and human metastatic prostate carcinoma (DU145) cell lines were purchased from ATCC. HT-29 and HCT116 cells were grown in McCoy's 5A media and DU145 cells were grown in DMEM; all cell lines were supplemented as recommended by ATCC. Human acute T-cell leukemia (Jurkat, Clone E6-1) and a dominant-negative fas-associated death domain (dnFADD) mutant of wild-type Jurkat cells (Jurkat, Clone I 2.1) were purchased from ATCC. These cells were cultured in RPMI-1640 medium supplemented with 10% FBS and 40 µg/ml gentamicin (GIBCO). Cultures were maintained at 5% CO_2 and 37°C.

Assessment of apoptosis

Apoptosis was detected by microscopy with cell-permeable Hoechst 33342 dye and/or Annexin-V AlexaFluor-488. To monitor phosphatidyl serine exposure, Annexin-V

binding assay was performed. Cells were treated as indicated, trypsinized and washed 2X in room temperature PBS, then resuspended in Annexin-V calcium-binding buffer (10 mM HEPES/NaOH pH 7.5, 140 mM NaCl, 2.5 mM $CaCl_2$), and incubated with Annexin-V AlexaFluor 488 conjugate (1:50) for 15 min at 25ºC. For microscopy, 5 min incubation with 10 µM Hoechst 33342 dye was included with the Annexin-V binding incubation. Brightly stained, condensed nuclei were visible with Hoechst dye, characteristic of apoptotic cells, as is phosphatidylserine externalization detected by Annexin-V binding. Images of DU145 cells were captured on an inverted fluorescence microscope (Leica DM IRB, Germany). The percent of condensed nuclei (indicative of apoptosis) was calculated as: [(number of cells with condensed, brightly stained nuclei / total number of cells)*100] with a minimum of 5 fields counted with 100 cells / field.

Cytotoxicity assays

Cytotoxicity was measured using the WST-1 colorimetric assay. HCT116 cells were seeded at 2500 cells/well in 96-well tissue culture plates. After treatment with PST as indicated, cells were incubated with WST-1 for 4 h at 37 °C. Absorbance was measured at 450 nm on a VICTOR^3 microplate reader. Absorbance is directly proportional to the number of living cells in culture. Each assay was performed in triplicate and the mean of three assays was calculated from the average absorbance of control-treated cells.

Mitochondrial functionality assays

Mitochondrial membrane potential (MMP) was observed using cell permeable JC-1 dye (1 µM final concentration). HT-29 and HCT116 cells were grown on cover-slips and following treatment JC-1 was added directly to the media and incubated for 30 min at 37°C in darkness; cell permeable Hoechst dye was added for the last 5 min of incubation, to observe nuclear morphology.

ROS Detection in Isolated Mitochondria

Isolated mitochondria from untreated DU145 cells were subjected to direct incubation with PST. Mitochondrial ROS generation was measured using Amplex Red dye and HRP. In an opaque 96-well plate, 100 µg mitochondrial suspension was incubated in (200 µl) reaction buffer (2.5 mM malate and 10 mM succinate, in PBS) with

50 µM Amplex Red reagent and 6 U HRP, and with control (Me_2SO), PST (1 µM), Tamoxifen (5 µM), or co-treatment of PST and Tamoxifen (PST+TAM). Fluorescence was measured in 1 min intervals over 2 h at excitation 560 nm and emission 590 nm using a SpectraMax GeminiXPS spectrofluorometer.

Assessment of caspase activity

To monitor caspase activity, cellular lysate was collected from dnFADD Jurkat cells and incubated with the desired fluorogenic substrate (caspase-3, DEVD-AFC; caspase-8, IETD-AFC) in assay buffer (0.1 M HEPES, pH 7.4, 2 mM DTT, 0.1% CHAPS, 1% sucrose) and allowed to incubate at 37ºC for 45 min. Fluorescence was measured at excitation 400 nm and emission 505 nm using a SpectraMax Gemini XPS spectrofluorometer. Caspase activity was calculated per microgram of protein, and expressed as a percentage of control activity.

Mitochondrial Toxicology Assay

A phenotype microarray plate was used to assess the effect of PST on mitochondrial function in DU145 cells, as per manufacturer's protocol. The PM-MTOX1 96-well microarray plates are pre-coated with 8 different energy substrates, designed to determine the metabolic pathways targeted by an unknown drug. Briefly, cells were seeded at 4 000 / well in 40 µl of serum-free, glucose-free RPMI media and allowed to attach overnight. Cells were treated with pancratistatin at increasing concentrations, or with rotenone, Antimycin A or tamoxifen for 18 h. Cells were then incubated with 10 µl BiOLOG redox dye "A" supplemented with 5 mM final concentration glucose / well for 4 h at 37°C. Absorbance was measured at 590 nm on a VICTOR^3 microplate reader. Higher absorbance (darker purple colour) is directly proportional to the number of living cells in culture, and thus the degree of mitochondrial function with the specific metabolite. The image presented depicts one assay of several that were run during the standardization of this protocol.

***In vivo* xenograft models**

Six-week old male homozygous CD-1 nude mice (25 – 30 g) were obtained from Charles River Laboratories, St. Constant, QC. Animals were housed in constant laboratory conditions of a 12 h light/dark cycle at 21°C in accordance with institutional

animal protocols (University of Windsor Research Ethics Board - AUPP05). Prior to injection, HT-29 and HCT116 cells were washed with PBS and centrifuged at 500 x *g* for 5 min; cell pellets were suspended in aliquots of 200 µl PBS (2 x 10^6 cells per mouse). The HT-29 ($p53^{mt}$) cell suspension was injected s.c. into the *left* hind flank of each mouse; The HCT116 ($p53^{wt}$) cell suspension was injected s.c. into the *right* hind flank of each mouse. Tumors were allowed to grow for 10 days and thereafter animals were randomized into treatment groups of 3 mice each. Animals were treated intra-tumor (I.T.) with vehicle (5 µl Me_2SO in PBS) or pancratistatin (3 mg/kg) twice a week for 5 weeks. Tumors were assessed at each treatment using standard calipers measuring length and width; tumor volume was calculated using the formula [$\pi/6$ x length x $width^2$]. All animals were weighed at each treatment during the study.

RESULTS

Chapter 2

Pancratistatin induces cell death and caspase-3 activation in dnFADD Jurkat cells

In this study, it was reported that Pancratistatin induces apoptosis in Jurkat cells by activating caspase-3, with minimal effect on non-cancerous peripheral blood cells. To extend this finding, the effect of 24 h treatment with 1 µM pancratistatin on Jurkat cells that express a dominant-negative Fas-associated death domain (dnFADD) was tested. FADD is a critical component of the death-inducing signalling complex (DISC) triggered upon death-receptor stimulation, leading to caspase-8 activation and subsequent activation of caspase-3. It was observed that dnFADD Jurkat cells were as sensitive to pancratistatin-induced apoptosis as wild-type Jurkat cells (Appendix Figure 1A; also refer to Chapter 2). Moreover, these cells had increased caspase-3 activity after only 3 h treatment with pancratistatin; caspase-8 activity did not increase, as expected (Appendix Figure 1B). This finding indictated that caspase-3 may reside upstream of caspase-8 in dnFADD Jurkat cells (Aouad *et al,* 2004), leading to rapid induction of apoptosis following pancratistatin treatment (also refer to Griffin *et al* 2007). Furthermore, this finding indicated that pancratistatin does not trigger the death-receptor mediated extrinsic pathway of apoptosis.

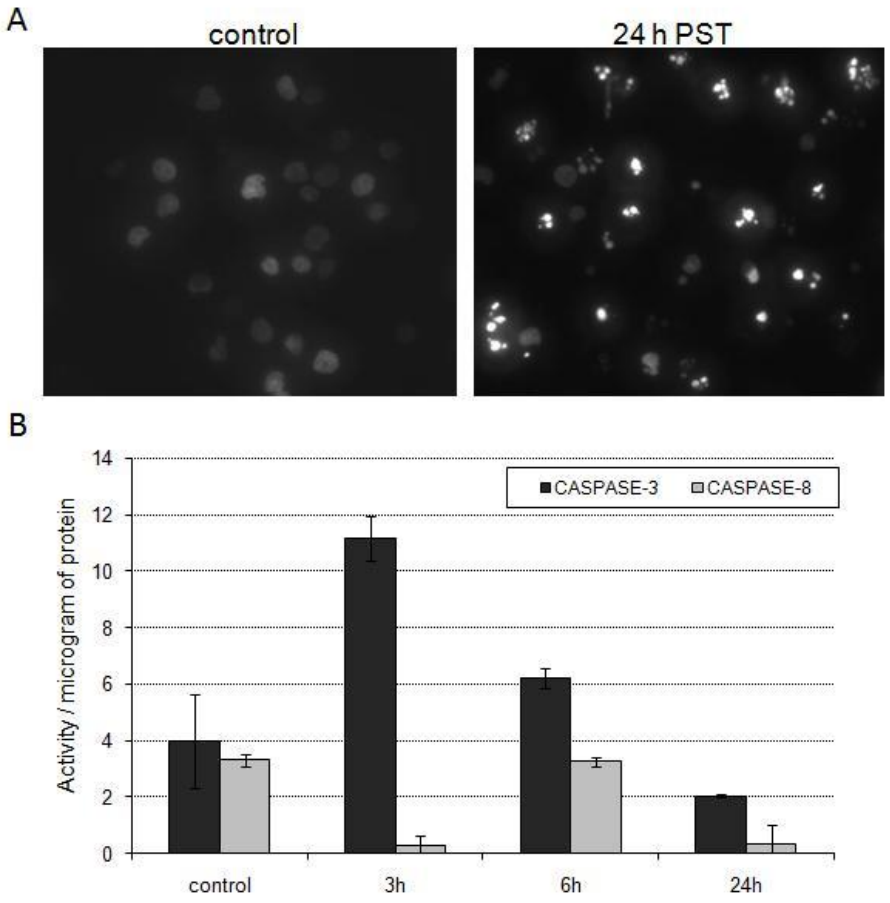

Appendix Figure 1. Effect of pancratistatin treatment on dominant-negative FADD Jurkat cells. (**A**) Hoechst staining was performed to observe nuclear morphology of dominant-negative FADD (dnFADD) Jurkat cells after 24 h control or 1 µM pancratistatin (PST) treatment. Condensed, brightly-stained nuclear morphology is a characteristic feature of apoptotic cells. (**B**) Caspase activity was measured in dnFADD Jurkat cells after the indicated treatment incubation with 1 µM pancratistatin. Results were calculated per microgram of protein and the standard error was calculated using the data from three separate sets of experiments. *Columns*, mean (n=3); *bars*, SD.

Chapter 5

Effect of pancratistatin on colon cancer cell mitochondria function

In a study similar to that reported in Chapter 5 (Supp. Figure 2), HCT116 cells were co-treated with and without pancratistatin and with and without anti-oxidants N-acetylcysteine (nac) or water-soluble coenzyme Q10 (q10), mitochondrial respiratory chain complex inhibitors rotenone (rot) or antimycin A (aa), or mitochondrial permeability transition pore inhibitor cyclosporin A (ca). In contrast to the results obtained with HT29 cells in Chapter 5, co-treatment of pancratistatin with any of these agents was not able to protect cells from pancratistatin-induced toxicity after 72 h exposure (Appendix Figure 2).

The effect of co-treatment with pancratistatin and cyclosporin A (CA) on mitochondrial membrane potential (MMP) in HT29 cells was also monitored. HT29 cells co-treated with pancratistatin and cyclosporin A retained JC-1 dye, which indicated that cyclosporin A, an inhibitor of the mitochondrial permeability transition pore (MPTP), offered protection against PST-induced MMP collapse (Appendix Figure 3, *top*). Furthermore, this co-treatment lead to a decrease in the number of apoptotic cells compared to treatment with pancratistatin alone (Appendix Figure 3, *bottom*). This finding strengthens our hypothesis that pancratistatin-induced cell death ultimately results from mitochondrial membrane permeabilization.

Additionally, the effect of co-treatment with pancratistatin and water-soluble coenzyme Q10 (Q10) on MMP in HT29 and HCT116 cells was observed. Use of a water-soluble formation of Q10 enables study of the anti-oxidant capability of Q10 *in vitro*. Co-treatment with pancratistatin and Q10 was unable to protect colon cancer cells from pancratistatin-induced apoptosis, as compared to pancratistatin treatment alone (Appendix Figure 4). This finding correlates with Chapter 5 data, where the anti-oxidant N-acetylcysteine was also unable to proctect cells from pancratistatin-induced cell death.

Complimentary to our *in vivo* findings presented in Chapter 5, the effect of pancratistatin *in vivo* against tumors with differential p53 expression was studied. Subcutaneous xenografts were established in immune-compromised mice with HT29 (mutant p53) and HCT116 (wt p53) cells. Pancratistatin effectively halted the growth of both HT29 (left hind flank) and HCT116 (right hind flank) compared to control-treated animlas (Appendix Figure 5). Moreover, pancratistatin did not have a significant effect on the body weight of immune-compromised mice when administered intra-tumor (3 mg/kg), compared to control-treated animals (Appendix Figure 5, *top*).

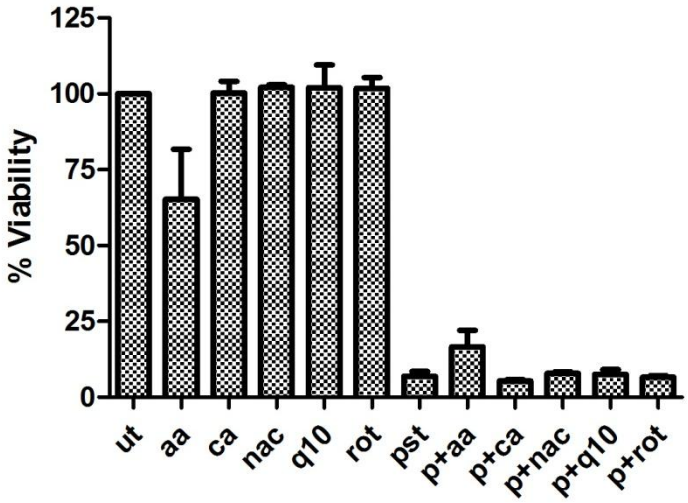

Appendix Figure 2. HCT116 colon cancer cells were treated with 1 µM pancratistatin (pst, p) with and without various antagonists. The effect of treatment on cell viability was determined by WST-1 assay after 72 h. Antagonists studied: 10 µM Rotenone (rot), 5 µM Antimycin A (aa), 5 µM cyclosporin A (ca), 5 mM N-acetylcysteine (nac), 50 µg/ml water-soluble Coenzyme Q_{10} (q10). *Columns*, mean (n=6); *bars*, SD. Co-treatment with anti-oxidants (nac, q10), mitochondrial respiratory chain complex inhibitors (rot, aa) or the mitochondrial permeability transition pore inhibitor (ca) was able to protect cells from decreased viability due to pancratistatin.

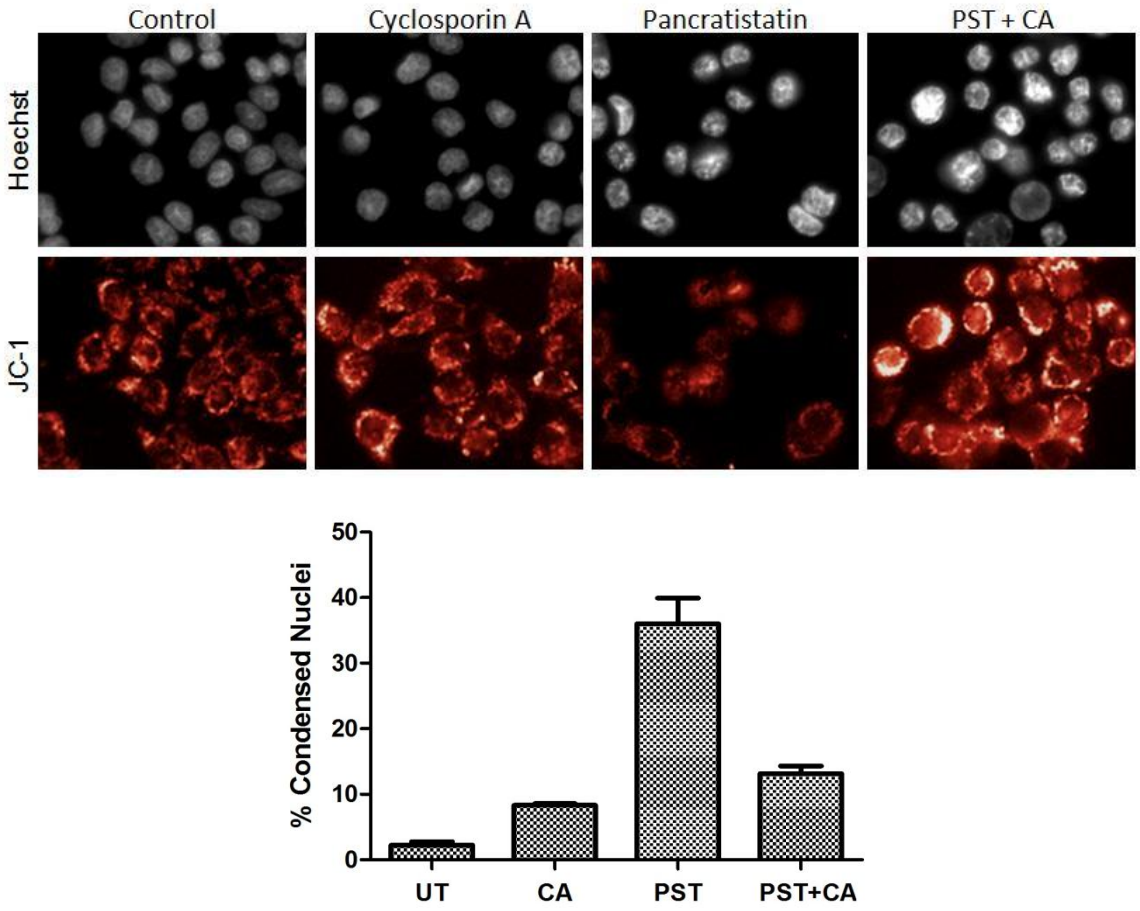

Appendix Figure 3. Effect of co-treatment with pancratistatin and cyclosporin A on mitochondrial membrane potential. Representative fluorescence micrographs of HT29 cells stained with Hoechst and JC-1 dye after 72 h with control (Me_2SO), 1 µM pancratistatin (PST), 5 µM cyclosporin A (CA) or co-treatment of PST and CA. Cyclosporin A binds to cyclophilin D, a component of the mitochondrial permeability transition pore (MPTP), inhibiting its opening and the subsequent collapse of mitochondrial membrane potential (MMP). Mitochondria of cells treated with PST and CA retained JC-1 dye, indicating that CA offered protection against the effects of PST-induced MMP collapse (top panel). Furthermore, there was a decrease in the percentage of cells with brightly stained condensed nuclei, indicative of apoptosis, in PST and CA co-treated cell compared to treatment with PST alone (bottom panel).

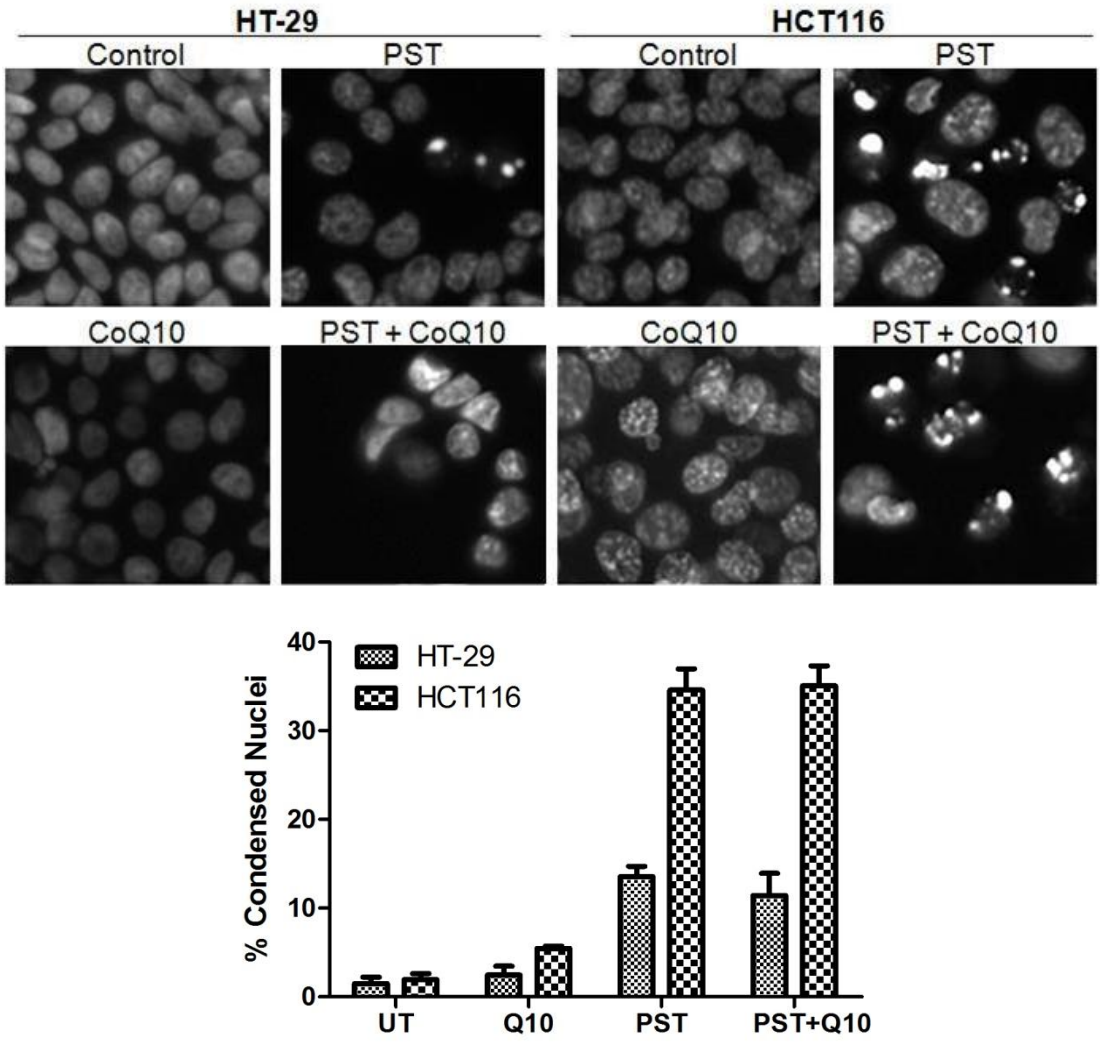

Appendix Figure 4. Effect of pancratistatin (PST) and water-soluble Coenzyme Q_{10} (ws-CoQ_{10}) co-treatment on colon cancer cells. Representative fluorescence micrographs of HT-29 and HCT116 cells stained with Hoechst dye after 48 h with control (Me_2SO), 1 µM pancratistatin (PST), 50 µg/ml ws-CoQ_{10} (Q10) or co-treatment of PST and Q10 (*top panel*). This water-soluble formulation enables study of the anti-oxidant capability of Q10 to protect cells against ROS generated in the mitochondria. Coenzyme Q10 (also referred to as ubiquinone) accepts electrons from complexes I (NADH-ubiquinone oxidoreductase) and II (succinate-ubiquinone oxidoreductase) and transports them to complex III (ubiquinone-cytochrome *c* oxidoreductase) of the mitochondrial respiratory chain. Co-treatment with ws-CoQ_{10} was unable to protect colon cancer cells from pancratistatin-induced apoptosis.

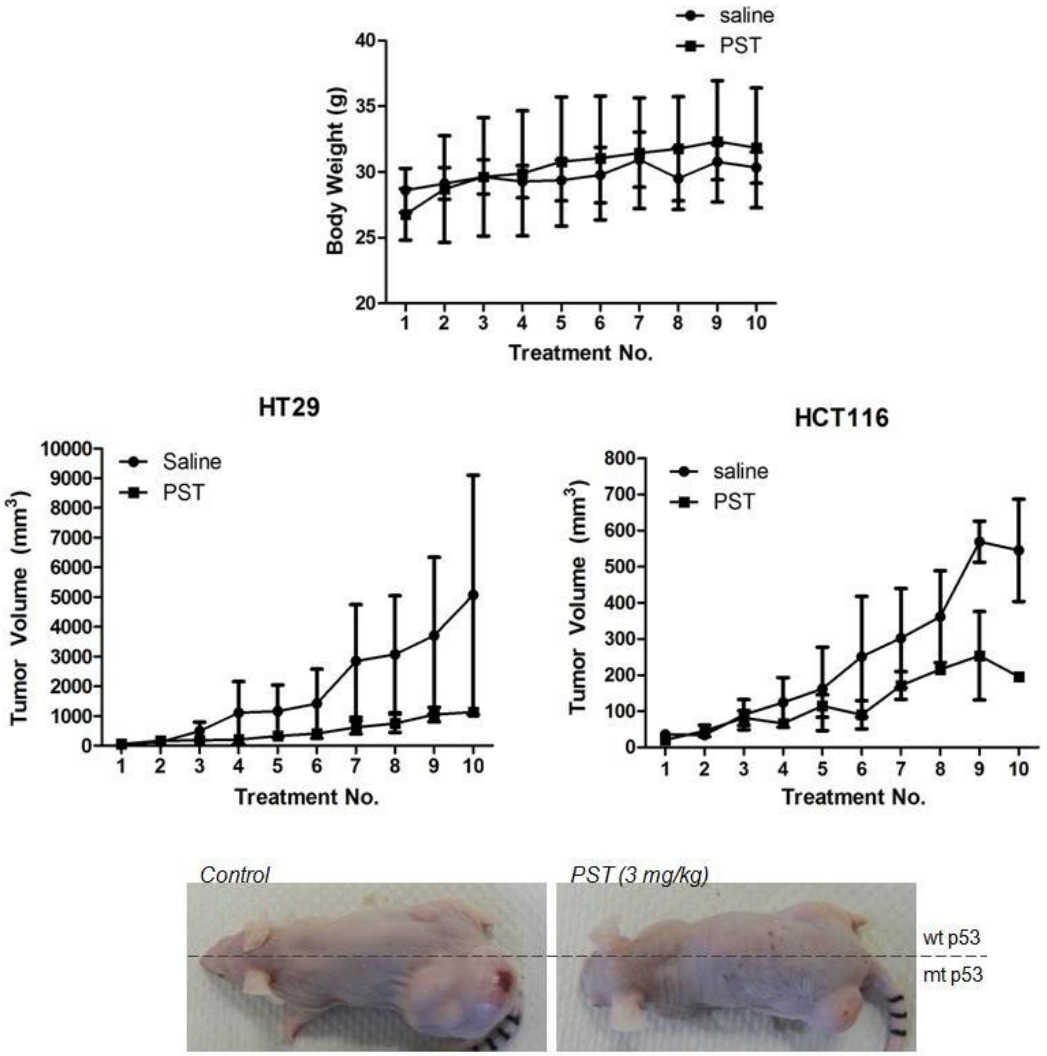

Appendix Figure 5. Evaluation of the effect of pancratistatin (PST) on colon cancer xenografts established from cells expressing wild-type or mutant p53. Average body weight of saline (5 µl Me_2SO in 200 µl PBS) and 3 mg/kg pancratistatin (PST) treated mice (*top panel*). The body weights of the saline and PST-treated mice did not vary significantly throughout the study. *Data points*, mean (n=3); *bars*, SD. Tumor growth curve of saline or pancratistatin (PST) (3 mg/kg) I.T. administration of HT-29 (mutant p53) tumors (*left panel*). Tumor growth curve of saline or PST (3 mg/kg) I.T. administration of HCT116 (wild-type p53) tumors (*right panel*). *Data points*, mean (n=3); *bars*, SD. Representative tumor size of HCT116 (wild-type p53) and HT-29 (mutant p53) xenografts in CD-1 nude mice at time of sacrifice (*bottom panel*).

Chapter 6

Pancratistatin induces apoptosis in human prostate cancer cells

Complimentary to the data presented in Chapter 6 (Figure 2), human prostate cancer cells (DU145) treated with pancratistatin for 24 and 48 h were positive for Annexin-V binding, which indicates exposure of phosphatidylserine, a characteristic feature of apoptosis (Appendix Figure 6).

In Chapter 6, our data suggested that pancratistatin induced reactive oxygen species (ROS) production in DU145 cells (Figure 4A) and that tamoxifen (TAM) induced non-lethal autophagy in DU145 cells (Figure 5A), which may be attributed to increased ROS generation (Chen *et al,* 2009). To extend these findings, we monitored the effect of pancratistatin and tamoxifen on DU145 isolated mitochondria. Our results suggested that pancratistatin and co-treatment with pancratistatin and tamoxifen induced increased ROS production after 2 h incubation (Appendix Figure 7).

Additionally, a preliminary metabolism-based experiment was performed with DU145 cells using a phenotype microarray – mitochondrial toxicity (PM-MTOX) 96-well plate. This PM-MTOX plate is pre-coated with various metabolites that allow study of the metabolic pathway affected by pancratistatin treatment at increasing concentrations. Preliminary findings suggested that the metabolic pathways that consume α-ketoglutarate and pyruvate for energy are not affected by pancratistatin treatment (Appendix Figure 8). This is an interesting finding that requires additional testing to be conclusive.

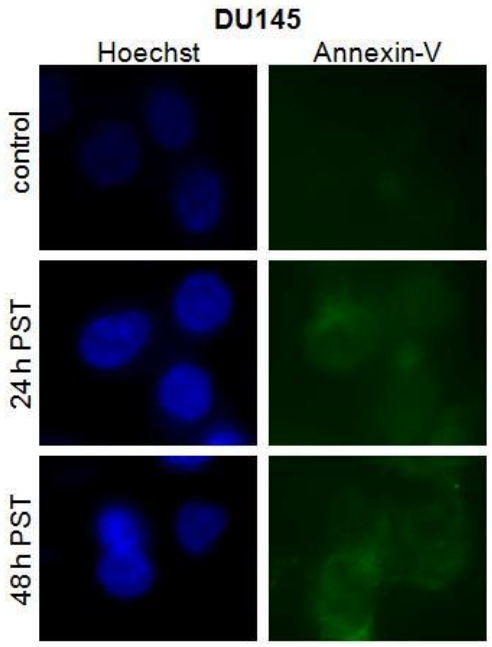

Appendix Figure 6. Monitoring the apoptosis-inducing effect of pancratistatin (PST) on human prostate cancer cells. Cells (DU145) were treated with PST for 24 or 48 h and stained with Hoechst to observe nuclear morphology; phosphatidylserine flipping from the inner to the outer leaflet of the plasma membrane was monitored with the Annexin-V binding assay. Pictures taken at 400x magnification.

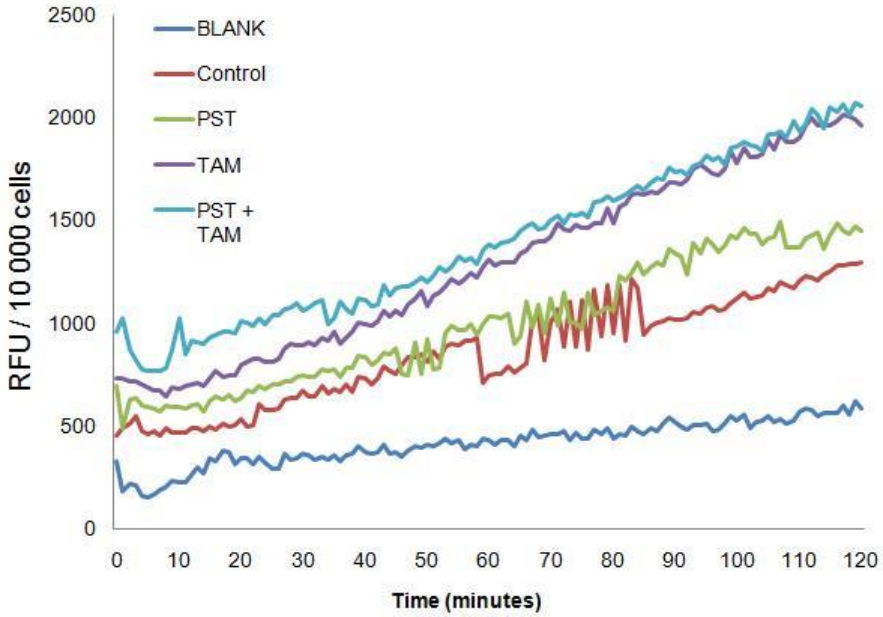

Appendix Figure 7. Effect of Pancratistatin and/or Tamoxifen treatment on the production of ROS from isolated mitochondria. ROS generation from isolated DU145 mitochondria treated with 1 µM pancratistatin (PST), 5 µM tamoxifen (TAM) or both. Measurements were recorded over 2 h in 1 min intervals and calculated as relative fluoresence units (RFU) per 10 000 cells using Trypan Blue exclusion dye.

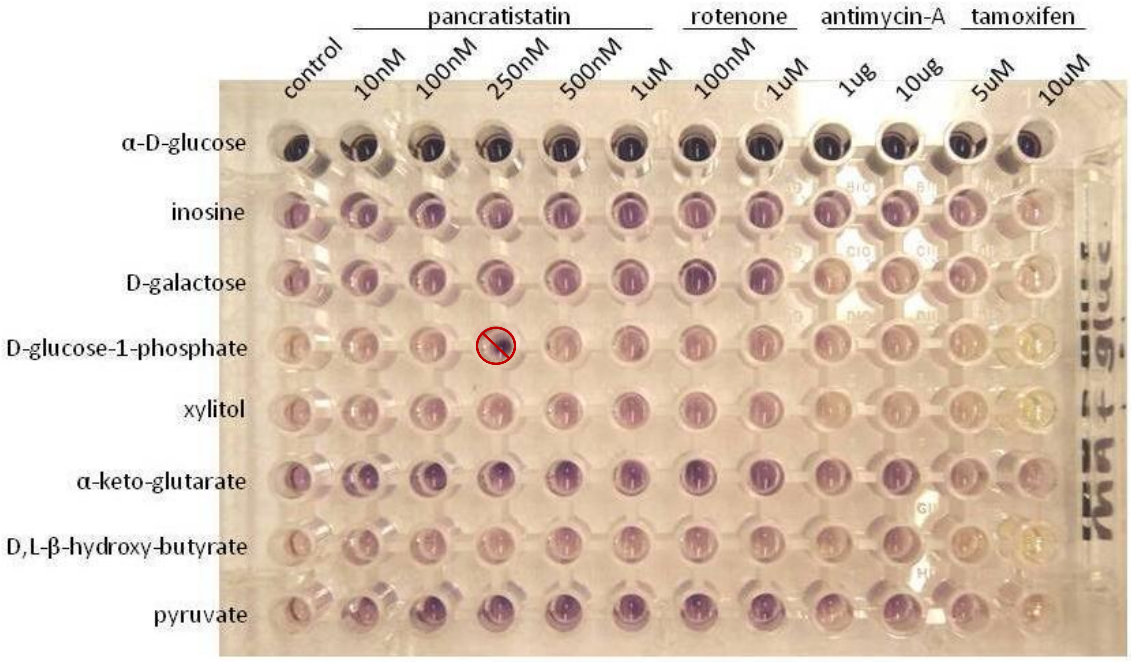

Appendix Figure 8. Assessment of mitochondrial toxicity in prostate cancer cells using a phenotype microarray plate. DU145 cells (4 X 10^3) were added to each well of a PM-MTOX-1 96-well microarray plate and allowed to grow in serum-free, glucose-free media and the indicated metabolite for 24 h prior to treatment. Cells were treated with pancratistatin at increasing concentrations, rotenone (complex I inhibitor), Antimycin A (complex III inhibitor), or tamoxifen (cited as a fatty acid β-oxidation uncoupler by the manufacturer) for 18 h. Representative image taken after 4 h incubation with the appropriate redox dye.

DISCUSSION

The unpublished findings presented here correlate with published data in Chapters 2, 5 and 6 of this thesis. Where appropriate, these results are indicated in the main body of the thesis. Collectively, this additional experimental data supports the overall hypothesis that pancratistatin treatment leads to increased ROS generation and mitochondrial membrane collapse/permeabilization, resulting in caspase activation and apoptotic cell death in cancer cells.

REFERENCES

Aouad SM, Cohen LY, Sharif-Askari E, Haddad EK, Alam A, Sekaly RP. Caspase-3 is a component of Fas death-inducing signaling complex in lipid rafts and its activity is required for complete caspase-8 activation during Fas-mediated cell death. J Immunol 2004; 172(4): 2316-2323.

Chen JQ, Cammarata PR, Baines CP, Yager JD. Regulation of mitochondrial respiratory chain biogenesis by estrogens/estrogen receptors and physiological, pathological and pharmacological implications. Biochim Biophys Acta 2009; 1793(10): 1540-1570.

Griffin C, McNulty J, Hamm C, Pandey S. Pancratistatin: a novel highly selective anti-cancer agent that induces apoptosis by activation of membrane-Fas-receptor associated caspase-3. *Trends in Cell Apoptosis Research.* NovaScience Publishers, Inc. 2007. Pgs. 93-110.

APPENDIX C

CHEMICAL REAGENTS

REAGENT NAME	COMPANY NAME	CATALOGUE No.
2',7'-dichlorodihydrofluorescein diacetate (H_2DCFDA)	Sigma	D6883
3-[4,5-dimethylthiazol-2-yl]-2,5-diphenyl tetrazolium bromide (MTT)	Sigma	M5655
40% Acrylamide/Bis Solution (37.5:1)	BioRad	161-0148
5,5',6,6'-tetrachloro-1,1',3,3' tetra-ethylbenzimidazolylcarbocyanine iodide (JC-1)	Invitrogen	T3168
Amplex Red	Sigma	90101
Annexin-V AlexaFluor 488	Invitrogen	A13201
Anti-AIF (Rb pAb)	AbCam	ab1998
Anti-Bax (Ms mAb)	Santa Cruz Biotech	sc7480
Anti-Bcl-2 (Ms mAb)	Santa Cruz Biotech	sc7382
Anti-Cytochrome c (Ms mAb)	AbCam	ab13575
Anti-Endo G (Rb pAb)	AbCam	ab9647
Anti-H2AX (Ms mAb)	Upstate (Millipore)	05-636
Anti-LC3 (pAb Rb)	AbCam	ab58610
Anti-Mouse FITC (whole molecule)	Sigma	F2266
Anti-Mouse HRP (rabbit pAb)	Abcam	ab6728
Antimycin A	Sigma	A8674
Anti-Rabbit FITC (whole molecule)	Sigma	F7512
Anti-Rabbit HRP (goat pAb)	Abcam	ab6721
Anti-SDHA (Ms mAb)	SantaCruz Biotech	sc59687
Anti-β-Actin (Ms mAb)	SantaCruz Biotech	sc81178
Bradford Reagent	BioRad	500-0006
Cyclosporin A	Sigma	C1832
DEVD-AFC (caspase-3 substrate)	MP Biomedicals	03AFC138
Eosin	Sigma	E4382
Etoposide (Vp-16)	Sigma	E1383
Hematoxylin	Sigma	H3136
Hoechst 33342	Invitrogen	H1399
Horse Radish Peroxidase (HRP)	Sigma	P6782
HTS-Tubulin Polymerization Assay Kit	CytoSkeleton Inc.	BK004
IETD-AFC (caspase-8 substrate)	MP Biomedicals	03AFC140
LEHD-AFC (caspase-9 substrate)	MP Biomedicals	03AFC154
Leupeptin	Sigma	L2023
MitoCasp Assay Kit	Cell Technology Inc.	000021

Mitotracker	Invitrogen	M7513
Mono-dansyl cadaverine (MDC)	Sigma	30432
N-acetylcysteine	Sigma	A9165
Paclitaxel (Taxol)	Sigma	T7402
Pepstatin A	Sigma	77170
Phenylmethanesulfonyl fluoride (PMSF)	Sigma	P7626
PM-MTOX-1 Assay	BIOLOG Inc.	PM-MTOX1
Rotenone	Sigma	R8875
Tamoxifen (TAM)	Sigma	T9262
Terminal deoxynucleotidyl transferase dUTP nick-end labelling (TUNEL) Assay Kit	Invitrogen	A23210
Tetramethyl rhodamine methyl ester (TMRM)	Invitrogen	T668
Trypan blue exclusion dye	Invitrogen	15250061
WST-1	Roche	11 644 807 001
z-VAD-fmk (pan-caspase inhibitor)	EMD BioSciences Inc.	627610

VITA AUCTORIS – CARLY GRIFFIN

EDUCATION

2005 – 2011 **Ph.D. Biochemistry – "Evaluation of the Selective Anti-Cancer Activity of Natural and Synthetic Alkaloids"**
Department of Chemistry & Biochemistry, University of Windsor
- Supervised by Dr. Siyaram Pandey, Professor
- In collaboration with: Dr. James McNulty, Organic Chemist, McMaster University, ON; Dr. Caroline Hamm, Oncologist, Windsor Regional Cancer Center, ON

2002 – 2005 **B.Sc. (Honours w/Thesis) Biochemistry – "Uncovering the Mechanism of Induction of Apoptosis by Pancratistatin in Human Lymphoma & Leukemia"**
Department of Chemistry & Biochemistry, University of Windsor
- Supervised by Dr. Siyaram Pandey, Professor

AWARDS

1. Natural Health Products Research Society Best Oral Presentation: 05/2010
2. Canadian Institute of Health Research (CIHR) Banting Canada Graduate Scholarship, Doctoral Fellowship: 09/2008 - 09/2011 (accepted)
3. Canadian Breast Cancer Foundation Doctoral Fellowship: 09/2008 (declined)
4. Ontario Graduate Scholarship: 01-12/2009; 01-12/2008; 05-12/2006.
5. University of Windsor "Chemistry at the Mall" Best Poster Award: 05/2009
6. Casino Windsor Cares / Gail Rosenblum Breast Cancer Scholarship: 2008
7. CIHR Canada Graduate Scholarship, Master's Award: 01-12/2007
8. University of Windsor Graduate Tuition Scholarship: 09/2005 - 12/2010
9. Canadian Prostate Cancer Research Initiative Research Travel Bursary: 09/2007
10. University of Windsor President's Excellence Scholarship: 05-12/2006
11. GoldenKey International Honor Society Academic Research Award: 02/2006
12. Cindy Hutnik Biochemistry (Hons.) Research Award: 04/2005

INVITED PRESENTATIONS

Griffin C, Hamm C, McNulty J, Pandey S. (**2010**) Evaluation of the selective anti-cancer activity of natural and synthetic alkaloids. *Departmental Seminar.* 11/16/10. Canada's Michael Smith Genome Sciences Centre, BC Cancer Agency, Vancouver, BC.

Griffin C, Hamm C, McNulty J, Pandey S. (**2010**) Evaluation of the selective anti-cancer activity of natural and synthetic alkaloids. *Weekly Departmental Seminar Series.* 10/29/10. Department of Chemistry & Biochemistry, University of Windsor, Windsor, ON.

Griffin C, Hamm C, McNulty J, Pandey S. (**2008**) Building a collaborative research effort to develop a non-toxic chemotherapeutic agent for the treatment of cancer. *Knowledge Translation Seminar*. 07/23/08. St. John's Research Institute, Bangalore, India.

Griffin C, Hamm C, McNulty J, Pandey S. (**2006**) Recent progress on research work on Pancratistatin: a novel anti-cancer agent capable of selectively inducing apoptosis in cancer cells. *'Fridays at Four' Seminar Series.* 02/24/06. Windsor Regional Hospital, Windsor, ON.

REFEREED PUBLICATIONS

Griffin C, Karnik A, McNulty J, Pandey S. Pancratistatin selectively targets cancer cell mitochondria and reduces growth of human colon tumor xenografts. *Mol Can Ther* 2011; 10(1): 57-68.

Ovadje P, Chatterjee S, Griffin C, Tran C, Hamm C, Pandey S. Selective Induction of Apoptosis through Activation of Caspase-8 in Human Leukemia cells (Jurkat) by Dandelion Root Extract. *J Ethnopharmacol* 2011; 133: 86-91.

Griffin C, Hamm C, McNulty J, Pandey S. Pancratistatin induces apoptosis in clinical leukemia samples with minimal effect on non-cancerous peripheral blood mononuclear cells. *Cancer Cell Int* 2010; 10: 6.

Collins J, Rinner U, Moser M, Hudlicky T, Ghiviriga I, Romero AE, Kornienko A, Ma D, Griffin C, Pandey S. Chemoenzymatic synthesis of Amaryllidaceae constituents and biological evaluation of their C-1 analogues. The next generation synthesis of 7-deoxypancratistatin and trans-dihydrolycoricidine. *J Org Chem* 2010; 75(9): 3069-84.

McNulty J, Nair J, Bastida J, Pandey S, Griffin C. Structure activity studies on the crinane alkaloid apoptosis-inducing pharmacophore. *Nat Prod Comm* 2009; 4(4): 483-88.

McNulty J, Nair J, Bastida J, Pandey S, Griffin C. Structure-activity studies on the lycorine pharmacophore: a potent inducer of apoptosis in human leukemia cells. *Phytochem* 2009; 70(7): 913-9.

McNulty J, Nair J, Griffin C, Pandey S. Synthesis and biological evaluation of fully functionalized seco-pancratistatin analogues. *J Nat Prod* 2008; 71(3): 357-63.

Griffin C, Sharda N, Sood D, Nair J, McNulty J, Pandey S. Selective cytotoxicity of pancratistatin-related natural Amaryllidaceae alkaloids: evaluation of the activity of two new compounds. *Cancer Cell Int* 2007; 7: 10.

Siedlakowski P, McLachlan-Burgess A, Griffin C, Tirumalai SS, McNulty J, Pandey S. Synergy of Pancratistatin and Tamoxifen on breast cancer cells in inducing apoptosis by targeting mitochondria. *Cancer Biol Ther* 2007; 7(3): 376-84.

McNulty J, Poloczek J, Larichev V, Werstiuk NH, Griffin C, Pandey S. Discovery of the Apoptosis-Inducing Activity and High Accumulation of the Butenolides, Menisdaurilide and Aquilegiolide, in Dicentra spectabilis. *Planta Med* 2007; 73(15): 1543-47.

McNulty J, Nair J, Codina C, Bastida J, Pandey S, Gerasimoff J, Griffin C. Selective apoptosis-inducing activity of crinum-type Amaryllidaceae alkaloids. *J Phytochem* 2007; 68: 1068-74.

McLachlan A, McCarthy S, Griffin C, Richer J, Pandey S. Differential response induced by exposure to low-dose ionizing radiation in SHSY-5Y and normal human fibroblast cells. *Appl Biochem Biotechnol* 2006; 135(2): 159-78.

Kekre N, Griffin C, McNulty J, Pandey S. Pancratistatin causes early activation of caspase-3 and flipping of phosphatidyl serine followed by rapid apoptosis specifically in human lymphoma cells. *Cancer Chemother Pharmacol* 2005; 56(1): 29-38.

ACCEPTED / SUBMITTED PUBLICATIONS

Griffin C, McNulty J, Pandey S. Pancratistatin induces apoptosis and autophagy in metastatic prostate cancer cells. 2011 [Submitted to *Int J Oncol* 2010 December 8].

COLLECTIVE WORKS / BOOK CHAPTERS

Griffin C, McNulty J, Hamm C, Pandey S. Pancratistatin: a novel highly selective anti-cancer agent that induces apoptosis by activation of membrane-Fas-receptor associated caspase-3. *Trends in Cell Apoptosis Research.* NovaScience Publishers, Inc. 2007. Pgs. 93-110.

Pandey S, Somayajulu M, McLachlan A, Gueorguieva D, Griffin C. The Cutting Edge: Apoptosis and Cell Therapy. *Artificial cell, Cell engineering & Therapy.* Woodhead Publishers, Ltd. 2007. Pgs. 117-136.

PLATFORM PRESENTATIONS

Griffin C, McNulty J, Pandey S. (**2011**) Evaluation of the selective anti-cancer activity of natural and synthetic alkaloids. *Bringing Together Communities: Student Research Conference.* 02/03/11 – 02/04/11. University of Windsor, Windsor ON. (PhD work)

Griffin C, Hamm C, McNulty J, Pandey S. (**2010**) Pancratistatin selectively induces apoptosis in cancer cells and reduces growth of colon xenografts. *7th Annual NHPRS Research Conference*. 05/23/10-05/26/10. Westin Nova Scotian, Halifax NS (PhD work, award winning)

Griffin C, Valero M, McNulty J, Pandey S. (**2006**) Pancratistatin: A novel anti-cancer agent that selectively induces apoptosis in cancer cells. "The Hawaiian flower with cancer killing power". *Golden Key International Honour Society Conference*. 02/18/2006. Le Royal Meridien Hotel, Toronto ON. (MSc work, award winning)

Griffin C, Pandey S, McNulty J. (**2005**) Uncovering the mechanism of induction of apoptosis by Pancratistatin in human lymphoma cells. *33rd SOUSC Conference.* 03/19/2005. University of Toronto, Toronto ON. (BSc work)

POSTERS

Griffin C, McNulty J, Pandey S. (**2010**) Pancratistatin selectively induces apoptosis in colon cancer cells by targeting the mitochondria and reduces tumor growth in xenograft models. *Keystone Symposia. Cell Death Pathways: Apoptosis, Autophagy & Necrosis.* 03/12/10 – 03/17/10. Fairmont Hotel Vancouver, Vancouver BC. (PhD work)

Griffin C, McNulty J, Pandey S. (**2009**) Pancratistatin induces apoptosis by targeting the mitochondria selectively in colon cancer cells and reduces tumor growth in xenograft models. Abstract #5498. *AACR 100th Annual Meeting*. 04/18/09 – 04/22/09. Colorado Convention Center, Denver CO. (PhD work)

Griffin C, Karnik A, McNulty J, Pandey S. (**2008**) The novel compound Pancratistatin induces apoptosis selectively in human prostate and colon cancer cells by targeting the mitochondria and reduces growth of human tumor xenografts. *CIHR Canadian Student Health Research Forum.* 06/08/08. University of Manitoba, Winnipeg MB. (PhD work)

Siedlakowski P*, Griffin C, McLachlan-Burgess A, Sridhar TS, McNulty J, Pandey S. (**2007**) Synergistic action of Pancratistatin and Tamoxifen on breast cancer cell lines leading to selective induction of apoptosis by destabilization of mitochondria. *National Cancer Institute of Canada's 60th Anniversary Conference.* 11/15/07 – 11/17/07. Intercontinental Toronto Centre, Toronto ON. (PhD work, national)

Griffin C, Siedlakowski P, Karnik A, McNulty J, Pandey S. (**2007**) Pancratistatin induces apoptosis selectively in prostate cancer cells by targeting mitochondria & reduces growth of prostate tumor xenografts. *Canadian Prostate Cancer Research Initiative.* 09/28/2007. Westin Harbour Castle, Toronto ON. (PhD work)

Griffin C, Kekre N, McNulty J, Pandey S. (**2004**) Pancratistatin induced early activation of caspase-3, flipping of phosphatidyl serine to outer leaflet of p.m. leading to efficient induction of apoptosis in human lymphoma (jurkat) cells: no effect on normal blood cells. *11th Annual International Life Sciences & Biotechnology Conference/Exhibition*. 11/29/04 – 12/01/04. Ottawa Congress Centre, Ottawa ON. (BSc work).